District of Columbia
Exceptional Event Demonstration and Analysis of the June 2023 Quebec Canada Wildfires and Their Impact on DC's Air Quality on June 29, 2023

January 26, 2024

DEPARTMENT OF ENERGY & ENVIRONMENT
GOVERNMENT OF THE DISTRICT OF COLUMBIA

Prepared by:
Air Quality Division
1200 First Street, NE, Fifth Floor
Washington, DC 20002

(This page is intentionally left blank)

Contents

Table of Figures

List of Tables

1.0 Overview

1.1 Introduction

Numerous wildfires were initiated by lightning, produced by a passing storm system across wildland areas of Quebec on June 1, 2023. Well over 100 fires were burning across the province by June 4. With strong and persistent winds behind the system fanning the flames, numerous fires grew to enormous sizes and spread uncontrolled. The two most significant areas of fires were over southwestern and northern Quebec, both of which burned out of control throughout the month of June.

During the week preceding the event that impacted the District of Columbia (the District) on June 29, roughly 1.7 million hectares of land, or approximately the size of Connecticut, burned across Canada, primarily in Quebec. Smoke was first concentrated across Quebec, where concentrations climbed to the upper AQI thresholds. The concentrations were so significant in some locations that they exceeded the AQI scale. This smoke then meandered from Quebec to over the Great Lakes, finally moving into the District, being guided by pin-wheel-like transport around a storm system. The wildfire smoke produced widespread ozone across the Mid-Atlantic and Great Lakes of the United States (US).

Ozone concentrations exceeded the 2015 National Ambient Air Quality Standard (NAAQS) of 70ppb on June 29, 2023, across a wide area of the central and eastern US. Ozone concentrations exceeding 70 ppb were seen not only in the District, but across northeast United States by June 29, 2023 (Figure 1). In the District, the maximum daily 8-hour average ozone (MD8AO) concentration reached a peak of 89 ppb with two of the District's ozone monitors exceeding the 70-ppb standard on June 29, 2023, due to the influences of the Quebec wildfire smoke. Those monitors that exceeded the 70-ppb standard are highlighted in Table 1. District sites are listed using the common site name and Air Quality System (AQS) identification number (AQSID). MD8AO concentrations for June 29th are shown in ppb. The final columns indicate the current fourth high and estimated design value with no exclusion of any data.

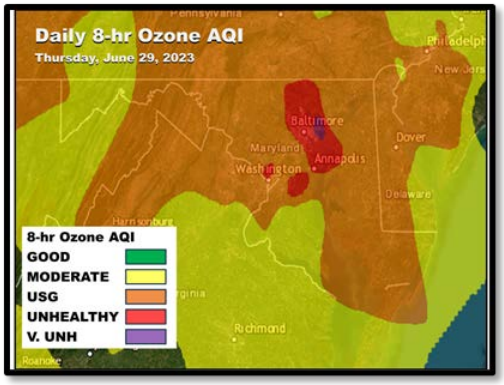

Figure 1: AQI maps from June 29, 2023.

Table 1: Maximum Daily 8-hour average ozone (MD8AO) concentrations on June 29, 2023, for both District sites.

		MD8AO, ppb	2023	
Site Name	**AQSID**	**29-Jun**	**Fourth High, ppm**	**Est DV, ppm**
McMillan Reservoir	110010043	89	0.075	0.071
River Terrace	110010041	73	0.058	0.060

*** 2023 data are not certified as of this writing, and therefore all DVs are estimated.**

Following the U.S. Environmental Protection Agency's (EPA) regulatory process for the Exceptional Events Rule (40 CFR § 50.14), the District of Columbia's Department of Energy and Environment (DOEE) flagged the data as being influenced by a Canadian wildfire and communicated to EPA, the District's intention of submitting an exceptional event package for ozone on June 29, 2023. This analysis demonstrates that the District's 8-hour ozone concentrations that exceeded the 2015 standard meet the requirements for having been influenced by an exceptional event and should therefore be excluded from design value (DV) calculations used to determine the District's ozone attainment status.

1.2 Exceptional Events Summary of Approach

The Exceptional Events Rule, as defined in 40 CFR § 50.14, states that an event may be excluded from regulatory use if it had the following characteristics:

1) *There is a clear, causal relationship between the event and the monitored exceedance that affects air quality.*
2) *The event was of human origins not likely to recur or was natural in origins.*
3) *The occurrence was not reasonably controllable or preventable.*

The 2016 Exceptional Events Rule at 40 CFR § 50.14(c)(3) states that an exceptional events demonstration must include the following elements:

1) *A narrative conceptual model that describes the event(s) causing the exceedance or violation and a discussion of how emissions from the event(s) led to the exceedance or violation at the affected monitor(s);*
2) *A demonstration that the event affected air quality in such a way that there exists a clear causal relationship between the specific event and the monitored exceedance or violation;*
3) *Analyses comparing the claimed event-influenced concentration(s) to concentrations at the same monitoring site at other times. The Administrator shall not require a State to prove a specific percentile point in the distribution of data;*
4) *A demonstration that the event was both not reasonably controllable and not reasonably preventable;*
5) *A demonstration that the event was caused by human activity that is unlikely to recur at a particular location or was a natural event; and*
6) *Documentation that the submitting air agency followed the public comment process.*

Furthermore, 40 CFR § 50.14(b)(4) states that the EPA:

> *"… Administrator shall exclude data from use in determinations of exceedances and violations where a State demonstrates to the Administrator's satisfaction that emissions from wildfires caused a specific air pollution concentration in excess of one or more national ambient air quality standards at a particular air quality monitoring location and otherwise satisfies the requirements of this section. Provided the Administrator determines that there is no compelling evidence to the contrary in the record, the Administrator will determine every wildfire occurring predominantly on wildland to have met the requirements identified in paragraph (c)(3)(iv)(D) [item (4) above] of this section regarding the not reasonably controllable or preventable criterion."*

The guidance document also recommends following a tiered approach to the analysis, providing evidence of "Key Factors" in each tier. Following the elements suggested in the Exceptional Events Guidance Document outlined above, DOEE contends and demonstrates here-in, that transported wildfire smoke had a direct role in amplifying ozone concentrations to a level that would not have been possible in the absence of smoke, and constituents and satisfies the three core exceptional event criteria. Based on recommendations from the EPA and the Guidance Document, the District used a Tier 3 weight of evidence approach for this analysis. DOEE addresses each of the necessary elements cited previously in the subsequent sections of this document.

The EPA Guidance Document offers suggestions for appropriate analyses to demonstrate the clear causal relationship between wildfire and excessive ozone levels. In addition, EPA recognizes that appropriate levels of analysis will vary for particular locations and conditions. EPA does not intend for the guidance to constrain the analysis. DOEE includes some of the suggested analytics and variations on those methods to support our conclusion that the high ozone concentrations throughout the District were caused or worsened by the wildfire smoke from Quebec fires in June of 2023.

1.3 Regulatory Significance of the Exclusion

1.3.1 June 2023 Exclusion Request

There are three ozone monitors in the District of Columbia (Figure 2) covering the Washington, DC-MD-VA nonattainment area. Those sites are Takoma Recreation Center (in the far north), McMillan Reservoir (central to the District), and River Terrace Education Campus (east of the Anacostia River). DOEE operates all three of these regulatory ozone monitors. On June 29, 2023, two of these three monitors had both MD8AO observations above 70ppb (Takoma Recreation Center was not operational at the time) exceeding the 70 ppb ozone NAAQS in the District and met the criteria for further analysis and potential exclusion according to those listed in 40 CFR § 50.14(a)(1)(i). Therefore, DOEE asks for the exclusion of both MD8AO observations for June 29, 2023, that exceeded 70 ppb at the following two monitors: McMillan (110010043) and River Terrace (110010041). DOEE requests that these observed ozone concentrations on June 29, 2023, at these monitors as listed in Table 1, be classified as an exceptional event and excluded from regulatory use.

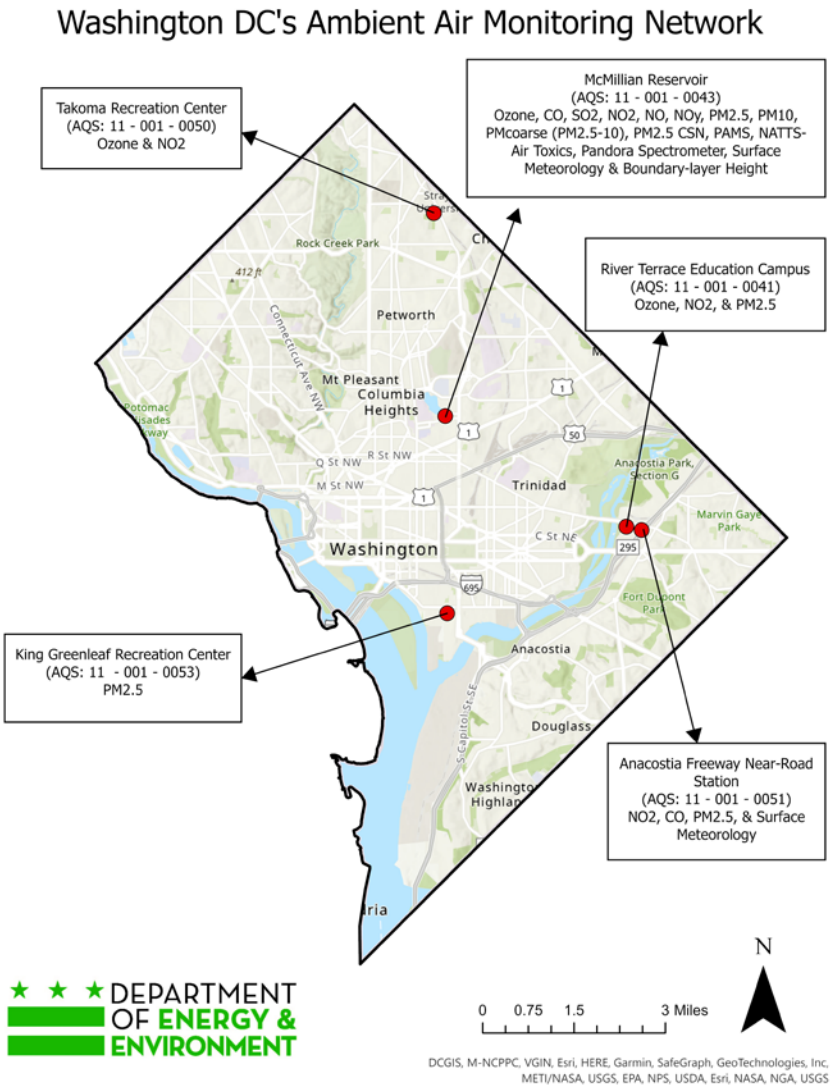

Figure 2: The District of Columbia's ambient air monitoring program as of June 2023. There are three sites that measure ground-level ozone.

		2023				
Site Name	AQSID	MD8AO, ppb	Fourth High, ppb		Design Value, ppb	
		29-Jun	Including	Excluding	Including	Excluding
McMillan	110010043	89	76	72	76	71
River Terrace	110010041	73	58	57	58	58

Table 2: Ozone monitors at which DOEE is seeking EPA data exclusion concurrence.

Local names and Air Quality System (AQS) identification numbers (AQSID) identify monitors in the text. Also given are the maximum daily 8-hour average ozone (MD8AO) concentrations in ppb. The final columns indicate the 2023 fourth high and design value with no exclusion of data (Including) and if the requested data from June 29th is excluded from the fourth high and design value calculations (Excluding).

1.3.2 Design Value and Fourth High Impacts

The exclusion of both MD8AO observations on June 29, 2023, will lead to lower DVs for two monitors in the District of Columbia. The June 29, 2023, smoke event is one of the most potent smoke events of the year, aiding ozone production across the entire District network. Due to the large amount of smoke during the 2023 season, there were at least four smoke-impacted events at the highest monitor in the District (McMillan).

The EPA designates an area's attainment status of the NAAQS via the DV metric. For 8-hour ozone, each monitor's annual fourth-highest daily 8-hour maximum concentration averaged over the past three years designates the attainment status for that particular area. Ozone concentrations on June 29 were within the fourth-highest 8-hour average observations of 2023 at McMillan and River Terrace Table 1. Excluding the June 29th concentrations at the two requested monitors, Table 2 would reduce the design values of both monitors, notably McMillan, which would drop below the 2015 70 ppb NAAQS level (from 71 to 70 ppb). Details of specific site DVs with and without exceptional event status, along with changes in the fourth highest concentrations for June 29, 2023, are provided in Table 2 for both District monitors that DOEE is requesting exceptional event data exclusion.

1.3.3 NAAQS Attainment Considerations

The Washington, DC-MD-VA ozone nonattainment area needs to demonstrate continued attainment of the 2015 ozone standard by August 2024. This continued attainment of the 2015 ozone standard would only occur if EPA concurs with this exceptional event demonstration for June 29, 2023.

EPA concurrence of the requested concentrations on June 29, 2023, in the District will bring the McMillan monitor (110010043), Washington, DC-MD-VA Non-Attainment Area (NAA) into attainment of the 2015 8-hour ozone NAAQS. At this time, the McMillan monitor is the only monitor that is violating the NAAQS in the nonattainment area, and the area would be eligible to be re-classified as in attainment of the 2015 NAAQS should EPA concur with the District's June 29, 2023 exceptional event demonstration. However, due to repeated smoke events and their impacts on ozone, this demonstration is one of two in the Washington, DC-MD-VA attainment area. DOEE will submit the other demonstrations to have a certain record of the events in the case that these monitored values become policy-relevant in future years. DOEE is also including the exceptional value at the River Terrace monitor in this demonstration for the same purpose.

1.4 Summary of Findings

This report demonstrates that:

- There was a clear causal relationship between the smoke and the MD8AO exceedances;
- The wildfire causing smoke was a natural event and
- The smoke event in question was not reasonably preventable and is unlikely to recur.

Key findings and evidence supporting these assertions include the following:

- Copious, network-wide ozone was generated due to the presence of wildfire-smoke-generated ozone upstream transported into the District with rapid local generation due to smoke augmenting transport;
- Ozone higher than historical norms within an environment of historically low anthropogenic precursors and weak in-situ meteorological support (e.g., low temperatures) for ozone;
- A Q/d analysis which meets EPA thresholds for clear causal influence;
- Fine Particle ($PM_{2.5}$), Carbon Monoxide (CO), and Nitrogen Oxides (NOx) were elevated during the event, consistent with a wildfire smoke plume;
- Elevated $PM_{2.5}$ surface concentrations tracked from the wildfire region; and
- Satellites captured a visual smoke plume transported to the northeastern US, which was also associated with satellite-retrieved CO, both of which were tracked from the Quebec area.

Several analysis methods were used to develop a weight-of-evidence demonstration that the 8-hour ozone concentrations above 70 ppb in the June 29, 2023 event meet the rules for data exclusion as an Exceptional Event. Satellite, meteorological data, trajectory analysis, and emissions data were used to assess whether conditions were favorable for the transport of smoke from the Quebec, Canada wildfires to monitors that showed 8-hour ozone concentrations above 70 ppb. The data also showed that the transported smoke degraded air quality northwest (upstream) of the District first, then this photochemically aging airmass was transported eastward, creating a prolonged period (June 27-30) of enhanced ozone from the Great Lakes eastward to the East Coast, including the District.

Substantial changes in chemistry in the eastern United States due to regional NOx emissions reductions have occurred over the last two decades. The following analysis puts the 8-hour ozone concentrations in the District during this ozone event in the context of these reductions and in comparison to ozone in previous months of June. A comparison of emissions during late June of 2023 shows that aggregate Electric Generating Unit (EGU) NOx emissions were lower than any other year on record during the smoke event. Yet, ozone concentrations in June of 2023 exceeded ozone concentrations in earlier years during meteorology less conducive (cooler, less sunlight reaching the surface) compared to years under heavier anthropogenic precursor emissions. Analysis of the airmass associated with the District's ozone exceedances on June 29, 2023, revealed a composition characteristic of wildfires, with an abundance of ozone precursors despite substantial reductions in anthropogenic sources.

DOEE's analysis strongly supports that both the MD8AO concentrations above 70 ppb in the District on June 29, 2023, meet the rules as an Exceptional Event, and both monitors and their corresponding MD8AO observations in Table 2 should be excluded from DV calculations.

The following documentation justifies these claims and is outlined as follows:

- Section 2 contains a conceptual model overview of the event, including a synopsis of the meteorological and air quality conditions, emissions, transport, and characteristics defining the event.
- Section 3 demonstrates a clear causal relationship between the exceedance via a tiered, weight-of-evidence approach.

- Section 4 demonstrates that this event fulfills the definition of a natural event that is unlikely to recur.
- Section 5 fulfills the requirements that demonstrate the event was not reasonably controllable or preventable.
- Section 6 documents the public comment process.
- Section 7 summarizes and concludes the analysis.

2.0 Conceptual Model and Overview of the June 26-30, 2023, Smoke and Ozone Event

2.1 District of Columbia Area Description

As part of the Clean Air Act (CAA), both local and state air quality agencies are required to maintain and operate ambient air quality monitoring networks. The Air Monitoring Branch (AMB) in DOEE's Air Quality Division (AQD) operates, maintains, and performs all functions of the ambient air monitoring program required by the CAA. As required by federal air monitoring regulations, the District's monitoring network is designed to study expected high pollutant concentrations, high population density, significant sources, general background concentrations, and regional transport. The District's network currently consists of five monitoring sites. DOEE is proposing to add a new monitoring station in an overburdened environmental justice community in 2024.

Sampling covers criteria air pollutants, $PM_{2.5}$ mass and chemical speciation, and enhanced monitoring for ozone and its precursor pollutants with a photochemical assessment monitoring station (PAMS) for measuring speciated VOCs, NO_x, carbonyls, air toxics, and surface and meteorological parameters. A full description of the various instrumentation used by DOEE is available in the DOEE Ambient Air Monitoring Plan.

The District of Columbia is an urban area with a geographic area of 68.3 square miles. It has an estimated population of 671,803 as of 2022, according to the US Census Bureau. The District of Columbia is surrounded by Northern Virginia on its southwest side and Maryland on its southeast, northeast, and northwest sides. The Washington, DC-MD-VA ozone nonattainment area comprises the District of Columbia, five counties in Maryland, four counties in Virginia, and five independent cities in Virginia, as shown in Figure 3. This figure also shows the location of the 14 air quality monitors used in determining compliance with the ozone NAAQS.

Figure 3: Metropolitan Washington 8-hour Ozone Nonattainment Region (Washington, DC-MD-VA).

2.2 Characteristics of Typical, Non-Event Ozone Formation

In the absence of atypical air mass composition (for instance, extraordinary events or smoke plumes), the primary mechanism driving ozone formation in the District stems from the photolysis of volatile organic compounds (VOCs) and a combination of regionally and locally originated anthropogenic NO_x. This interplay is often accentuated by the densely populated areas and topographical features, leading to concentrated regions that historically have caused ozone-related challenges, particularly to the northeast of the District.

The key contributors to these challenges are human-made emissions from various sources: fixed point sources such as EGUs, mobile sources like cars, trucks, boats, locomotives, and non-road equipment, and area sources encompassing industrial processes and consumer goods. The predominant share of locally generated NO_x, a precursor to ozone, originates from urban pollution plumes that form along the I-95 corridor between the District and Baltimore, along with surrounding point sources, like EGUs. Nonetheless, these emissions alone frequently fall short of generating ozone concentrations exceeding 70 ppb in the District as measured by the MD8AO standard. Photochemical modeling underscores the argument that, excluding instances of light winds and recirculation that result in the accumulation of local emissions, the emissions from EGUs and mobile sources within the District are insufficient to

cause ozone levels to surpass regulatory thresholds. However, the District also lies at the downstream end of the EGU-rich Ohio River Valley, where a large density of EGU point sources generates a regional NO_x plume upstream, transporting NO_x and/or ozone into the District. Historical instances of ozone exceedances in the District are predominantly associated with this kind of transport phenomenon. Hence, the influx of ozone and ozone precursors, notably NO_x, within the residual layer (the layer of air immediately above the surface, typically situated around 500-2,000 meters above ground level) that enters the District through transport contributes to elevating local ozone levels, often surpassing NAAQS thresholds. In the absence of substantial transport, the District has experienced a reduction in widespread or frequent ozone exceedances of NAAQS standards.

Over the past five years, the District has experienced a dearth of pollution transport cases. From 2019 to 2023, the concentration of ozone and its precursors in the residual layer has reached its lowest recorded levels. This reduction has led to a decrease in the maximum daily ozone concentration in the District, resulting in a decline in the frequency of ozone exceedance days. Consequently, local factors such as meteorology and emissions, which used to be overshadowed by regional signals, have gained more significance. This has led to isolated and infrequent exceedances, as illustrated in Figure 4. Emissions of NO_x from point sources in states upstream of and including the District (such as Maryland, Virginia, West Virginia, Pennsylvania, Ohio, and Indiana, represented as "Total NO_x" in Figure 4) during the ozone season have reached historically low levels. In fact, the total 2023 emissions in these upwind states were the lowest ever recorded.

This decline has been consistent monthly throughout the season, resulting in a significant regional reduction of almost 50% over the past five years, as shown in Figure 4. NO_x emissions from mobile sources have also decreased during the same period. However, this reduction is overshadowed by the substantial decrease in EGU-related NO_x emissions. It is important to note that while mobile-source NO_x has decreased less compared to EGU-related NO_x, the current emissions from mobile sources in the District, even when combined with additional local EGU emissions, are insufficient to cause anything but isolated and infrequent ozone exceedance days within the state.

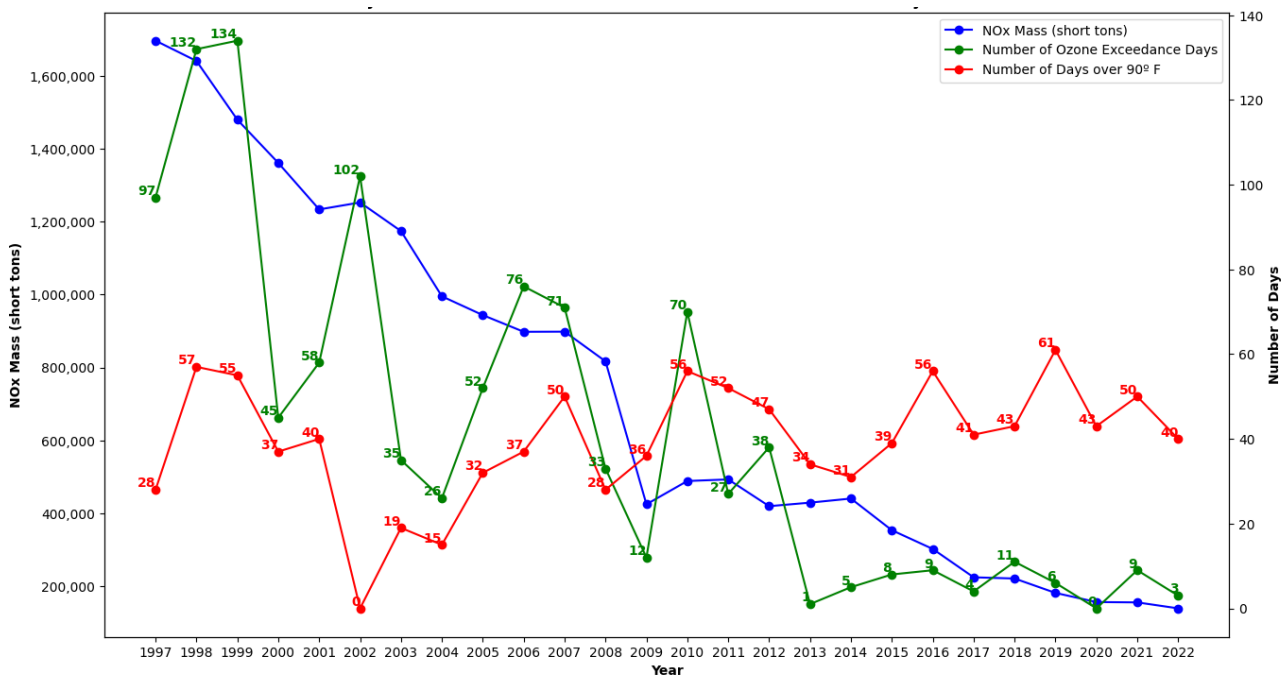

Figure 4: Annual EGU NO_x from the District of Columbia and upwind states, number of days at or above 90°F at National Arboretum (90 DD), and exceedance days at various standards.

2.2.1 Emissions Trends

In the context of a standard scenario involving a District ozone exceedance day, as described earlier, the primary source of NO_x transport into the state stems from upwind EGU point sources. These source emissions can result in elevated ozone concentrations the next day, which compounds the local emissions issue. The Clean Air Markets Database (CAMD) records the NO_x emissions originating from EGU point sources across the nation. Over the past 15-20 years, there have been notable and sustained reductions in NO_x emissions throughout the eastern United States, as illustrated in Figure 3. In 2023, the cumulative NO_x emissions from upstream states had dwindled to a mere 20% of their 2010 levels, marking a substantial decrease of approximately 80%. Regulatory ozone season in the District of Columbia is March 1st through October 31st. This analysis focuses on the months of May through September. Figure 5 depicts the collective monthly total NO_x emissions from May to September 2023. These were the lowest recorded values ever from upwind states, including Indiana, Ohio, West Virginia, Virginia, Pennsylvania, and Maryland. These states together constitute a significant source region for ozone or ozone precursors transported into the District during typical summer conditions of favorable meteorology. In June 2023, NO_x emissions from these areas were approximately 15% of what was observed in 2010.

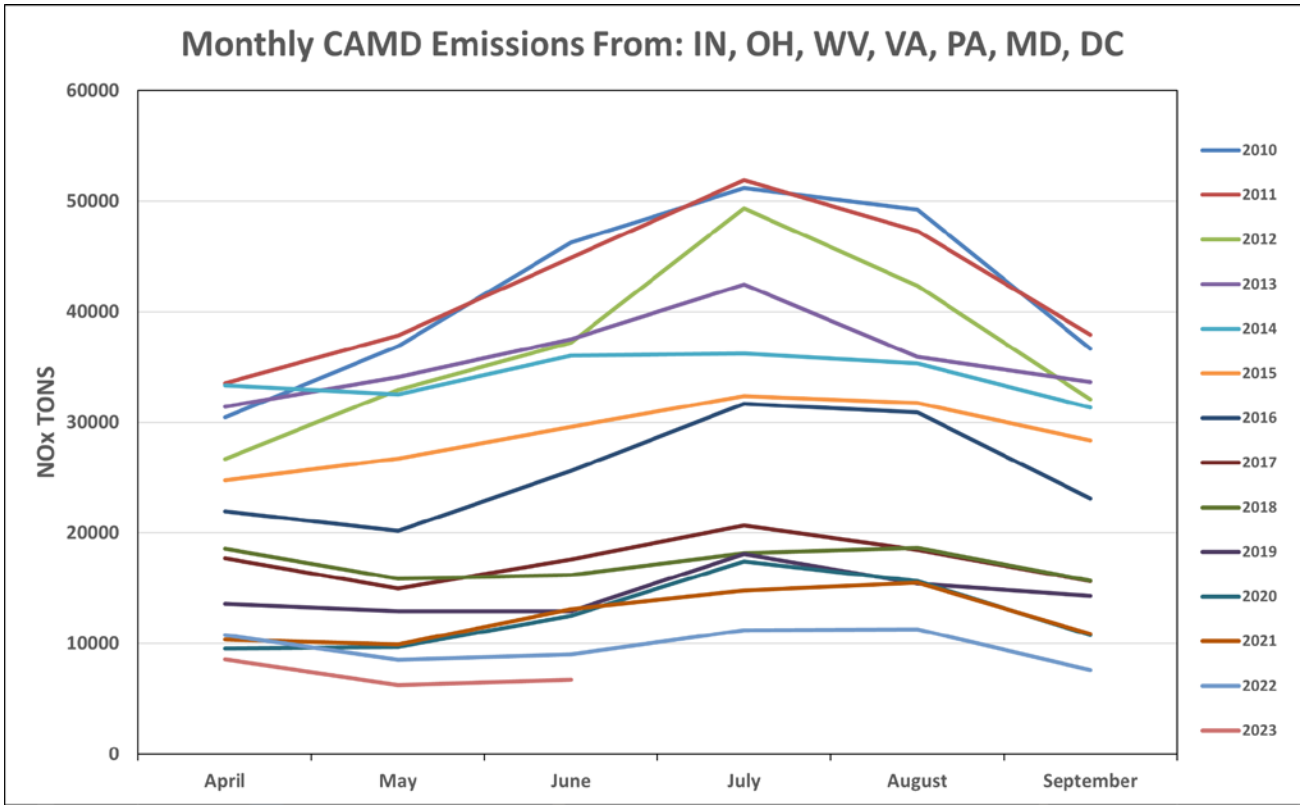

Figure 5: Monthly NO_x-aggregated from the group of upwind states, including the District by Month of ozone season.

The daily emissions data for these same states reflects identical reductions. When we examine the daily combined NO_x emissions from Indiana, Ohio, West Virginia, Virginia, Pennsylvania, Maryland, and the District of Columbia, focusing solely on the month of June from 2017 to 2023 as extracted from CAMD, it becomes evident that the total emissions in June 2023 reached an all-time low (indicated by the black line in Figure 6). A steady downward trend is observed. Despite these historically low emissions in June 2023, the District experienced one of the worst air quality days in over ten years (June 29th, 2023), with two of the District's three ozone monitors exceeding the daily maximum 8-hour ozone standard of 70 parts per billion (ppb) (as represented by the green bars in Figure 6).

Aggregate NO_x emissions from EGU point sources for states upwind of the District (Indiana, Ohio, Pennsylvania, West Virginia, Virginia, DC, and Maryland) from the CAMD database for 2017 – 2023 are shown with the blue points. The maximum 8-hour average ozone at any monitor in the District for each day in June 2017-2023 (orange bars) and the number of monitors exceeding 70 ppb in the District (green bars) is also shown. A downward trend in emissions is noticeable throughout the period, with the lowest emissions in 2023. An increase in NO_x emissions towards the end of June 2023 is apparent, but the increase only matches the mean of the 2022 season, which was the lowest year up to that point.

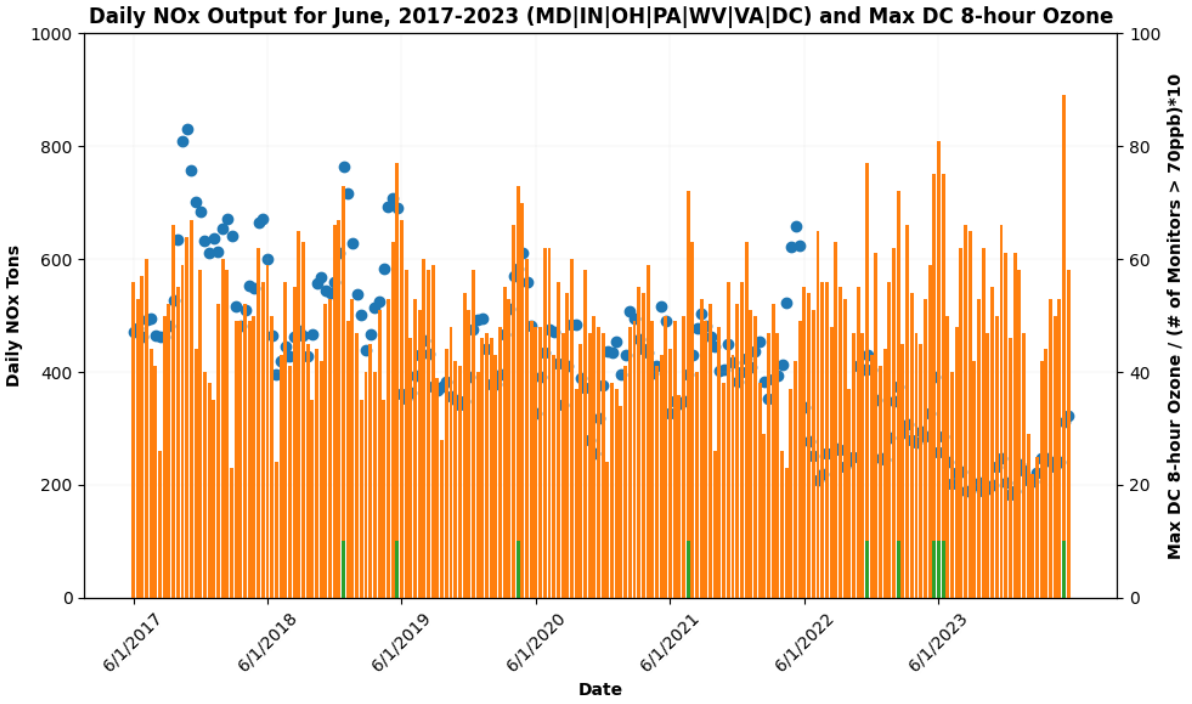

Figure 6: Daily aggregate NO_x, maximum DC ozone, and monitors exceeding 70 ppb in May 2017-2023.

2.2.2 Ozone Production in the District

Research has found that the generation of ozone in the District involves a complex interplay between volatile organic compounds (VOCs) and nitrogen oxides (NO_x), and the atmospheric balance of each required to produce bi-products like ozone. In the past, the balance between these two precursor groups was insignificant compared to their absolute atmospheric concentrations. Both precursors were consistently abundant for ozone exceedances and were primarily influenced by weather conditions. For instance, the fluctuations in exceedances depicted in Figure 4 at the 70 parts per billion (ppb) level strongly correlate with the number of days reaching 90° Fahrenheit between 2000 and 2015. However, in more recent years, this correlation has diminished. The District has now transitioned into a NO_x-limited regime due to regional reductions in NO_x emissions (Roberts, et al., 2022). Consequently, the stoichiometry of ozone production is no longer in equilibrium, and daily ozone production depends on the availability of either precursor group and/or the quantity of ozone already formed upstream and transported into the state. As a secondary consequence, high temperatures are no longer a dependable predictor of daily ozone exceedances of the NAAQS.

Ozone production hinges on the availability of NO_x, and VOCs, as well as favorable meteorological conditions of ample heat and sunlight. In the District, the VOCs relevant to ozone production encompass both naturally occurring and human-made sources. Although there has been a noticeable reduction in anthropogenic VOCs in tandem with the decrease in NO_x emissions, it's crucial to acknowledge that daily ozone production driven by biogenic (naturally occurring) VOCs cannot be controlled and remains a significant contributor to ozone chemistry in the District. For example,

isoprene, a naturally occurring VOC, has the highest maximum incremental reactivity (i.e., easily makes more ozone) of VOCs tested in the District, and is the highest VOC contributor on high ozone days. Isoprene is emitted by the biosphere, particularly trees, in response to environmental stressors such as elevated temperatures. Due to increased energy demand, NOx emissions from stationary sources also tend to rise on warm summer days. In contrast, mobile emissions exhibit relative consistency on workdays and diminish over the weekend, unaffected by temperature. Simultaneously, as NO_x output rises relative to temperature, biogenic VOCs are released into the local environment. When exposed to sunlight and heat, these biogenic VOCs facilitate the creation of local ozone. When this locally generated ozone and ozone precursors mix with those transported into the state, the District observes MD8AO above 70 ppb and exhibits its fundamental non-event ozone exceedance. In this NO_x-constrained environment, absent additional transported ozone or ozone precursors, the District's local emissions are insufficient to produce ozone exceedance days.

2.2.3 Weather Patterns Leading to Ozone Formation

The District experiences variable meteorological conditions during the summer. While occasional April days may witness ozone levels surpassing standard limits, many occur mainly from May to September. Changing weather conditions within the ozone season result in diverse meteorological patterns that favor ozone formation. These include lee-side troughing (where downward air movements on the lee side of the Appalachian Mountains create a zone of pollutant convergence along the I-95 corridor). Other such meteorological patterns or processes include airmass and ozone transport and mixing, as well as local recirculation and stagnation, including reverse I-95 corridor flow from the northeast. On the local scale, meteorological factors on which ozone concentrations depend are the amount of available sunlight (ultraviolet range), temperature, and the amount of space (volume) in which precursor emissions mix. Sunlight drives the critical photochemical reactions for ozone and its key precursors, and the emissions rates of many precursors (isoprene, for example) are temperature dependent (Ryan and Dickerson, 2000, p2-1).

Ozone production within each pattern depends on favorable local weather conditions, such as warm, sunny days with light to moderate surface winds. The positioning of the Bermuda High ultimately dictates which of these scenarios prevails. During an average summer, the Bermuda High is positioned off the southeast Atlantic coast of the United States, resulting in westerly transport of air towards the District, varying in direction depending on altitude. This creates conditions favorable for cross-Appalachian flow. Lee-side troughing relies on weak cross-mountain flow, creating compressional heating and column stretching on the mountains' lee side, often aligning with the I-95 corridor and leading to increased ozone concentration. Both transport and lee troughing can occur simultaneously or independently. In the presence of downward mixing of transported ozone, lee troughing may lead to ozone exceedance days. Over several days, recirculation and stagnation can also elevate local pollution concentrations, exceeding NAAQS levels. These patterns are most likely to occur during the summer months of June through August, historically the peak period for ozone production in the District. Shoulder seasons, like Spring and Fall, are typically cooler, with active weather patterns that prevent the buildup of local or regional emissions. Winter, on the other hand, is too cold for ozone exceedances.

As temperatures rise, there is an increase in the release of super-regional NO_x emissions from power plants located upstream, such as those in the Ohio River Valley and western Pennsylvania. This elevated output leads to higher concentrations of ozone and ozone precursor compounds in the residual atmospheric layer. Over time, these substances mix down and blend with locally sourced pollutants, contributing to instances of ozone exceedances in the District.

2.3 Exceptional Event Description: June 2023 Quebec Fires

Abnormally warm and dry conditions during the winter and early spring of 2023 set the stage for a record Canadian wildfire season. North American snow cover in May was the lowest it has ever been since measurements began being taken in 1966 (over 55 years) (see Figure 7). The little amount of snow that fell across Quebec melted sooner, exposing fire fuels sooner than typical. The Canadian wildfire season typically runs from May through October, peaking in July. However, with snowpack far less than average, wildfires across Canada started considerably earlier, with seasonal fires being detected as early as March.

Numerous wildfires sparked by lightning broke out across Quebec beginning in early June. Fires burned out of control for the entire month as surges of smoke poured from hundreds of large source regions. Firefighters from as far as Spain, Portugal, and France assisted local teams in battling the flames. In late June, a resurgence of the fire brought on by favorable meteorology led to an extremely rapid uptick in the area burned and associated smoke (Figure 8). Figure 8 depicts accumulated hectares burned reported by the Canadian Wildland Fire Information System (CWFIS) daily over the last ten years. The burn area is estimated by satellite. There was a burn area increase equivalent to the size of Connecticut between June 21 and June 26, 2023, leading to an increase in emissions in that time period. The area circled highlights the late June period of intense burning across Quebec.

Burning across Canada in 2023 is unprecedented compared to any recent year. Between June 21st and 26th, nearly 1.7 million hectares (4.2 million acres) of land burned across the Quebec province, a burn area larger than the size of Connecticut (circled area in Figure 8). Smoke from this period stretched as far as Europe, a distance of over 3000 miles.[i] Hundreds of fires were analyzed by the NOAA Daily Hazard Mapping System (HMS) smoke analyses (McNamara, et al., 2004) in Quebec over this timeframe (Figure 8). Fires and associated smoke plumes analyzed by HMS were derived from the GOES Imager, the POES AVHRR, MODIS satellites, and expert subjective analysis. The analysis for the remaining demonstration will focus on the emissions from the late June Quebec fires alone, which were extremely large, long-lasting, and produced prolific smoke (Figure 9 and Figure 10).

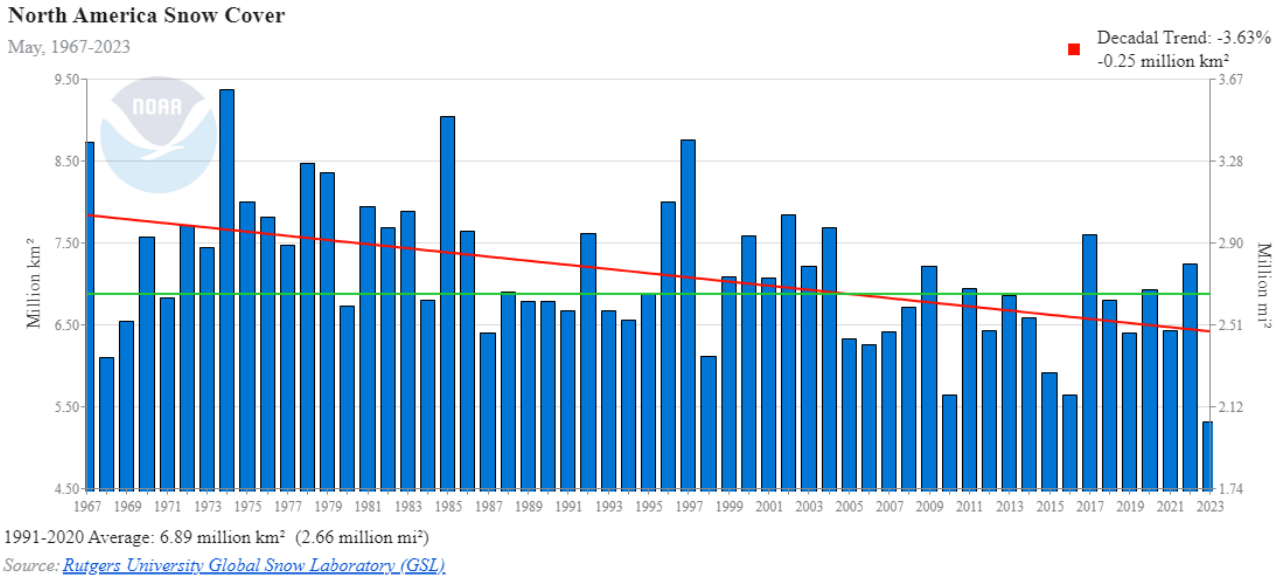

Figure 7: North American Snow Cover (Millions km^2) each May between 1967 and 2023. Average line in green and decadal trend line in red.

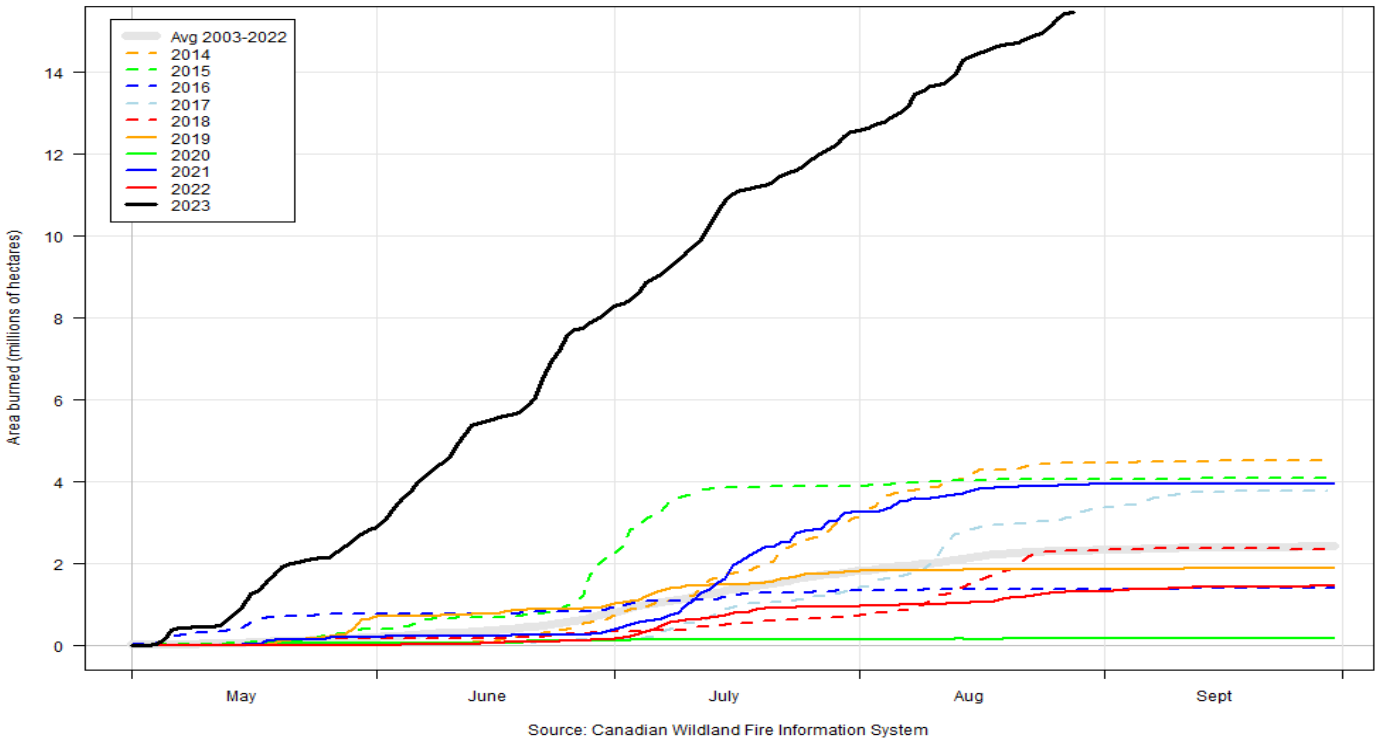

Figure 8: Cumulative hectares burned reported by the Canadian Wildland Fire Information System (CWFIS) by day over the last ten years. The burn area is estimated by satellite.

Figure 9a: June 2023 Quebec Wildfire.
Image showing wildfire and associated smoke at Lebel-sur-Quevillon in Quebec, Canada, on June 23, 2023. One of over 100 fires burning across the Quebec province at the time[ii].

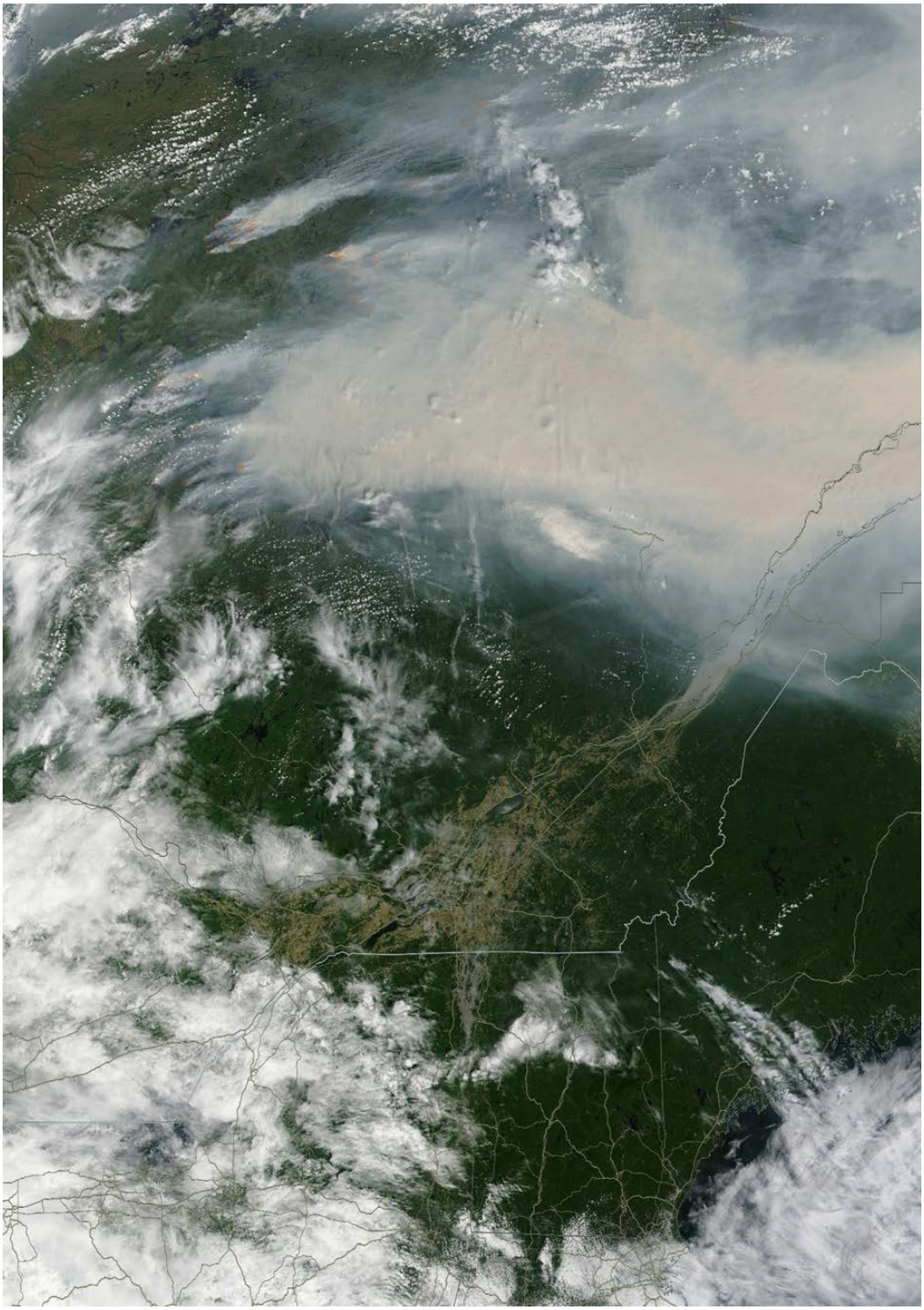

Figure 10: June 23, 2023, Terra/MODIS Corrected Reflectance with overlaid Terra/MODIS Fires and Thermal Anomalies

Source: https://wvs.earthdata.nasa.gov/

2.4 Conceptual Model of Ozone Formation from June 2023 Quebec Fires

2.4.1 Overview and Literature Review

Wildfires are known sources of emissions responsible for both primary and secondary pollutants, including CO, PM2.5, NOx, VOCs, as well as ozone (Andreae and Merlet, 2001; McKeen et al., 2002; Bytnerowicz et al., 2010). Similar to the study presented here, Canadian wildfires have increased ozone concentrations in Houston, TX (Morris et al., 2006) and as far away as Europe (Spichtinger et al., 2001). Evidence of Canadian wildfire smoke and biomass burning affecting the Mid-Atlantic's particulate matter (PM) air quality was also previously reported (Adam et al., 2004; Colarco et al., 2004; Sapkota et al., 2005; Dreessen et al., 2016) but wildfire smoke has also been recognized in high-ozone events on the East Coast (Fiore et al., 2014). DeBell et al., (2004) presented a chemical characterization of the July 2002 Quebec wildfire smoke plume and its impact on atmospheric chemistry in the northeastern United States. More recently, Dreessen et. al., (2016) presented a case where a Saskatchewan, Canada wildfire smoke plume amplified ozone in Maryland in June of 2015.

While historically infrequent in the Mid-Atlantic, wildfire smoke has been an increasing fractional contribution to high-ozone exceedance days, particularly in light of increased fire frequency in a warming climate (Flannigan and Wagner, 1991; Marlon et al., 2009; Westerling et al., 2006; Spracklen et al., 2009; Pechony and Shindell, 2010), decreasing regional NOx emissions (Gégo, et al., 2007) and tighter ozone NAAQS (https://www.epa.gov/ground-level-ozone-pollution).

2.4.2 Ozone Generation from the Fire

Wildfires generate precursors that may directly lead to ozone formation or indirectly foster ozone through atmospheric composition that disproportionately generates ozone when impacted by anthropogenic precursors. Dreessen et al. (2016) previously showed that smoke plumes from Central Canada are capable of transporting ozone to the Mid-Atlantic and causing NAAQS exceedances, even in the contemporaneously low NO_x emission environment. As in the June 2015 ozone case covered in Dreessen et al. (2016), the June 2023 ozone events across the Northeast and Mid-Atlantic U.S. were characterized by smoke plumes associated with ozone, increasing in concentration as the smoke plume aged.

During the late June 2023 Quebec wildfire event, ozone was transported into the District after being produced in a modified airmass upstream of the District. Furthermore, active chemistry within the plume exacerbated any local de minimis emission contributions (in relation to the plume concentrations) to foster rapid ozone chemistry. In other words, in addition to 'already formed ozone' transported in the smoke, chemistry in the smoke enhanced local ozone production beyond expected concentration outcomes. In the 2015 case study examined by Dreessen et al. (2016), it was hypothesized that once the smoke-sourced VOC-rich plume interacted with anthropogenic NO_x sources, that copious ozone production began, which was capable of being transported long distances as either ozone or within ozone reservoir species. Dreessen et al. (2016) also acknowledged NO_x

contribution from the fire itself, though focused on the plume's interaction with anthropogenic sources. In that 2015 study, smoke subsided across the eastern Midwest and northern Mid-Atlantic and took over 24 hours of aging before ozone above 70 ppb was widespread across the region. This delay in ozone production while the airmass aged is consistent with previous studies such as Putero et al. (2014), which observed the largest increases in ozone from fires five days (120 hours) after the initial pollutants were emitted from the fire (Figure 10).

In the current June 29 case, the smoke generated by the worst burn period on June 22 was already seven days old when it reached the District. While sufficient NO_x and VOCs were generated by the Quebec fires in late June 2023 for 'primary' ozone concentrations already at exceedance levels, as the plume aged and mixed with anthropogenic NO_x (albeit the lowest NO_x on record), ozone concentrations were augmented to and above levels exceeding the NAAQS not possible without the smoke.

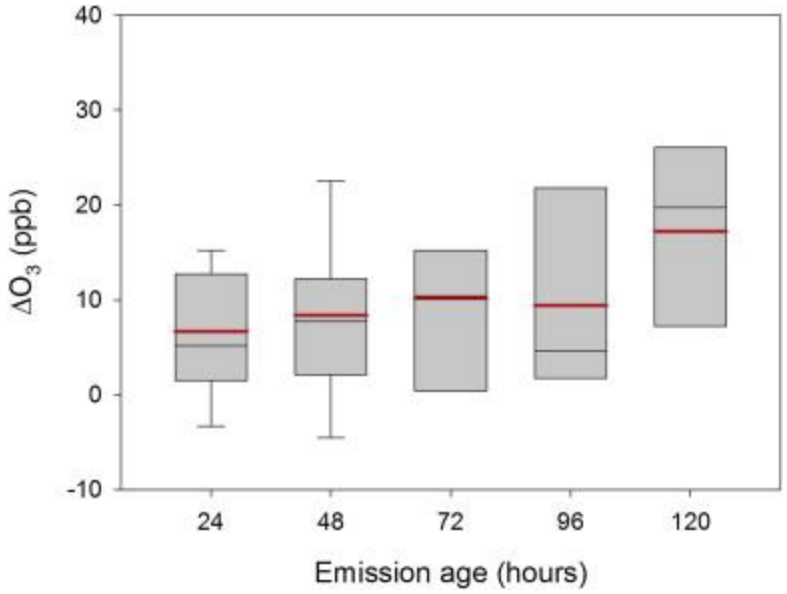

Figure 11: Ozone enhancement with smoke plume age.
(from Putero et al. (2014), Figure 7)

Fires were ongoing across Quebec for the entire month of June 2023, starting with lightning strikes on June 1. Prior to the June 29 event impacting the District, copious smoke had filtered across the upper Midwest and Great Lakes, creating widespread $PM_{2.5}$ and ozone exceedances there due to smoke from Quebec. While exceedances existed there prior to June 21, we consider that date an evidential beginning that the relevant burn period and area produced 'primary' ozone which eventually impacted the District. Meteorological conditions fostered intense fire growth beginning June 19, peaking on June 22 for the newly burned area. Relatively stagnant transport and poor boundary layer ventilation across Quebec from June 21 through June 24 fumigated a vast region of Quebec, with $PM_{2.5}$ concentrations exceeding 500 AQI (250 $\mu g/m^{-3}$) at some locations across Quebec. This smoke then made its way southward, curling counter-clockwise towards Maryland by June 28/29. As such, most of the smoke

reaching the District may have been older than five days. Prior to that time, MD8AO across northern Illinois and Indiana, Michigan, and Wisconsin were greater than 70 ppb with temperatures in the upper 70s to mid-80s. By June 27, locations in Illinois and Indiana remained in the upper 70s yet exceeded the ozone standard as the thickest smoke plume from the burn period reached the Midwest and lower Ohio River Valley. Ozone concentrations further worsened on June 28 as the smoke plume curled eastward, with widespread unhealthy for sensitive groups (USG) conditions and several locations in the unhealthy AQI range for MD8AO. These highest locations were typically downwind of urban centers, showing how readily the smoke augmented ozone production where 'new' NO_x was available. Thus, high ozone concentrations were transported into the District, which, while similar in nature, were not associated with the historical, conceptual, non-exceptional-event-type transport pattern. The path, residency, and meteorological setup of the smoke plume indicate a dispersing smoke plume conducive to ozone transported from Canada, pushing through the upper Midwest and Great Lakes, then moving into the Mid-Atlantic and Northeast states of the US.

While ozone exceedance days in late June in the District are not unusual due to peak sun angle, length of day, and associated increased seasonal temperatures, the magnitude and spatial scale of the June 29, 2023 exceedance were beyond contemporary norms. Meteorological conditions and emissions in the District on June 29, 2023, were insufficient to cause the large spatial scale, multi-day, and intense magnitude exceedance event without additional wildfire-related ozone precursor emissions.

Historical comparisons during the month of June show ozone concentrations and the number of monitors exceeding the standard at these magnitudes are rare (reference Figure 5), even rarer considering massive emissions reductions evident during that time period across the entire eastern US. Thus, it is unlikely that such a widespread area exceeding the standard would have occurred without additional supportive atmospheric chemistry from the wildfire smoke.

2.4.3 Meteorological Conditions Driving Smoke and Ozone Transport

2.4.3.1 Conceptual Model Overview

A generalized omega-like pattern existed for much of June across the North American continent. Apart from the earlier June smoke episode, transient mid-latitude cyclones (MLCs) kept smoke confined to northern US states and Quebec and/or in relatively diffuse concentrations for the middle portion of June. High pressure and dry weather generally persisted over the Quebec fire region through the month of June, allowing fires to continue unabated. An intense burn period beginning around June 19-20 burned an area the size of Connecticut in about five days (Figure 12). During this burning, stagnation existed over Quebec, allowing smoke to accumulate to concentrations over parts of southern Quebec, which exceeded the EPA AQI scale with a maximum 24-hour average concentration of 593 $\mu g/m^{-3}$, achieved on June 25. Around June 26, a disturbance along the US/Canadian border broke down this persistent pattern, opening transport from Quebec to the Mid-Atlantic. This passing MLC 'pin-wheeled' the smoke southward. Winds were not excessive, and the smoke took several days to move from Quebec to the District. Ridging and developing surface high pressure in the wake of the departing MLC pushed and kept smoke towards the surface as it moved southward. By June 29, the densest smoke mixed down to the surface layer in the District, raising fine particle concentrations in excess of 100

$\mu g/m^{-3}$ district-wide. Under the center of high pressure, the surface smoke was stagnant on June 29, with intense concentrations persisting throughout the day. Despite intense solar attenuation, abundant to extreme ozone concentrations were realized locally in the District as a combination of transport from upstream and local generation beyond typical in the contemporary Washington, DC area atmosphere. As surface high pressure departed on June 30, west and southwesterly winds above the planetary boundary layer (associated with the trough that created the surface high pressure), along with a mesoscale convective system (line of storms), relieved the burden of smoke across the region from west to east.

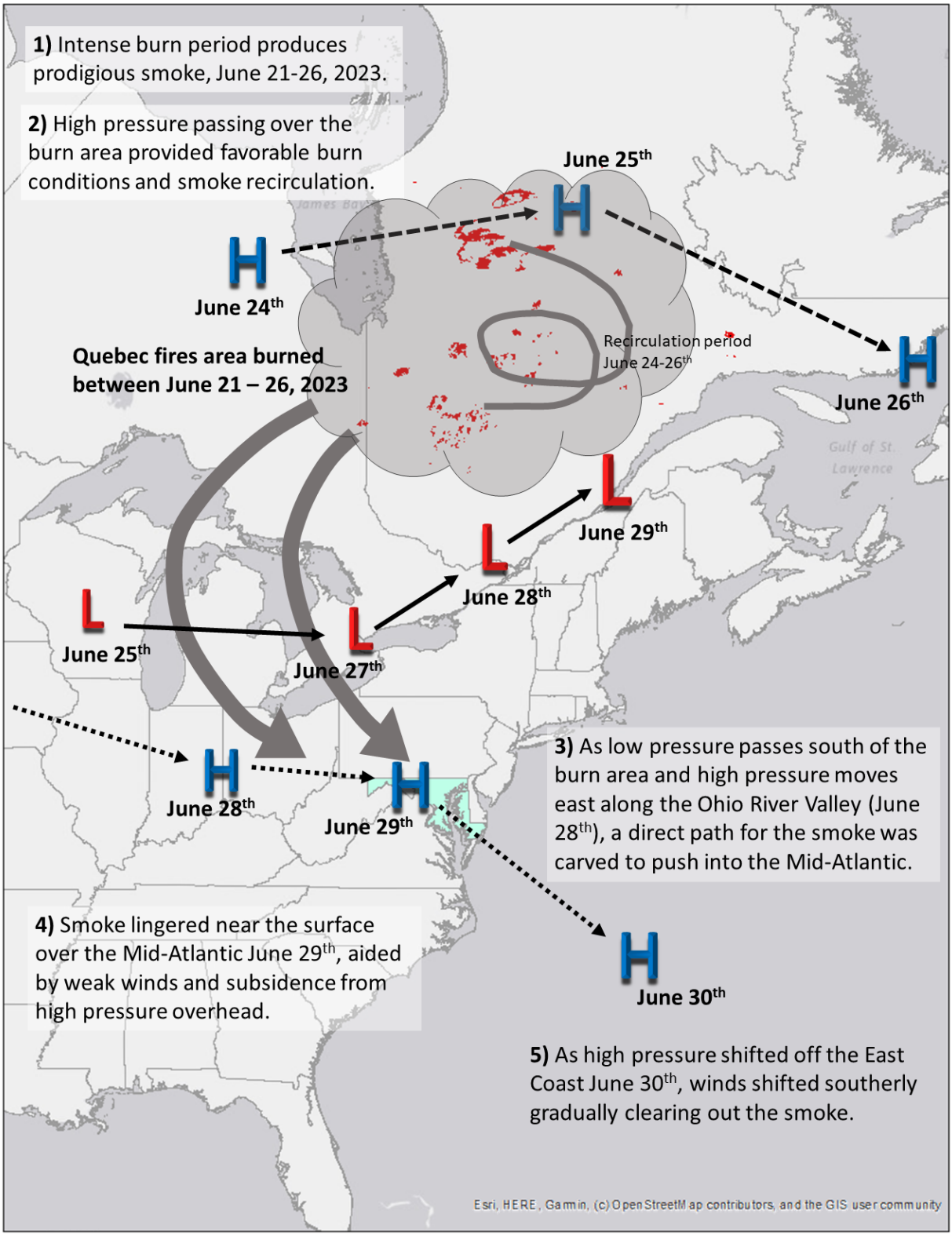

Figure 12: A simplified, illustrated conceptual model of the June 29, 2023, wildfire-influenced ozone event.

2.4.3.2 Upper-Level Pattern Overview

The 850 mb level (approximately 1500m above sea level) sits near the top of the planetary boundary layer, the atmospheric layer in which ozone pertinent to surface observations and human health develops. The 850 mb height level can serve as a guide for the transport of pollutants. The analysis of this atmospheric level is given for June 21-30 in Figures 12-15. Initially, the ridge of high pressure ("H" in the figures) was located directly over the wildfire area across central Quebec. Fires that had been burning over the entire course of the month were provided a resurgence period under the dome of high pressure. Meanwhile, a weak low pressure ("L" in the figures) over the Southeastern US gradually began to lift north and east over the next two days. A concurrent easterly flow over the Washington, DC, region turned southwesterly as the low-pressure system initially over the Southeastern US passed to the west (Figures 12a and 12b). This brought clouds and unsettled weather, unfavorable for ozone production through June 23.

By June 24, the high pressure, which was initially over the fire region, shifted north and out of the frame (Figure 12c) as the low-pressure system passed to the District, weakening in the process. A reasonably strong temperature gradient is noted around and just south of the central burn regions. This frontal boundary acted as a barrier, keeping the bulk of the clouds and precipitation associated with the low-pressure system from reaching the burn regions. Meanwhile, a secondary low-pressure system began to intensify over the Northern Plains. Between June 25 and 26 (Figure 13a and 13b), the Northern Plains low intensifies as it becomes cut off from the main synoptic scale flow, gradually shifting towards the Great Lakes. A weak ridge of high pressure tracks west to east over the burn region of central Quebec, providing another period of intense burning and smoke recirculation. Ridges of high pressure are associated with subsidence (sinking vertical motions) that brings air toward the surface. Air that resides or subsides under the ridge tends to remain since near-surface winds under the ridge are generally weak. This led to air mass persistence beneath the ridge, which occurred over central Quebec at this time.

By June 27, the cut-off low-pressure system, which is beginning to weaken, shifts to the District (Figure 13c). Ridging begins to build over the Central Plains over this same period. The circulation around these two systems provided a channel for the wildfire smoke to push south into the Great Lakes region. General subsidence around the outskirts of the low-pressure system, along with the subsidence associated with the ridging, helped to keep the smoke near the surface in the process. On June 28, the still weakening cut-off low-pressure system shifted far enough east that the smoke was able to wrap around and into the state (Figure 14a). Minimal change in the synoptic scale features and positioning on the 29 allowed for a continued stream of smoke into the state from the north and west (Figure 14b).

As the ridge of high pressure continued to weaken and move east on June 30 (Figure 14c), it essentially phased with the Bermuda High (a semi-permanent high-pressure area off the southeast coast of North America in the summer). As the ridge of high pressure and the Bermuda High phased and the weakening low continued its trek northeast, the transport winds turned to the southwest across Maryland. These winds began to remove the air mass that had settled across the area on June 28 and 29.

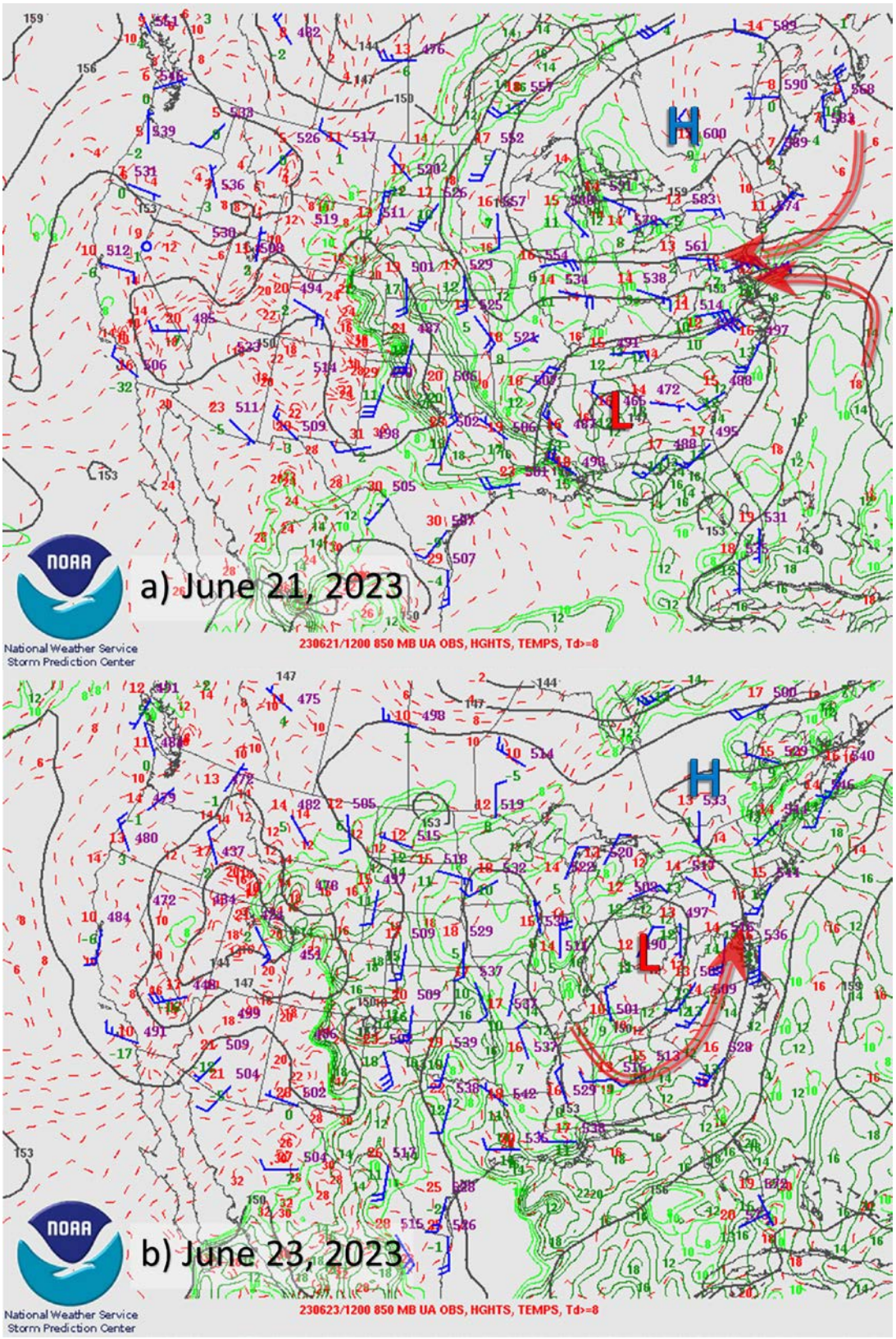
a) June 21, 2023
National Weather Service
Storm Prediction Center
230621/1200 850 MB UA OBS, HGHTS, TEMPS, Td>=8
b) June 23, 2023
National Weather Service
Storm Prediction Center
230623/1200 850 MB UA OBS, HGHTS, TEMPS, Td>=8

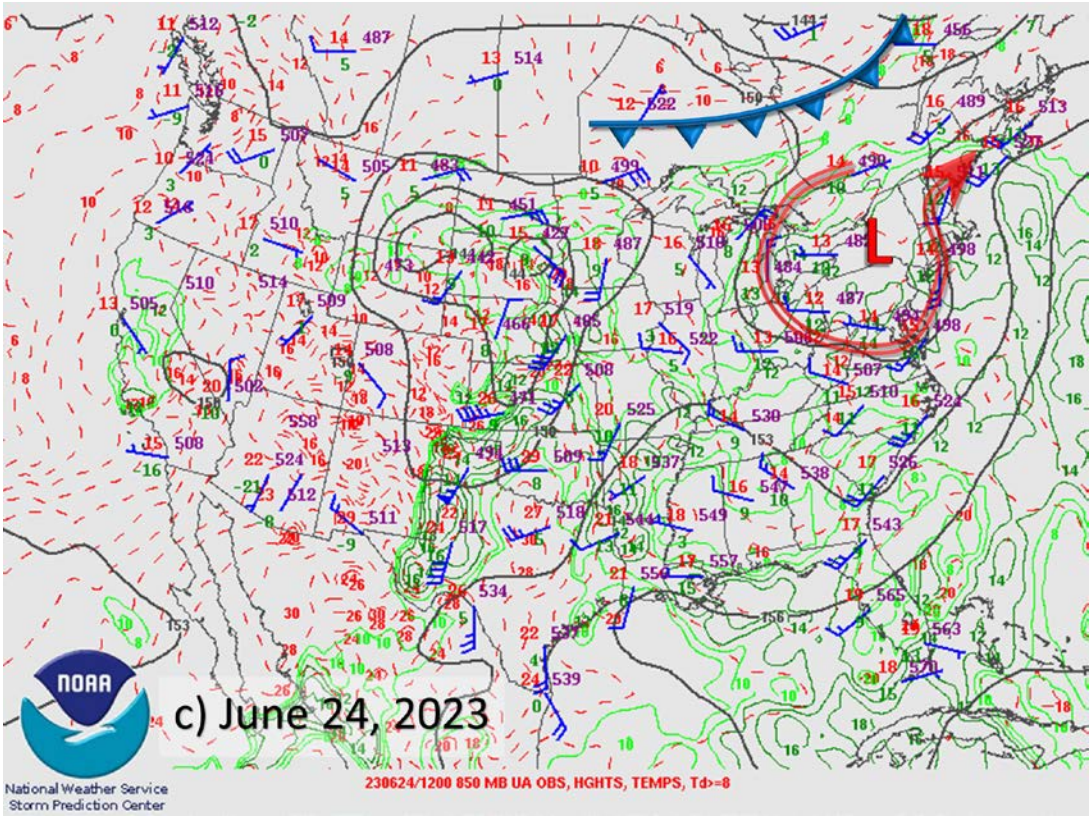

Figure 13: The 1200 UTC 850mb pattern for the CONUS on a) June 21, b) June 23, and c) June 24, 2023.

Red arrows show the general transport pattern. Capital letter "H" is high pressure, capital letter "L" is low pressure. Heights (black lines), temperatures (dashed red lines), dewpoint (green lines), and winds (blue barbs) are also analyzed. The frontal boundary location in Figure 12c is noted as a solid blue line with forward-facing triangles.

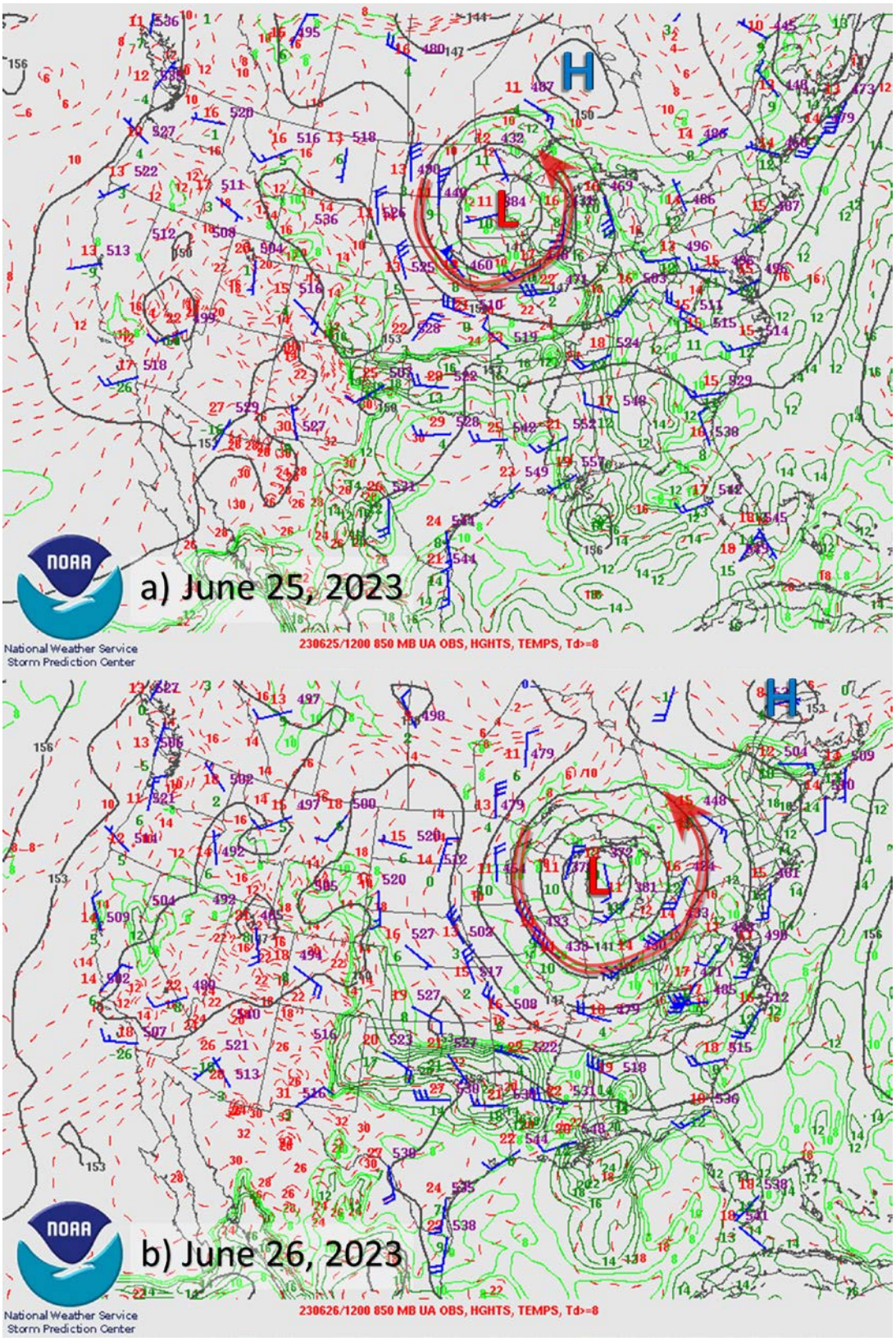
a) June 25, 2023
National Weather Service
Storm Prediction Center
230625/1200 850 MB UA OBS, HGHTS, TEMPS, Td>=8
b) June 26, 2023
National Weather Service
Storm Prediction Center
230626/1200 850 MB UA OBS, HGHTS, TEMPS, Td>=8

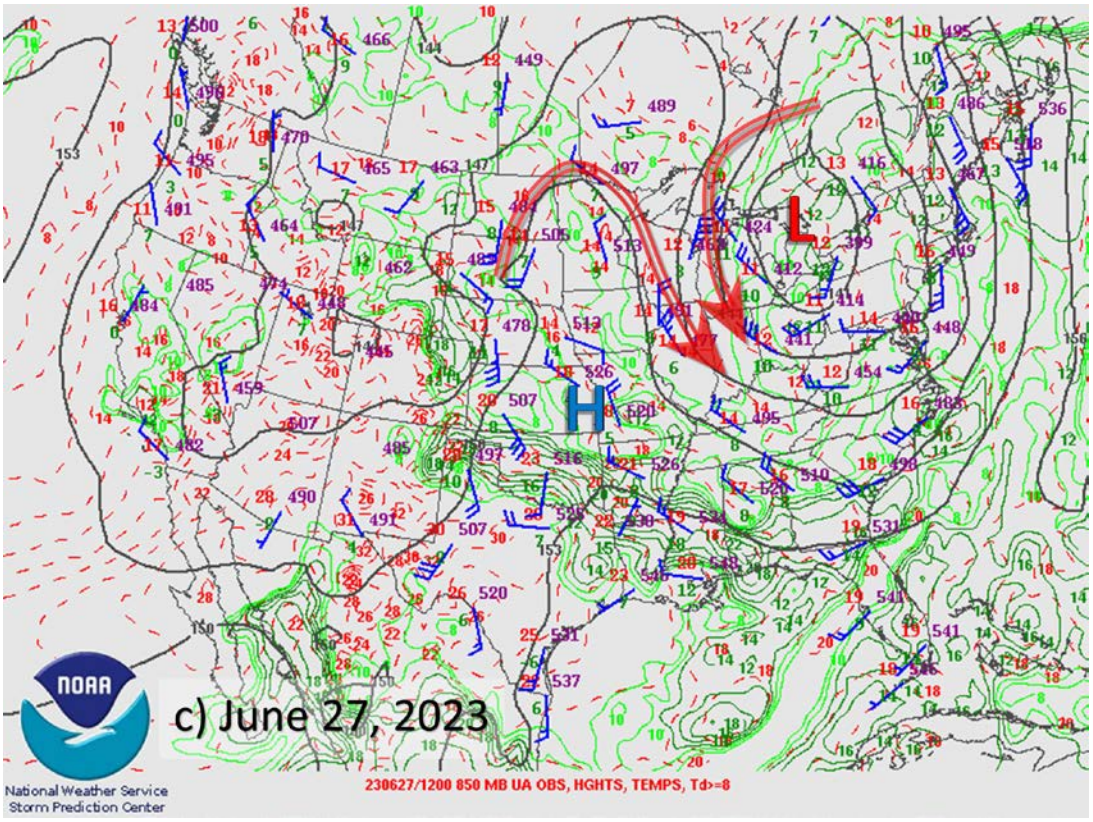

Figure 14: Figure 13, as in Figure 11, but for a) June 25, b) June 26, and c) June 27.

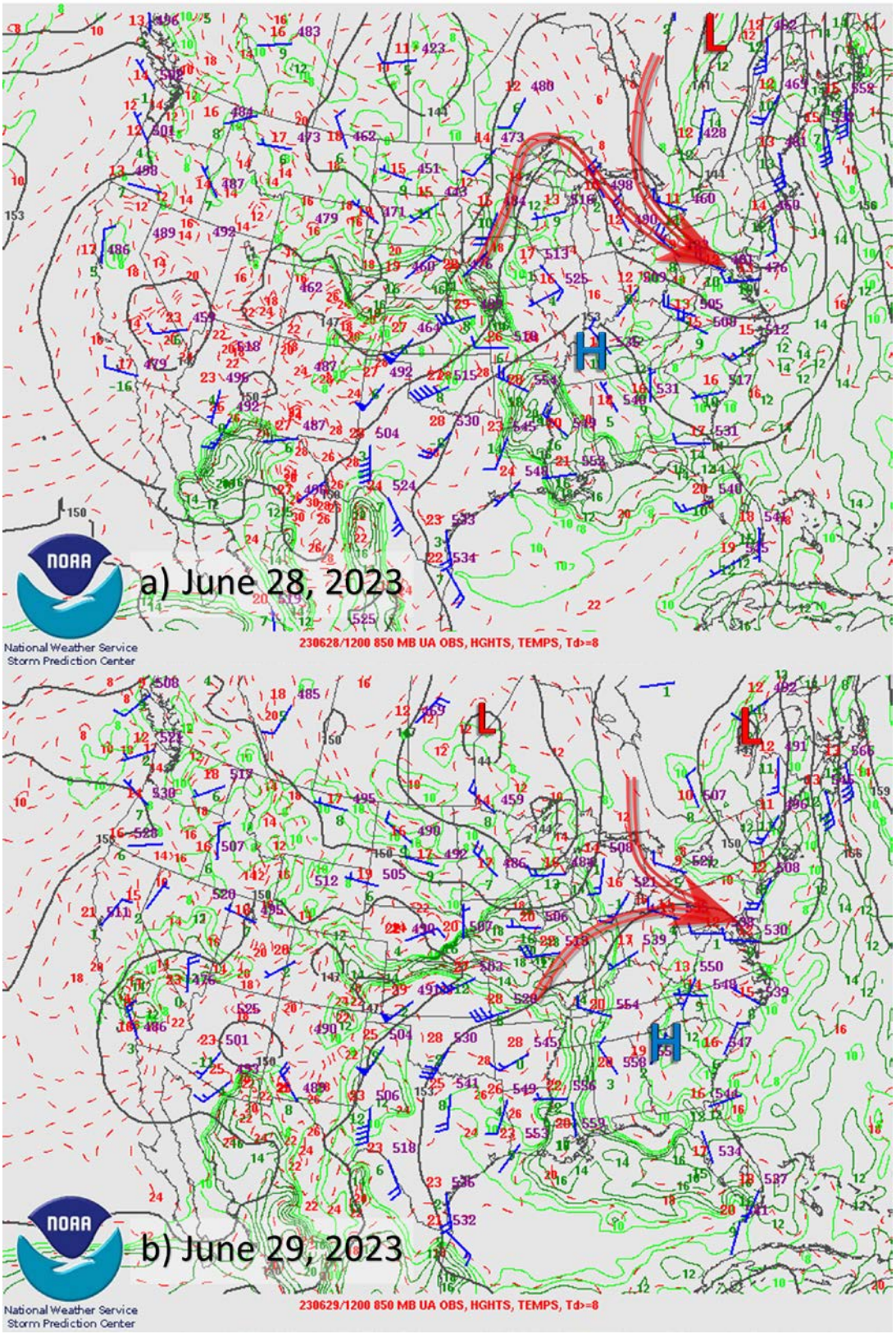

Figure 15: Figure 14, as in Figure 11, but for a) June 27, b) June 28, and c) June 29.

2.4.3.3 Surface Pattern Overview

While transport winds at 850 mb provide information on the movement of airmasses and weather systems, surface conditions and features dictate whether an airmass is capable of ozone production. The surface layer (ground level) where ozone monitors and humans reside, makes the layer paramount to understanding ozone morphology. As of June 25, a broad area of high pressure existed across Quebec (Figure 15a). Winds were weak with little dispersion occurring near the fires. High pressure over the Mid-Atlantic was slowly being pushed east with the approach of a mid-latitude cyclone (low pressure; "L") across the western Great Lakes, consistent with the aloft pattern at 850mb (Figure 13a). Clouds and unsettled weather were found in these areas. Light winds over the northern Great Lakes and southern Ontario and Quebec were only beginning to pull smoke southwestward. As the mid-latitude cyclone moved east, it began to pull more smoke from Canada southwestward over the Great Lakes by June 26, 2023 (Figure 15b). As the low was occluded and closed aloft at 850 mb (Figure 13b), the movement eastward slowed. This allowed north winds on the western side of the low to begin to pull smoke southward on June 26 and 27 over the Great Lakes, as high pressure developed across the Midwest and Ohio River Valley resulting in a broad area of divergent winds from Wisconsin through Ohio and Pennsylvania (Figure 15c). Winds through this area were light, thus, smoke movement was gradual. Furthermore, much of the smoke close to the low on June 26 and 27 was tucked under cloud cover associated with the center of the mid-latitude cyclone. The general pattern at the surface mimics the pin-wheel type transport seen at 850mb (Figure 13a-c and 14a).

High pressure developed further east on June 28 (Figure 15d). Wind patterns and smoke movement were largely dictated by the evolution of the surface high pressure. As winds remained light, smoke transport and steering were also slow, with smoke often stagnant over areas such as eastern Ohio for several days starting on June 28. The heaviest smoke generally did not cross the Appalachians under the surface setup on June 28. High pressure consolidated, increased in intensity, and formed directly overhead of the District on June 29, 2023 (Figure 15e). Air within high-pressure systems is characterized by subsidence (sinking motion), and the development of the surface high over the Washington, DC region was consistent with the arrival of the highest $PM_{2.5}$ concentrations across the state, as well as the greatest ozone concentrations.

2.4.3.4 Temperature

Temperatures were below normal in the District for the duration of the ozone exceedance event on June 29th (Table 3). Perhaps more key in the surface temperature fields was the first ozone exceedance in the Chicago area on June 27. On that day, a daily maximum high temperature of only 78°F at O'Hare Airport was enough to be associated with an ozone exceedance. After that time, an increase in temperature followed, and persisted near or above average, keeping ozone a persistent problem. A slight increase in temperature was experienced for most locations. After the initial low-temperature ozone onset, the increased temperature supported an increase in ozone intensity. This was similar to that described in Dreessen et al. (2016), that a smoky air mass produced increasing ozone as surface temperatures warmed, though in this case the surface temperatures were not extreme (e.g., >8°F above normal). Still, at the onset of ozone exceedances upstream on June 27, surface and upper-level winds showed air coming from the Great Lakes region with temperatures only in the 70s and low 80s sufficient for ozone exceedances from Chicago through Ohio, long before arriving into the District.

Daily high temperatures at Ronald Regan National Airport were still below normal by the time ozone exceedances were realized in the District. It should be noted that "normal" high temperatures are 88°F in late June, which is neither extreme nor typical for ozone events, which historically are associated with high temperatures above 90°F in the District.

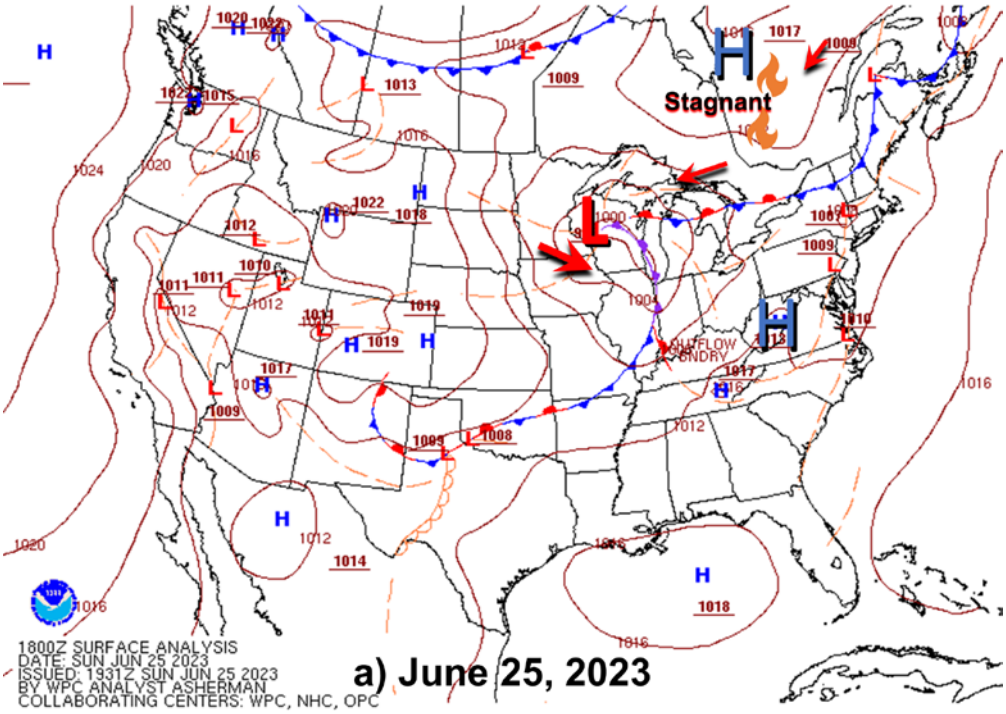

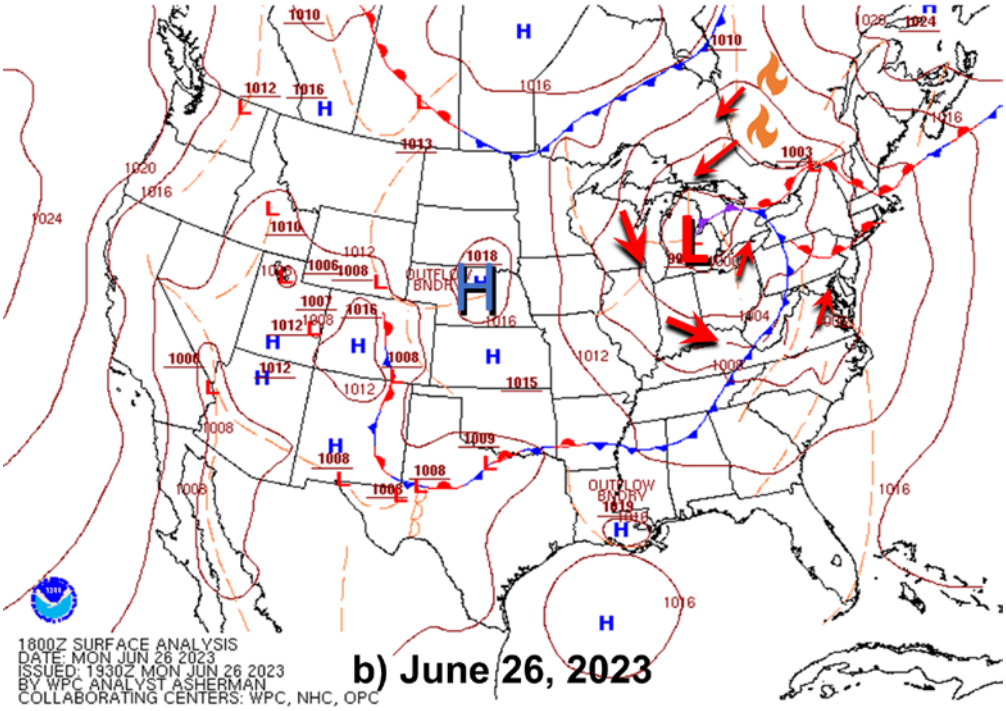

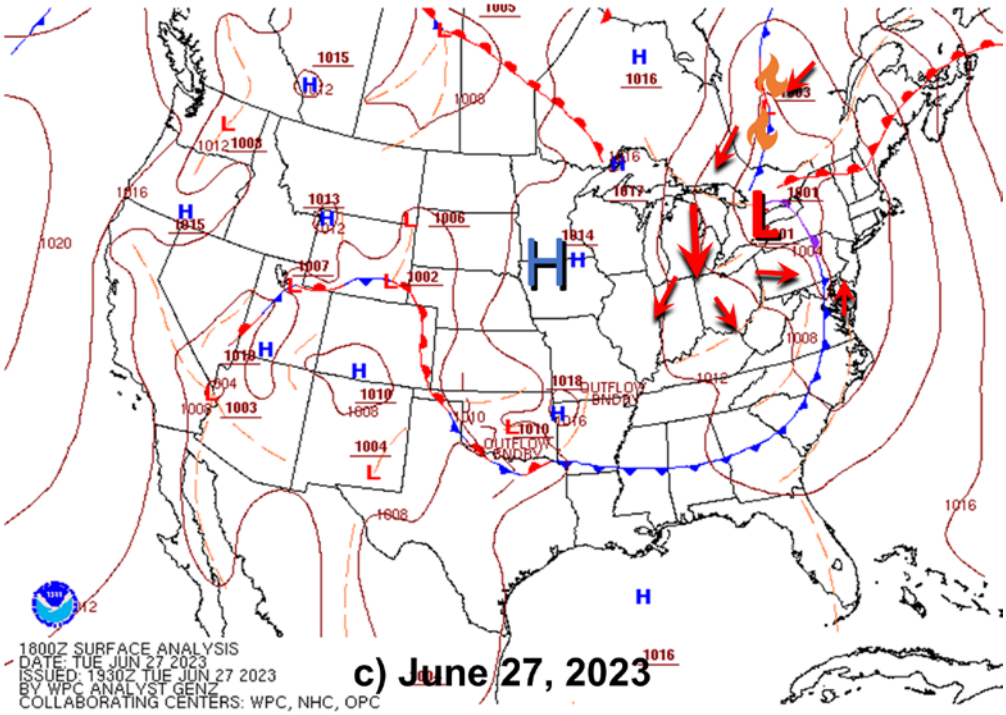

c) June 27, 2023

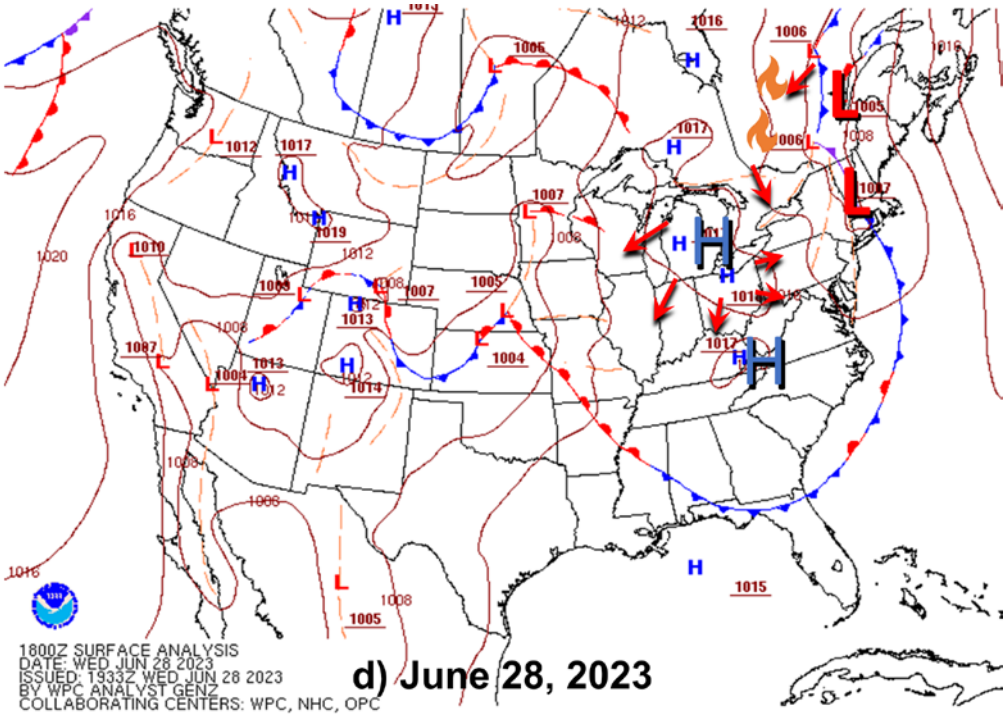

d) June 28, 2023

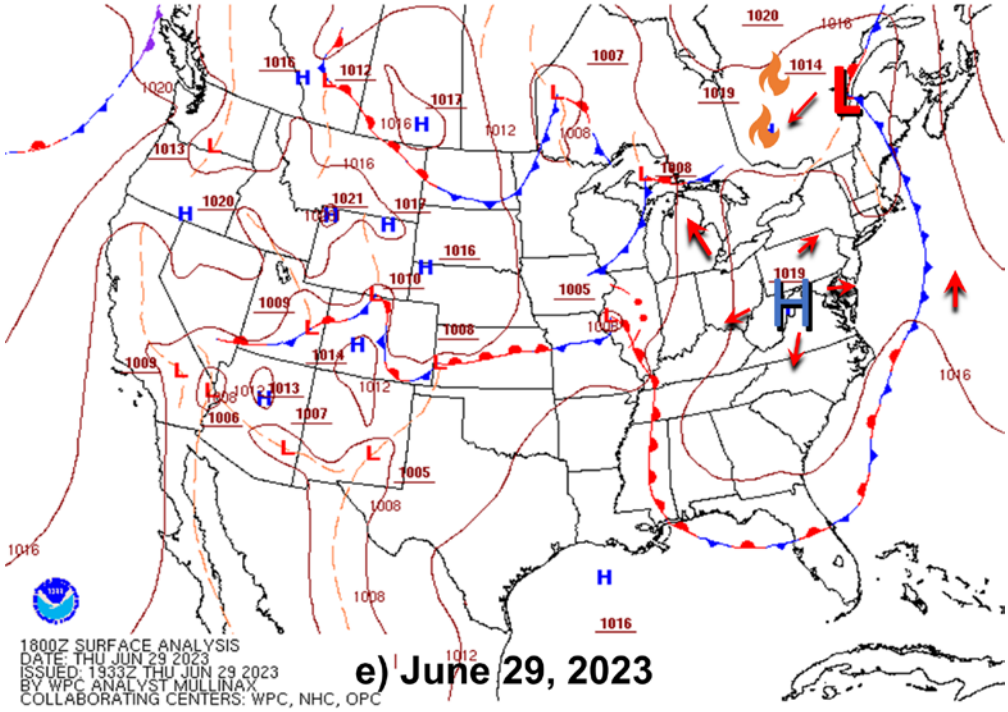

Figure 16: Surface analysis at 1800 UTC for a) June 25, b) June 26, c) June 27, d) June 28, e) June 29

Red arrows show the general pattern of surface winds. Capital letter "H" is high pressure, while the capital letter "L" is low pressure. Isobars (brown lines) and fronts are also analyzed.

Date	27-Jun	28-Jun	29-Jun	30-Jun	1-Jul
Chicago, IL	78	85	88	91	86
Normal	83	84	84	84	84
Departure	-5	1	4	7	2
Cincinnati, OH	76	83	86	87	83
Normal	85	85	85	85	86
Departure	-9	-2	1	2	-3
BWI, MD	88	83	86	86	85
Normal	88	88	88	88	88
Departure	0	-5	-2	-2	-3
Ronald Regan	88	82	87	89	88
Normal	88	89	89	89	89
Departure	0	-7	-2	0	-1

Table 3: Maximum daily temperature, average maximum daily temperature, and departure from average.

Maximum daily temperature, average maximum daily temperature, and departure from average (observation minus average) for various sites across the domain impacted by the smoke are provided for June 27-July 1, 2023. All temperatures are in degrees Fahrenheit. Colored boxes show maximum daily 8-hour average ozone AQI at locations where nearby sites had ozone exceedances of 70 ppb.

Near-ozone exceedances occurred near the fire sources in Canada, with temperatures slightly above normal across Quebec during the burn period. On June 24, 2023, temperatures were as much as 8°C greater than normal over parts of Quebec (Figure 17a). This not only was helpful for fire maintenance, but also photochemistry. As will be shown, MD8AO near the fire sources even as early as June 24 were close to 70 ppb in remote areas of Canada impacted by the smoke. Afternoon temperatures (2 pm) were around 27°C (81°F) on June 24 (Figure 16b). This is lower but relatively similar to the initial temperatures associated with ozone exceedances across the Great Lakes.

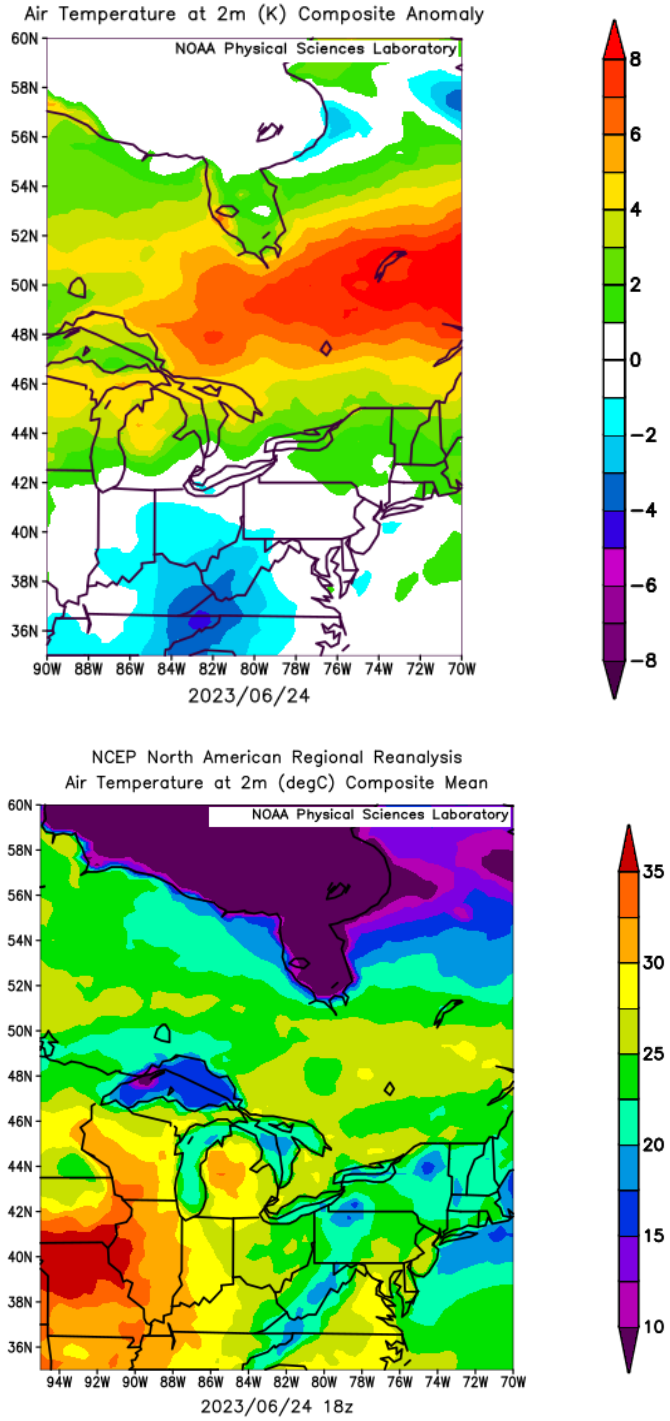

Figure 17: 2 pm (EDT) temperature on June 24, 2023, from the North American Regional Reanalysis (NARR).

Afternoon temperatures on June 24 were in the low 80s (~25-30°C) across southern Quebec. Temperature Reanalysis Link

2.4.4 Smoke and Ozone Transport Overview

Abundant smoke was produced across Quebec during an intense burn period from June 21-25 (Figure 18a-j). Before newly generated smoke from this burn period could reach the U.S., consistent, light northeastern flow across the western Great Lakes had tapped into previous smoke (fires were ongoing and intensified from June 21-25), fueling widespread ozone exceedances across Illinois, Wisconsin, Minnesota and other surrounding states. The newest, concentrated plume of smoke was recirculated across Quebec. Ozone was already responding in this new smoke across remote Quebec; on June 24, an 8-hour concentration of 69 ppb was observed in southwestern Quebec (Figure 18g). This area is remote, with no appreciable anthropogenic sources nearby, indicating the smoke alone was generating ozone approaching NAAQS exceedance levels. Additionally, adjacent monitors just on the fringe of the smoke were observed to be ~20 ppb lower, illustrating the smoke's impact on photochemistry.

By June 25, smoke was prolific in scope and concentration across Quebec due to the recirculation of the past few days of burning (Figure 18j). Due to an approaching mid-latitude cyclone along the U.S.-Canada border, smoke across Quebec, already producing ozone in remote areas of Canada, was pin-wheeled southwestward. On June 26, the smoke became obscured due to copious amounts of cloud cover associated with the mid-latitude cyclone (Figure 18 k,l). However, fine particle ($PM_{2.5}$) concentrations, which act as a primary pollutant indicator for smoke at the surface, show the abundance of smoke pulled into the cyclone's circulation across the western Great Lakes (Figure 18l). Smoke largely remained obscured from the satellite due to cloud cover on June 27, 2023. However, areas of eastern Wisconsin and northern Illinois were devoid of clouds, and instead, the satellite picked up on the western extent of the smoke plume (Figure 18 m,n). Below the cloud deck over the upper Ohio River Valley (Michigan, Indiana, Ohio, northern parts of Kentucky, and western Pennsylvania), surface 24-hour $PM_{2.5}$ concentrations revealed smoke beginning to reach as far east as western Pennsylvania, largely still west of and/or stopped by the Appalachian Mountains.

High pressure centered roughly over Indiana on June 28 continued to fan-out smoke in a divergent pattern, pushing smoke as far northwest as Minnesota, as far south as St. Louis, and then farther east as far south as Tennessee (Figure 18 o,p). The eastward extent of the smoke just started to filter into the western half of Maryland. The most significant concentrations were over the western Maryland panhandle, where $PM_{2.5}$ exceedances occurred (Figure 18 p). Widespread USG and Unhealthy AQI ozone were experienced from Wisconsin through Ohio and northern Kentucky. Less concentrated smoke continued to filter into the District on June 28, with concentrations generally increasing through the day and into the night. However, movement of the highest concentrations of smoke in western Pennsylvania was prolonged, and a significant disparity of smoke concentration existed between that area and the District on June 28 and to start June 29. With lower smoke concentrations and more clouds than sun, no appreciable increase in ozone was noted in the District on June 28.

While intense, smoke concentrations on June 29 were initially much lower than anticipated (~50 $\mu g/m^3$ instead of 100 $\mu g/m^3$). Around 9 a.m., coincident with the development of surface high pressure directly over the Washington, DC region (and more importantly on the eastern side of the mountains) and the onset of delayed, albeit weak, boundary layer mixing, smoke concentrations more than doubled over the next few hours as the densest smoke concentrations of the event finally arrived over

eastern portions of the state (Figure 18 q,r). Upon the arrival of the thickest smoke, the 8-hour ozone concentrations in the District were equal to and/or greater than what occurred across the vast area of high ozone upstream on June 28.

2.4.5 Smoke and Ozone Discussion and Analysis

Chronological spatial analysis of MD8AO concentrations and VIIR satellite and/or surface $PM_{2.5}$ observed smoke matched and showed that the development of high ozone concentrations in Maryland was dependent on smoke transport from the Quebec fires across the Great Lakes and into the Mid-Atlantic and northeast CONUS (Figure 17). MDE contends that substantial ozone was already present within the smoke transported into Maryland, and that precursors with the smoke enabled extraordinary ozone production locally from any anthropogenic precursor emission, far and beyond anything possible in the absence of smoke.

Initially high ozone concentrations existed across Illinois, Wisconsin, and surrounding nearby states (Figure 18a-). This ozone built up over time, under high pressure in the presence of diffuse smoke transported from the Quebec fire area. This culminated in an ozone exceedance on June 24 over these areas. After June 24, unsettled weather and/or cloudy skies associated with a mid-latitude cyclone reduced ozone concentrations over this area, mainly into the Good range on June 25 and 26 (Figure 18 g-j). At the same time, smoke from burning over Quebec was producing ozone nearing exceedance concentrations (upper 60s) at sparse monitors not covered by clouds of the cyclone (e.g., Figure 18 g, i). This smoke and associated ozone were pulled southwards. On June 27, clouds clearing west to east across Wisconsin, Iowa, and Illinois allowed an increase in sunlight and temperatures supportive of photochemistry (Figure 18 m). A few locations were already nearing the "Unhealthy" threshold across Illinois, with MD8AO of 81 ppb observed near Rockford. For reference, Rockford's high temperature for June 27, 2023, was 81°F, per NOAA records [https://www.weather.gov/wrh/climate?wfo=lot], similar to the low high temperature experienced at O'Hare airport in Chicago (Table 3).

As high pressure developed over a wide area on June 28, smoke and USG to Unhealthy AQI spread across a vast expanse from Minnesota to Kentucky and Maryland (Figure 18 o). Note that the ozone exceedances lagged the smoke slightly, as smoke was apparent across these areas and as far east as Virginia, Maryland, and Pennsylvania either visually (via satellite) or with instrumentation (surface PM2.5). Fine particle exceedances were realized in Maryland over the Western Panhandle but not over the Washington, DC area by June 28 (Figure 18 p). The lack of substantial ozone increases associated with the initial smoke arrival was due to partial cloud cover, initial temperatures in the low 80s, increasing but not significant smoke (e.g., compared with concentrations upstream), and most especially, the spatial separation of the portion of the smoke receiving the most sunlight. The portion of the smoke reaching the region on June 28 had spent several days under heavy cloud cover. On June 29, the most serious smoke, per satellite observation, moved into the Washington, DC area. A band of heavier smoke appears to exist from southwestern Pennsylvania into central Maryland and northwestward into Michigan and Wisconsin/Chicago (Figure 18 b). The map background is provided as the MODIS Aqua/Terra Reflectance TrueColor. Overlaid are maximum daily 8-hour average ozone concentrations (colored circles), with concentration (blue) and AQI-associated color, and daily winds

(barbs). Smoke is visible as light gray haze while clouds appear brighter white. Note that smoke is not always visible in satellites due to cloud cover, and as such, surface observations outline the extent and intensity of smoke. Ozone is provided first for each day, followed by daily average $PM_{2.5}$.
Not coincidentally, ozone exceedances on June 29 mainly existed in this same band from southeast Wisconsin southeastward through the Washington, DC area (Figure 18a). Thus, the same airmass with smoke produced similar ozone magnitudes across an area similarly impacted by smoke (per similar surface $PM_{2.5}$ concentrations), showing the connection of the smoke to ozone.

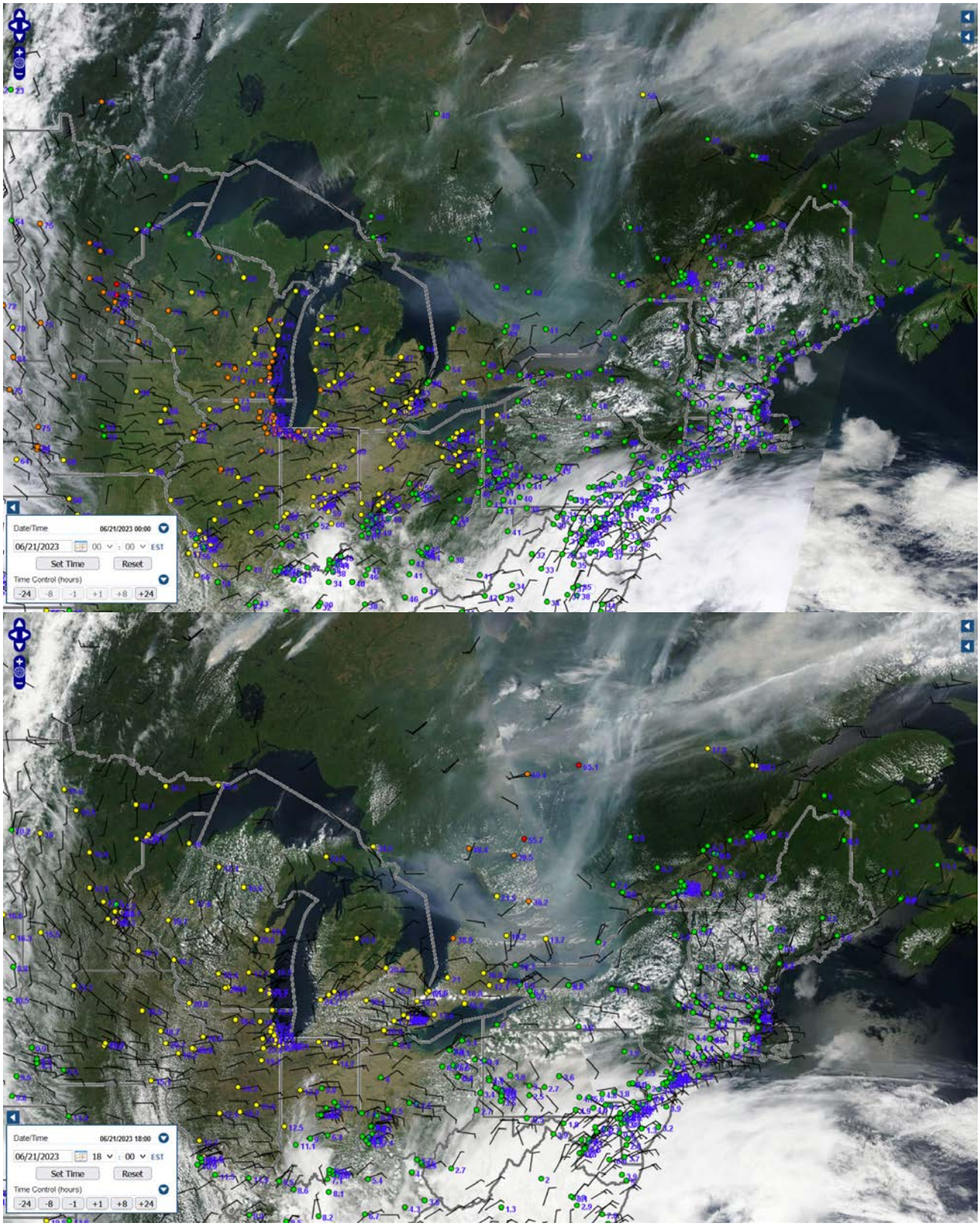
Date/Time 06/21/2023 00:00
06/21/2023 00 : 00 EST
Set Time
Reset
Time Control (hours)
-24 -8 -1 +1 +8 +24
Date/Time 06/21/2023 18:00
06/21/2023 18 : 00 EST
Set Time
Reset
Time Control (hours)
-24 -8 -1 +1 +8 +24

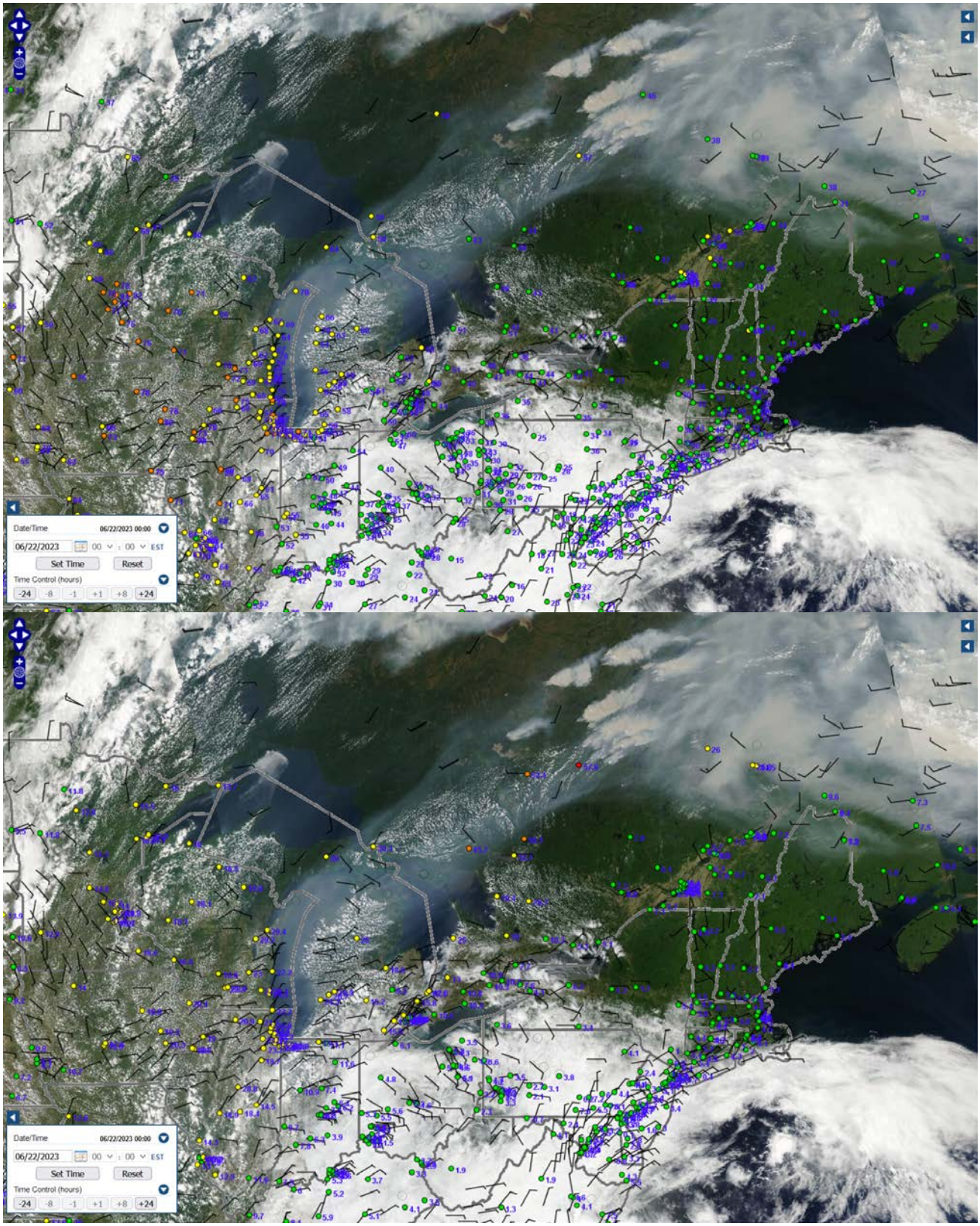
Date/Time
06/22/2023 00:00
06/22/2023
00 : 00 EST
Set Time
Reset
Time Control (hours)
-24 -8 -1 +1 +8 +24
Date/Time
06/22/2023 00:00
06/22/2023
00 : 00 EST
Set Time
Reset
Time Control (hours)
-24 -8 -1 +1 +8 +24

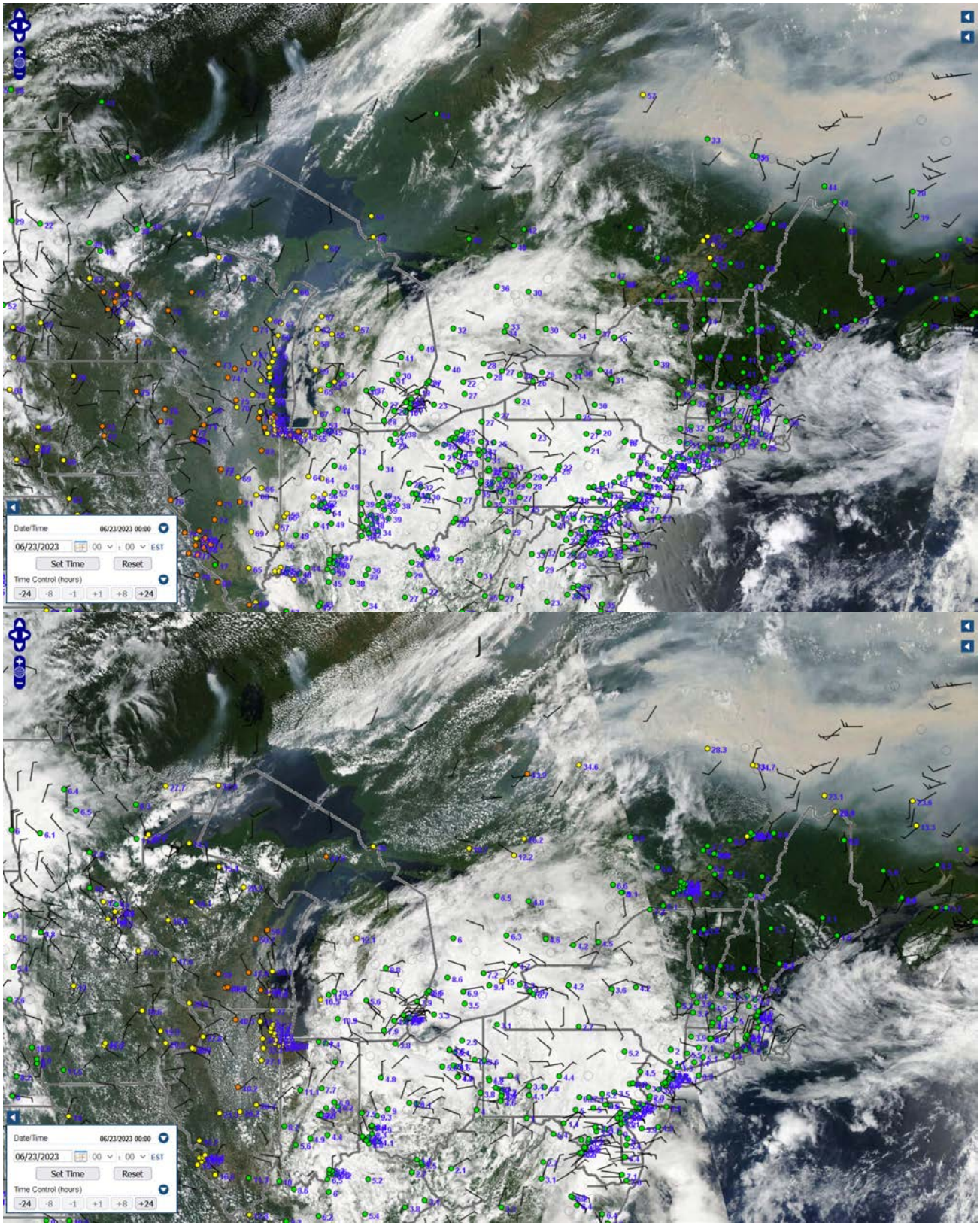
Date/Time
06/23/2023 00:00
06/23/2023
00 : 00 EST
Set Time
Reset
Time Control (hours)
-24 -8 -1 +1 +8 +24
Date/Time
06/23/2023 00:00
06/23/2023
00 : 00 EST
Set Time
Reset
Time Control (hours)
-24 -8 -1 +1 +8 +24

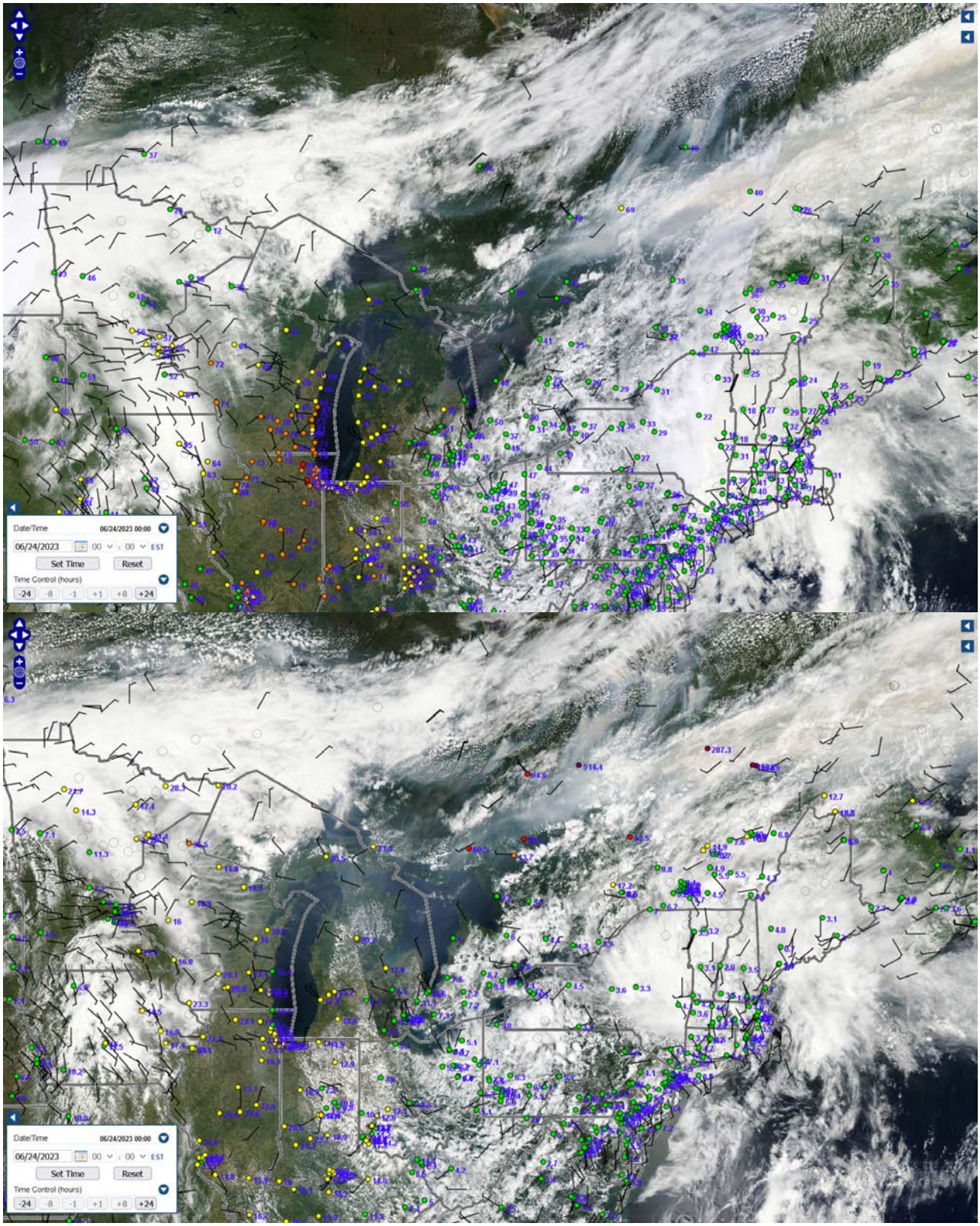
Date/Time
06/24/2023 00:00
06/24/2023
00 : 00 EST
Set Time
Reset
Time Control (hours)
-24 -8 -1 +1 +8 +24
Date/Time
06/24/2023 00:00
06/24/2023
00 : 00 EST
Set Time
Reset
Time Control (hours)
-24 -8 -1 +1 +8 +24

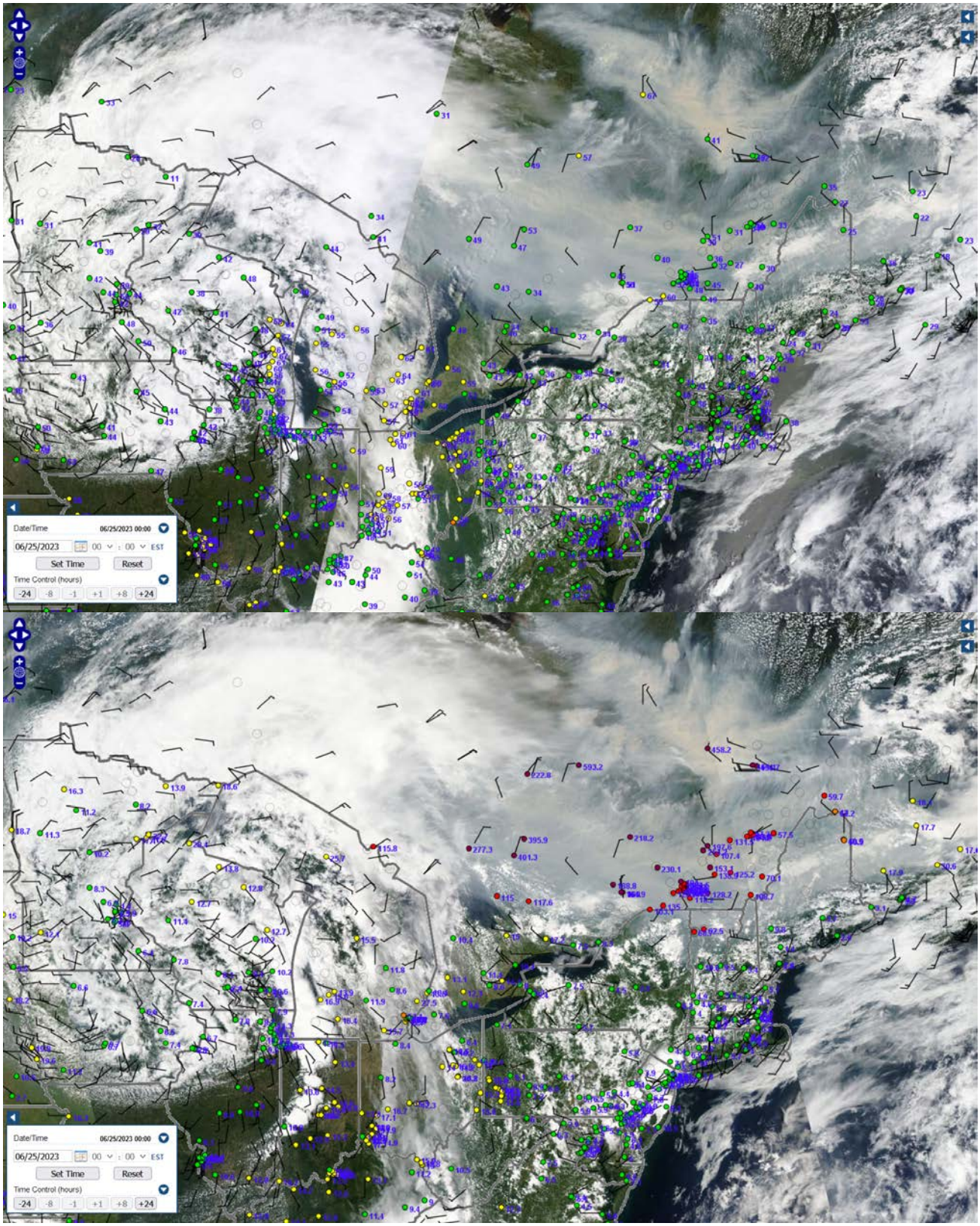
Date/Time
06/25/2023 00:00
06/25/2023
00 : 00 EST
Set Time
Reset
Time Control (hours)
-24 -8 -1 +1 +8 +24
Date/Time
06/25/2023 00:00
06/25/2023
00 : 00 EST
Set Time
Reset
Time Control (hours)
-24 -8 -1 +1 +8 +24

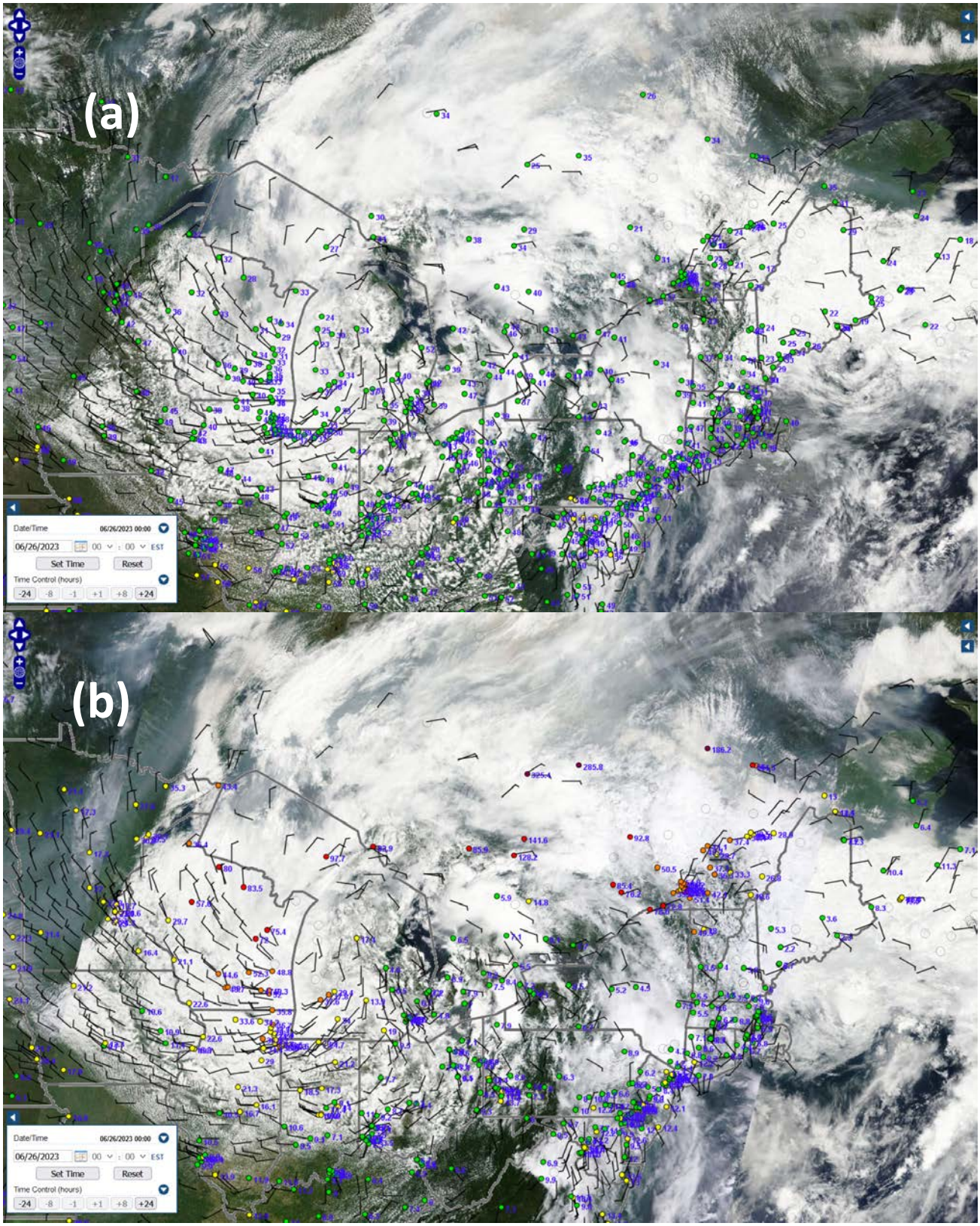
(a)
(b)
Date/Time
06/26/2023 00:00
06/26/2023
Set Time
Reset
Time Control (hours)
-24
-8
-1
+1
+8
+24

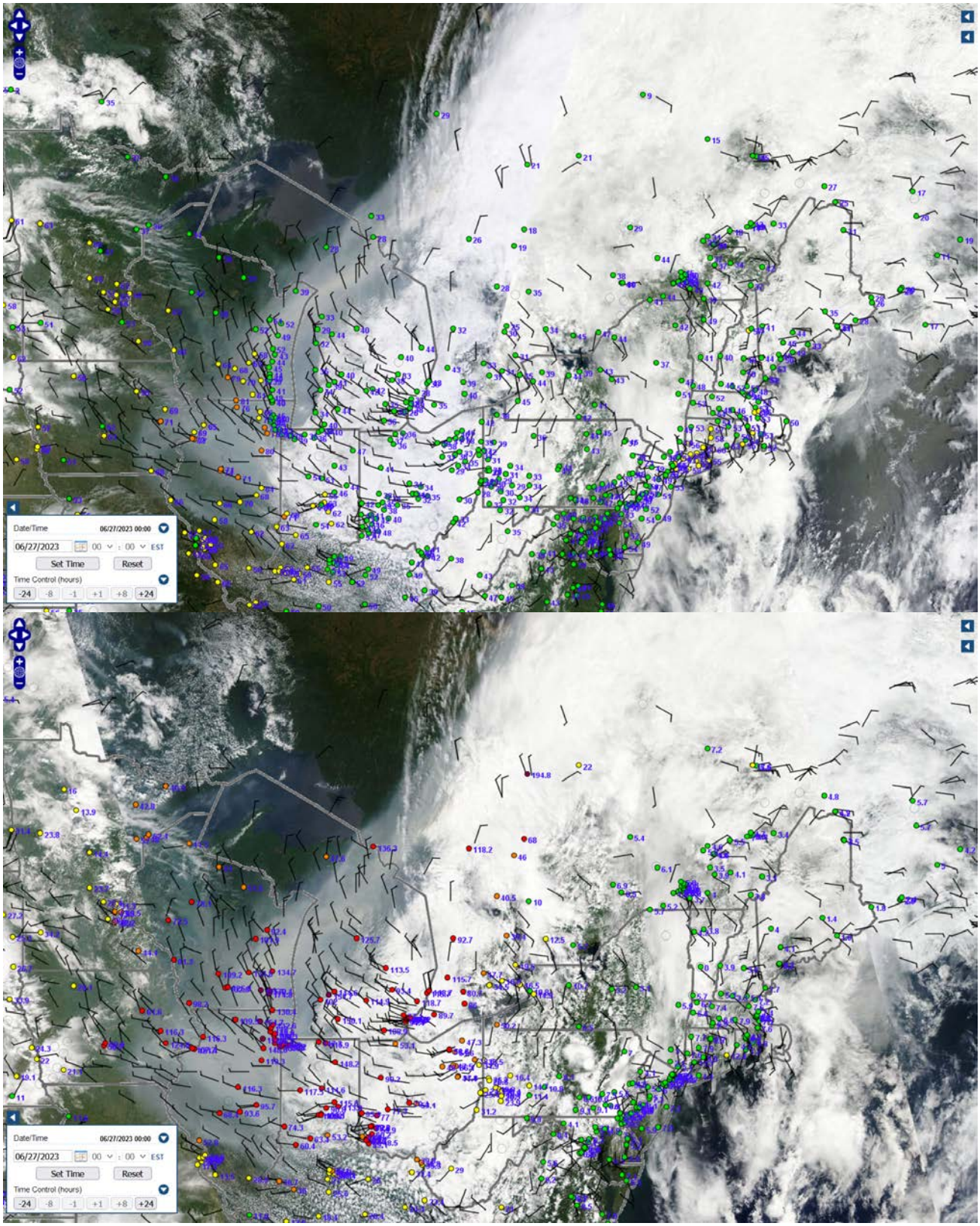
Date/Time
06/27/2023 00:00
06/27/2023
00 : 00 EST
Set Time
Reset
Time Control (hours)
-24 -8 -1 +1 +8 +24
Date/Time
06/27/2023 00:00
06/27/2023
00 : 00 EST
Set Time
Reset
Time Control (hours)
-24 -8 -1 +1 +8 +24

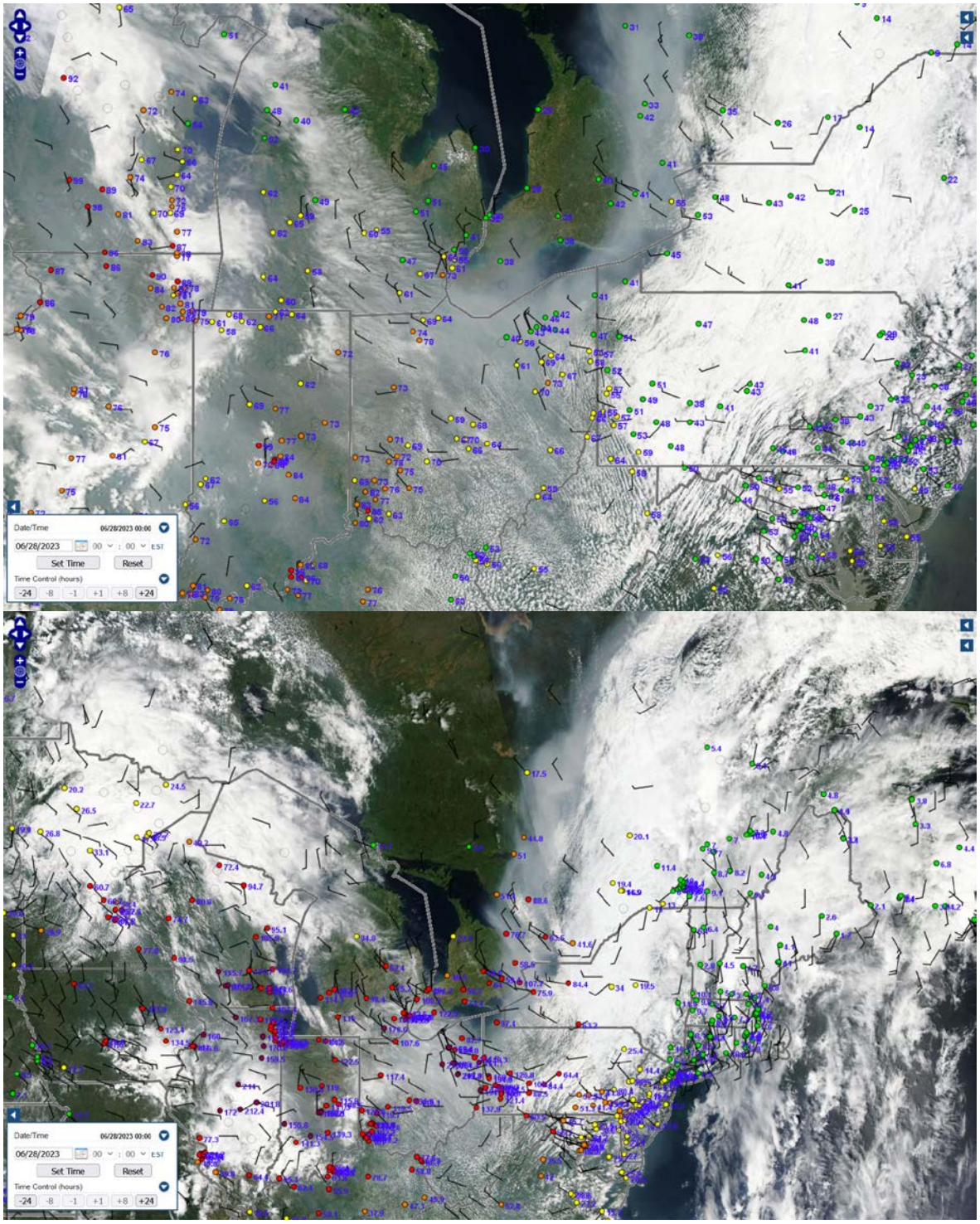

Figure 18: June 21-28 maximum daily 8-hour average ozone and daily average PM2.5 concentrations across eastern CONUS.

The map background is provided as the MODIS Aqua/Terra Reflectance TrueColor. Overlaid are maximum daily 8-hour average ozone concentrations (colored circles), with concentration (blue) and AQI-associated color, and daily winds (barbs). Smoke is visible as light gray haze while clouds appear brighter white. Note

that smoke is not always visible in satellites due to cloud cover, and as such, surface observations outline the extent and intensity of smoke. Ozone is provided first for each day, followed by daily average PM2.5.

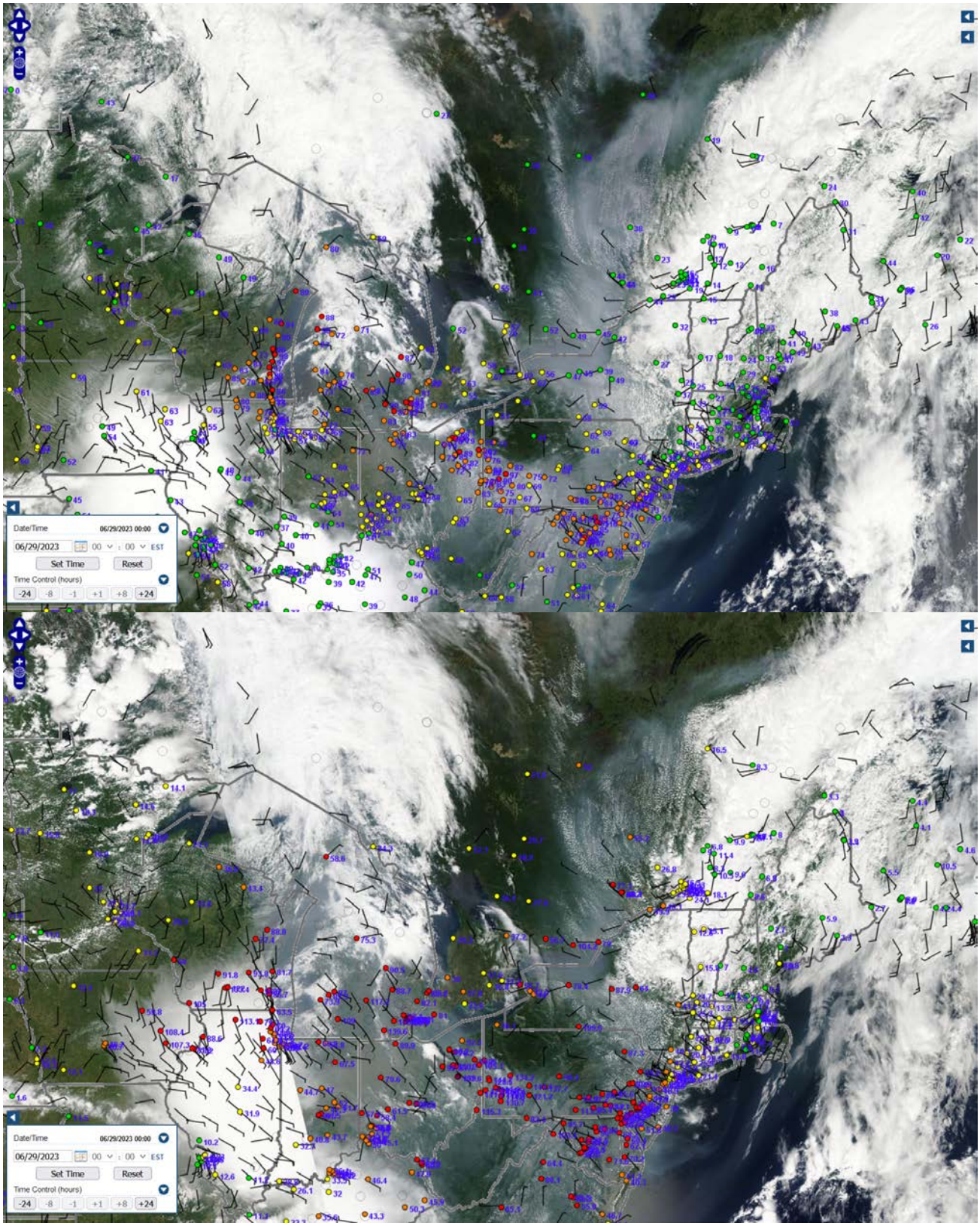

Figure 19: As in Figure 17, but for June 29th

3.0 Clear Causal Relationship Between the Event and Monitored Ozone Concentrations

The case presented in this analysis illustrates an example of the impact of smoke on ozone concentrations via the transport of smoke-augmented, ozone-laden air into the District. DOEE here presents necessary evidence to show that the smoke event affected air quality in the District and clearly was associated with ozone concentrations beyond what otherwise is expected in the absence of smoke and/or that smoke caused the exceedance days.

Comparisons to historical concentrations and a Q/d analysis (Tier 1 and 2 steps) are provided. While DOEE believes these analyses alone show a causal relationship between the ozone and smoke, the complicated nature and long transport of the event may not clearly demonstrate a clear causal relationship. However, it was deemed that further analysis was necessary to further establish and demonstrate a clear causal relationship was prudent. Therefore, a weight of evidence (Tier 3) approach is used to build an irrefutable case that smoke transport was responsible for the ozone concentrations and the ozone exceedance days in the District.

3.1 Historical Concentrations

Scatter plots of MD8AO at the District monitors exceeding the 70 ppb NAAQS on June 29th showed the exceptional nature of the exceedances (Figures 20-21). Ozone data during the 2019-2023 ozone seasons (for the months of April 1 to September 30) were plotted for each monitor against that monitor's multi-season and June-only 99th percentile. Recall that significant and sustained reductions in ozone precursors across the eastern US have occurred in the past ten years. These reductions have been particularly evident in NO_x, leading to lower ozone concentrations. Consequently, this has led to a noticeable decrease in ozone exceedance days despite an increasing number of hot days; four of the lowest five years based on exceedance days have occurred in the 2018-2022 period. COVID lockdowns lowered exceedance frequency in 2020, but 2022 had an equal number of exceedance days as 2020.

June 2023 had the lowest aggregate EGU emissions ever (Figure 4 and Figure 5). While June 29, 2023, had a notable increase in 2023 aggregate NO_x emissions, the total NO_x on June 29 (311 tons) was close to the mean of 2022 (300 tons), which had only three total exceedance days in the District as a year. Therefore, amplified MD8AO concentrations in late June 2023 represented substantially more ozone generated from available NO_x than in 2022 or a more historical scenario, when emissions were significantly higher. For comparison, mean aggregate emissions in June 2019 were 430 tons. Even so, 2022 EGU emissions experienced a substantial decrease of 30% compared to the 2019-2021 daily average (per Figure 5). The 2023 average daily output for June was 225 tons per day, or 47% lower than the 2019-2021 average (428 daily tons). Since 2019-2021 is within the previous five years of data that EPA requests for historical comparisons, DOEE feels the data from 2019-2021 raises the 99th percentile higher than what is otherwise now representative of the District's ozone. Thus, DOEE also offers two additional 99th percentiles to compare each monitor's MD8AO on June 29th. These additional 99th percentiles are calculated using data from only June in 2022 or June 2022 and 2023 combined. DOEE believes this increases the robustness of the historical comparison.

This can be seen in Figure 20; the days that exceeded the NAAQS on June 29 or 30, 2023, and for which DOEE is seeking exclusion of the data are colored red. Textual annotations give the MD8AO for the red-colored data points. Along with the 70 ppb NAAQS (red solid line), four additional lines provide the 99th percentiles to account for the changing NO_x emissions and ozone levels in D.C. over the past five years. The 99th percentile for all ozone season data, 2019-2023, is given in dashed purple. All June ozone data from 2019-2023 is shown in green dash. Data from June 2022 is only given in dashed orange, while all June ozone data from 2022 and 2023 combined are given as a blue short-dashed line.

Both monitors exceeded the 99th percentile threshold on June 29th. The River Terrace site, which exceeded 70 ppb during this event, has a 99th percentile, well below the 70 ppb standard, showcasing the cleaner environment the District has experienced in recent years.

It is safe to say the event caused one of the highest ozone concentrations at all monitors, which exceeded the standard (and even at those that did not – see Appendix B). The following scatter plots from both monitors show the above data (Figures 20-21). Along with the 70 ppb NAAQS, four additional lines indicate the 99th percentiles for all ozone season data from 2019 through 2023, all June ozone data from 2019 through 2023, only ozone from June 2022, and ozone from June of 2022 and 2023 combined.

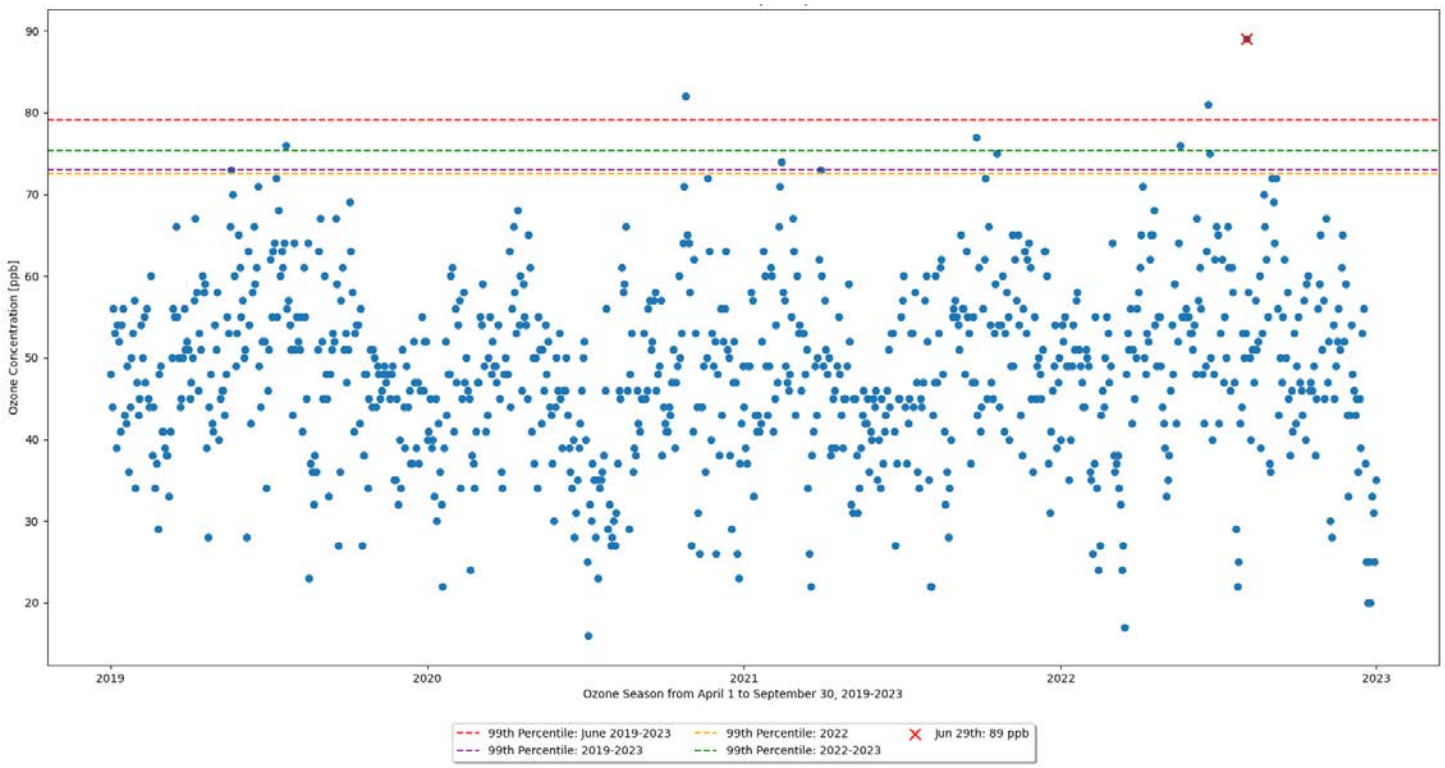

Figure 20: Scatterplot of Maximum Daily 8-hour Average Ozone (MD8AO) concentrations at McMillan (blue dots), April 1 – September 30, 2019-2023.

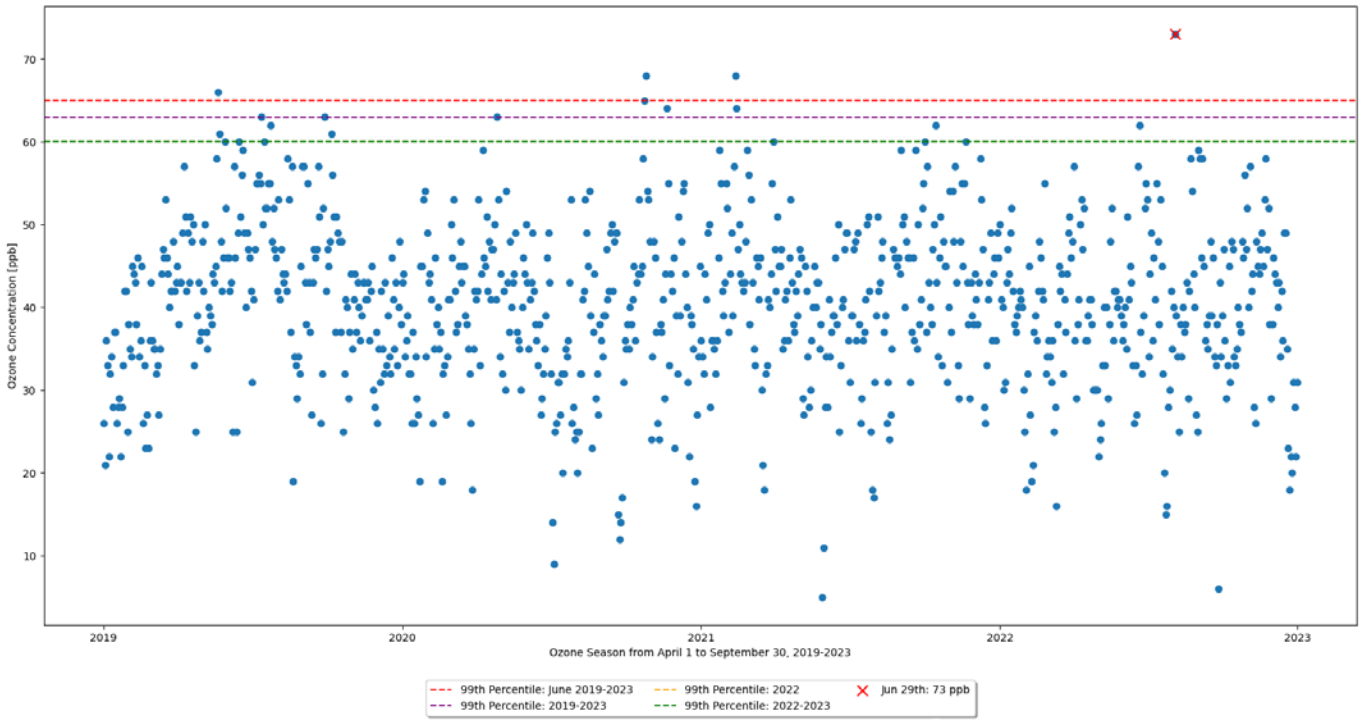

Figure 21: Scatterplot of Maximum Daily 8-hour Average Ozone (MD8AO) concentrations at River Terrace (blue dots), April 1 – September 30, 2019-2023.

3.2 Evidence that Fire Emissions were Transported to the District

To further demonstrate that Quebec wildfire emissions were transported to the District, the Hybrid Single-Particle Lagrangian Integrated Trajectory (HYSPLIT; Rolph, 2015; Stein et al., 2015) model was used to approximate the movement of air parcels both forward from the fire and smoke region and backwards from the District and according to the conceptual model, an intense burn period from June 21-25 underneath stagnating and recirculating conditions across Quebec created a prodigious smoke plume that was observed at the surface, with $PM_{2.5}$ 24-hour concentrations in Canada *beyond* the EPA AQI of 500. The smoke slowly moved southwestward across the Great Lakes and Midwest from June 26-27, 2023. The smoke path was trackable using the ground-based network of fine particle sensors across Canada and the United States, but trajectories further confirm and outline the evolution of the smoke. On June 28, the smoke finally moved eastward and impacted the District by June 29, much of the northeastern U.S.

A matrix of forward trajectories centered on the area in which the HMS analyzed smoke and which surface $PM_{2.5}$ concentrations were in excess of 200 $\mu g/m^3$ measured across Quebec were run (Figure 22). The 3km High Resolution Rapid Refresh (HRRR) was the meteorological data driving these trajectories. Running a matrix of trajectories (several trajectories which start from a gridded pattern over the source area) instead of a single trajectory allows the matrix to show a spread of possible dispersion of the smoke plume while increasing the confidence in the general transport pattern. Due to increasing model error with time (an intrinsic occurrence when modeling the atmosphere), no single

trajectory should be considered representative of the exact path of the smoke plume, and the longer the trajectory is run, the greater the error of the modeled path is likely to be. Therefore, clusters of trajectories increase confidence in the path of the smoke. In this case, a clear, consistent pattern was modeled, showing the southwestward movement of air out of Quebec towards the Great Lakes, then turning eastward (Figure 22). The forward trajectories stop just short of reaching the District by June 29, 2023, the day the full impact was felt in the District.

Backward trajectories had a similar origin but a more direct path to western Quebec by June 25, the start date of the forward trajectories (Figure 22). The trajectories show general counter-clockwise transport and well-clustered trajectory members running through the Great Lakes and into the upper Ohio River Valley by day 4 (June 29). Matrix: lower left: 46.065470N 80.420521W; upper right: 51.860224N 70.64703W; Spacing 0.5N, 1.0W. (b) 96-hour back trajectories from DCA airport in Virginia beginning at 2 p.m. on June 29, 2023, showing transport from the area of the smoke in Quebec to the District over the course of 4 days. Trajectories in both runs show relatively little vertical displacement due to the presence of the smoke within the planetary boundary layer through the entire transport process to the District. As discussed in the conceptual model, the smoke plume was transported across the Great Lakes southwestward before turning eastward toward the District over the course of ~4-5 days. Smoke remained in the boundary layer throughout this time and was trackable within the surface monitoring network of Canada and the United States. The lack of a strong or significant vertical displacement of the trajectories is consistent with transport of the smoke primarily in the boundary layer from Quebec, across the Great Lakes and the Ohio River Valley to reach the District. The length and origin of the back trajectories, while skewed more eastward than was observed by the surface network, connected the densest smoke from west central Quebec on midday June 25 to peak concentrations on June 29th in the District, consistent with the time of transport (4-5 days) outlined in the conceptual model.

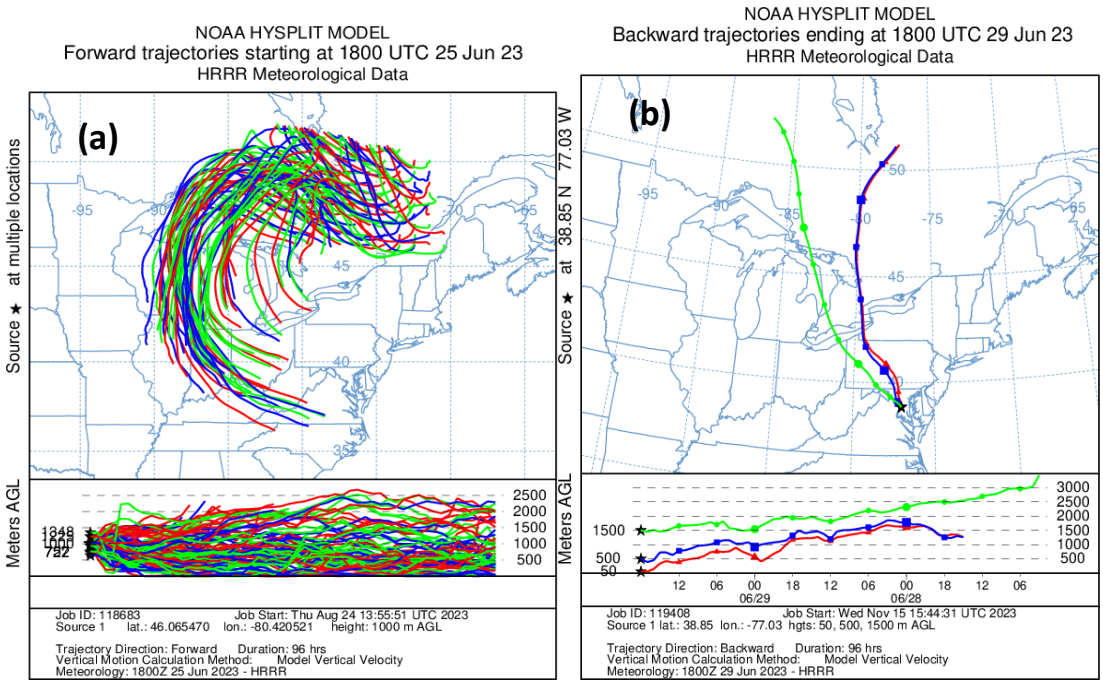

Figure 22: Forward and Backward Transport Trajectories (a) A Matrix of 96-hour (4-day) High Resolution Rapid Refresh (HRRR) forward trajectories with starting points centered around the location of the maximum smoke concentrations in Quebec on June 25, 2023.

3.2.1 Visibility

Aside from the surface observations of $PM_{2.5}$, smoke impacted visibility dramatically in the District. The images below were taken in both Northern Virginia and in the District.

Figure 23: Pictures from June 29, 2023, at various times and locations around Baltimore. a) Arlington, a community in Northern Virginia at 7 am EDT; b) A picture taken that shows the Lincoln monument on the horizon; c) A picture taken by a resident of the District that shows early morning traffic on the day of the event. The view of the Capital is impaired because of the smoke.

3.2.2 Evidence of Ozone Transport via Ozonesondes

DOEE contends ozone formation from the Quebec fires occurred upstream of the District and was then transported to the state as a cause of the ozone exceedances above the 99th percentile of recent historical data. With a heavy smoke burden evident by $PM_{2.5}$ concentrations greater than 100 µg/m^3 across the entire upstream airmass over the Midwest and Great Lakes as of June 27/28, MDE requested ozonesondes be launched June 29th from Maryland Department of Environment's Howard University (HU-)Beltsville site. These ozonesondes recorded substantial ozone concentrations within the nocturnal residual layer (i.e., pre-dawn ozone above the surface).

At night, ozone is removed from the layer of air a few tens of meters from the surface as it interacts with other molecules or objects and/or is chemically removed through reactions with nitric oxide (NO). However, the layer of air immediately above the surface at night "preserves'' ozone overnight, making it the "transport relevant" layer for the next day or simply known as "the residual layer." The residual layer is usually found from around 500 m to ~1,500-2,000 m above ground level at night. Therefore, surface ozone may be at or near zero at night, while just a few hundred meters above the ground, ozone may still be 50-80+ ppb. During the pre-dawn hours of June 29, ozone concentrations within the residual layer (0.25 – 1.5 km) were 50-65 ppb Figure 25). Wind direction at the time showed transport in this layer from approximately 330° to 50°, or northerly.

The 2 am launch was prior to the arrival of the greatest concentration of smoke. The ceilometer at McMillan Reservoir observed heightened aerosol returns above the surface at the time of the 2 am launch, indicating the thickest smoke was above the surface in a layer from 500 m to roughly 1600 m (Figure 25). Darker oranges and reds identify areas of thicker aerosol returns. In this case, the backscatter is hitting the smoke. Initially, the smoke is aloft and detached from the surface. A little after 12:00 UTC, the colors become more uniform and darker near the surface (indicating more returns at ground level) as the peak smoke concentrations reached the site later in the morning. The morning ozonesonde observed ozone concentrations increasing with height through this residual layer,

consistent with the idea that greater ozone concentrations were associated with thicker smoke, which was highest aloft. Furthermore, the highest concentrations of the entire event had yet to arrive, with hourly surface PM2.5 concentrations 2-3 times greater by late morning on June 29 than at 2 am. This was also reflected as higher aerosol returns on the McMillan ceilometer after about 13:00 UTC (9 am). As such, the morning ozonesonde observed only the 'fringe' of the smoke, but in so doing, already observed ozone concentrations nearing the NAAQS in the upper residual layer.

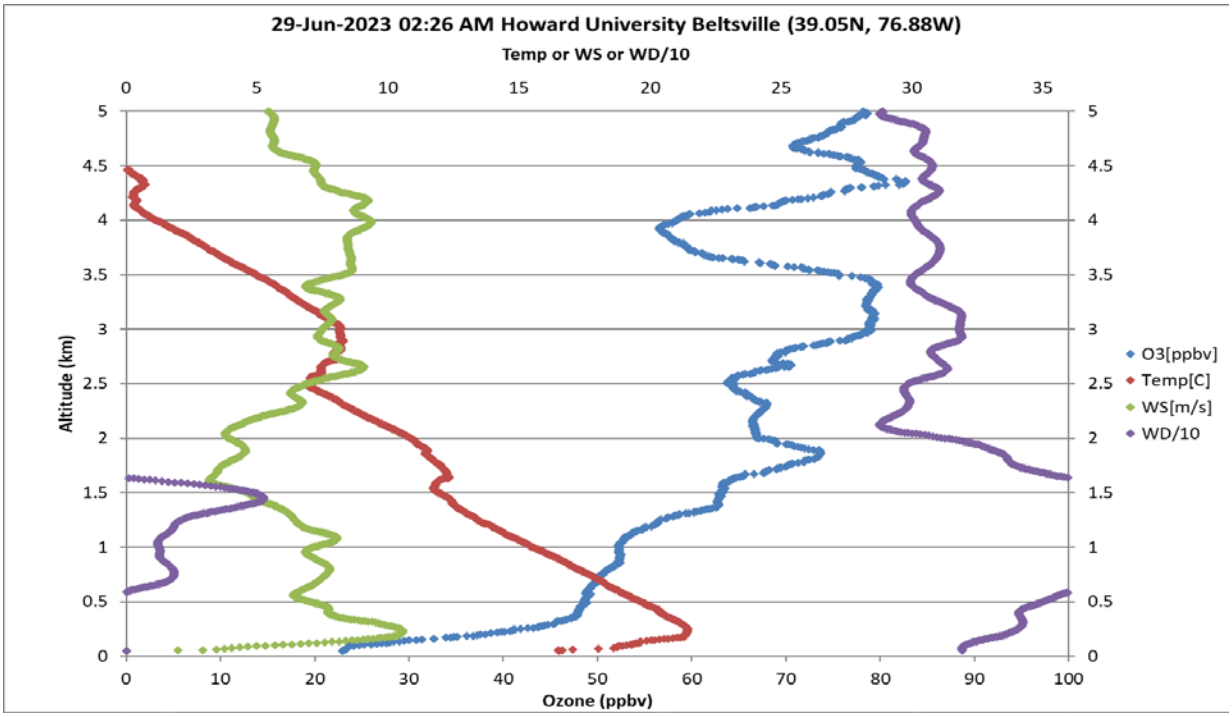

Figure 24: Ozonesonde launched from Howard University Beltsville on the morning of May 25, 2016. 2:26 am is equivalent to 06:26 UTC.

Temperature (red, squares), wind direction (green, triangles), wind speed (blue, diamonds), and ozone (purple, dashes) are shown from the surface through 5 km AGL. Ozone concentration is given on the top horizontal axis. Temperature and winds are given by the bottom horizontal axis.

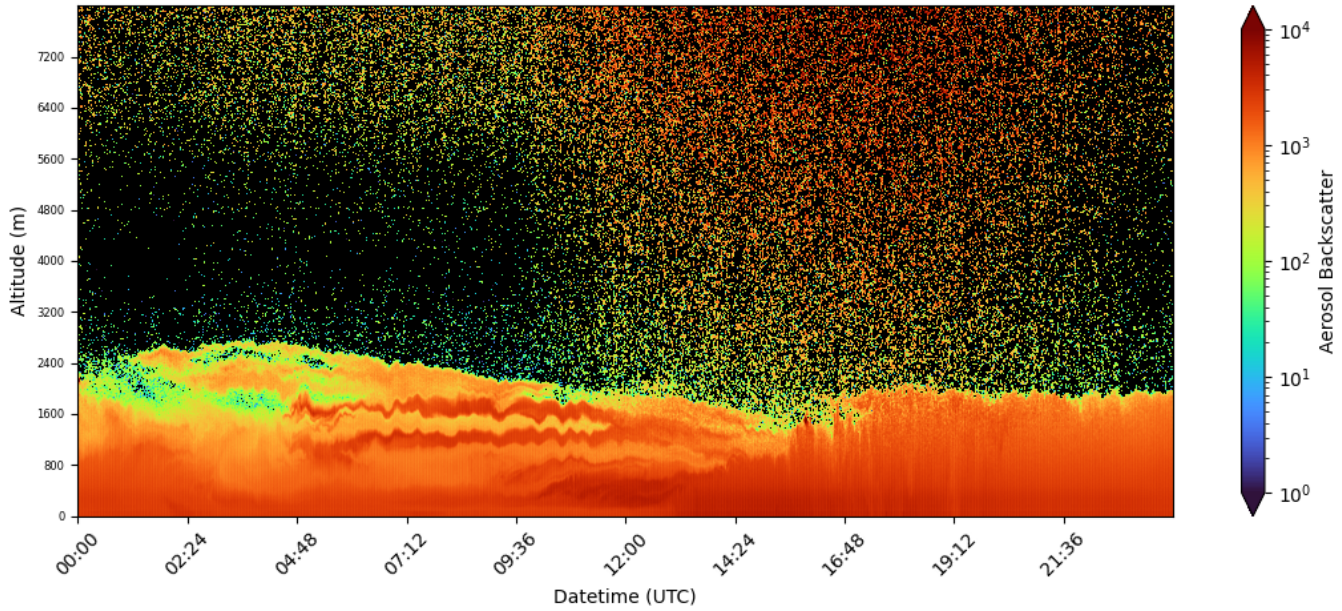

Figure 25: Ceilometer backscatter (colors) from a) The McMillan Reservoir site on June 29, 2023.

The vertical white lines and blue stars correspond to the times of ozonesonde launches from Howard University Beltsville on June 29 at 06:26 UTC (2:26 am) and 18:00 UTC (2:00 pm)

Inspection of the ozone concentrations across areas of densest smoke across the Great Lakes and Mid-Ohio River Valley on June 28 revealed areas of maximum 8-hour ozone concentrations in excess of 70 ppb. Ozone exceedances occurred from eastern Ohio west and northwestward through Wisconsin on June 28 across a wide region influenced by smoke with 24-hour average concentrations in excess of 100µg/m^3, with some areas in excess of 200 µg/m^3 (see Figure 18o,p) As this denser smoke moved into the District, so too did the ozone. In the weakly forced atmosphere, HYSPLIT trajectories did poorly, taking the smoke from the eastern Ohio River Valley to the District on June 29, 2023 (Figure 26).

As such, a better proxy is to track fine particle concentrations, which rose significantly in the District beginning around 9 am on June 29, as smoke just above the surface finally mixed downwards. While the distance covered by HRRR trajectories from western Pennsylvania from June 28 to June 29 do not cover the adequate horizontal distance to be consistent with smoke concentrations at the surface, the trajectories show clear downward motions, indicative of smoke transported a few hundred meters above the surface being dropped downwards and significantly increasing surface concentrations, consistent with the intense rise in concentrations seen around 9 am. As outlined in the conceptual model of the event, subsidence coincided with the final movement of the surface high pressure to over the District from the Ohio region on the morning of June 29.

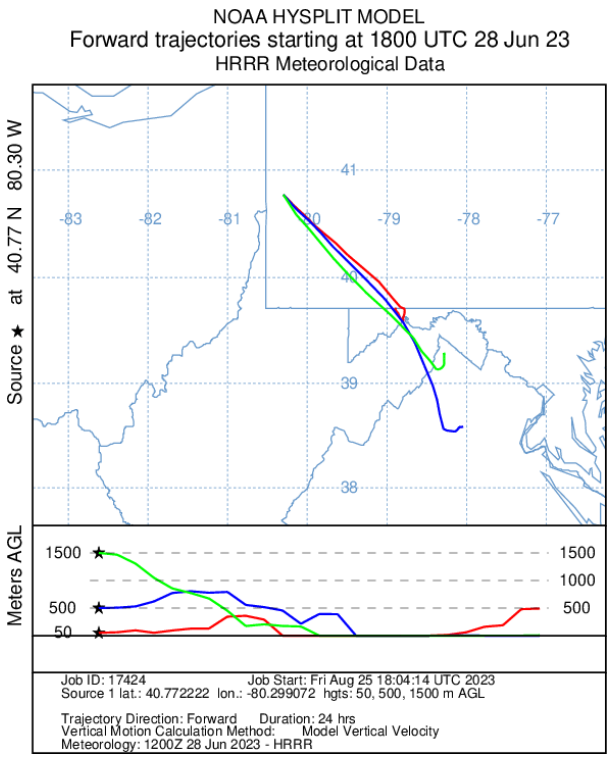

Figure 26: HYSPLIT 24-hour forward trajectories based on HRRR meteorology on June 28, 2023, at 2 pm (1800 UTC) from an area of dense smoke observed over western Pennsylvania.

Ozone concentrations increased markedly at both the surface (despite muted sunlight) and within the column as observed by ozonesondes. An ozonesonde was launched at 2 pm EDT (1800 UTC) from the HUB site (Figure 27). Ozone concentrations were generally at 80 ppb from 250 m through 1 km, then linearly increased to 110 ppb) at 2 km. Cross-referencing this sounding with the ceilometer returns lines up the highest ozone concentrations at 2 km with the top of the smoke aerosol layer for the McMillan ceilometer. This is a strong indication that the portion of the smoke plume getting full sun (e.g., the top layers of smoke) had extremely active photochemistry supportive of concentrations of 89 ppb. However, even muted sun still supported ozone concentrations at the surface above 70 ppb, consistent with upstream concentrations the previous day.

Ozone concentrations decreased on June 30 along with declining smoke concentrations.

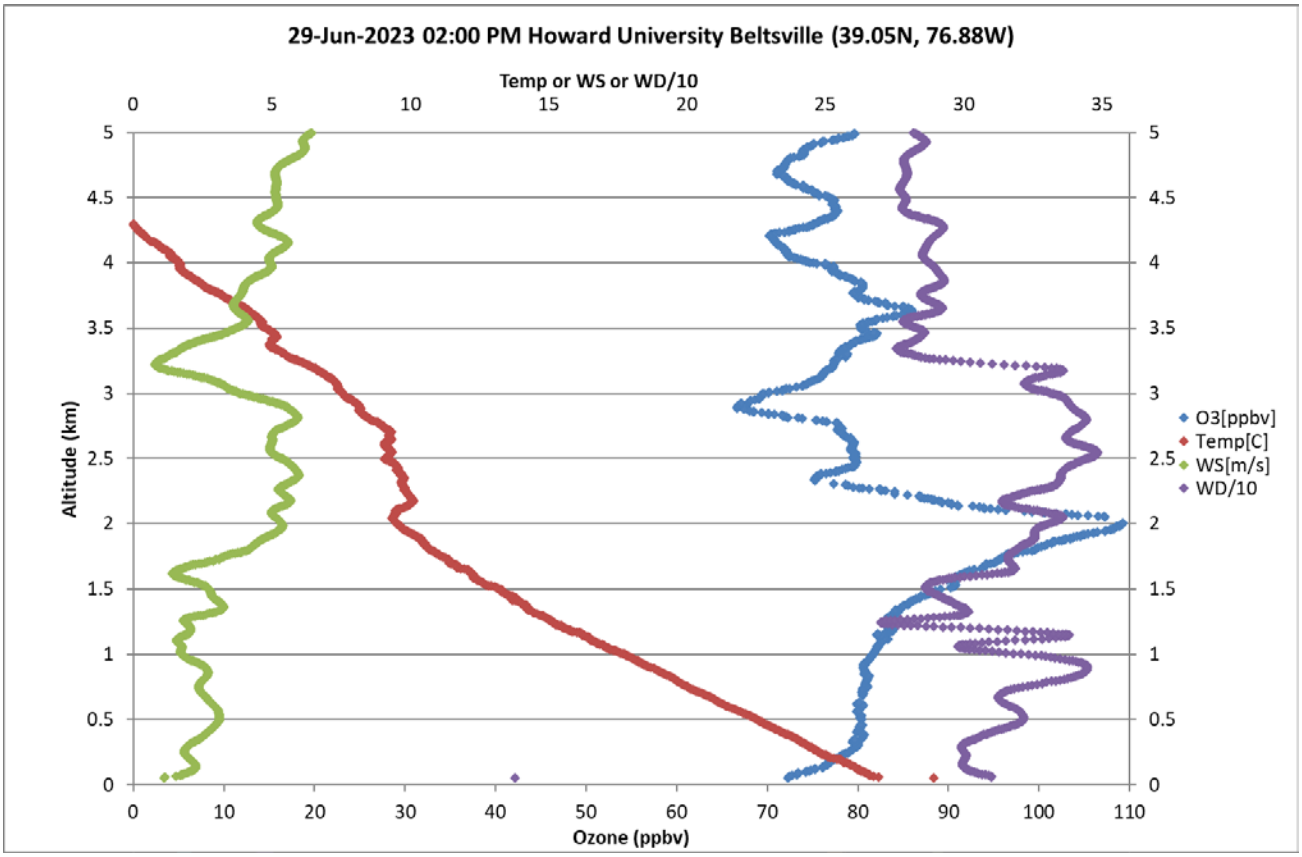

Figure 27: Same as figure 22 but for June 29, 2:00pm (1800 UTC)

3.3 Q/d Analysis

EPA guidance recommends conducting a Q/d analysis as a rough assessment of the ability of a wildfire to cause increased ozone concentrations. The Q/d analysis is a simple comparison of the ratio of Q, the daily tons of VOC and NO_x emitted from the fire to d, the distance in kilometers from the fire to the point of concern. If the Q/d value compares favorably to analytical data from other fires, then the fire can be presumed to have had a causal effect on ozone concentrations at the point of concern. The comparison to other fires is a key point that will be brought up again.

EPA guidance indicates that a fire should have a Q/d more than 100 tons per day, per kilometer (tpd/km) to be considered to have a clear causal impact on ozone. EPA developed this value based on analyses of four fires which occurred in 2011. Due to the large distances which Canadian wildfire plumes must travel to the District; the Q/d analysis will regularly fail to achieve the 100 deemed acceptable by the EPA guidance. Therefore, DOEE feels the 100 value is not representative for long-range east-coast smoke events. DOEE instead presents several alternatives based on this analysis.

3.3.1 Estimate of Q

The emissions from the fire can be estimated using information from EPA's AP-42 Compilation of Air Emission Factors Section 13.1 Wildfires and Prescribed Burning. The equations given are as follows:

Fi = Pi * L (Equation 1)
Ei = Fi * A (Equation 2)

Fi = emission factor (mass of pollutant/unit area of forest consumed)
Pi = yield for pollutant "i" (mass of pollutant/unit mass of forest fuel consumed)
= 12 kg/Mg (24 lb/ton) for total hydrocarbon (as CH4)
= 2 kg/Mg (4 lb/ton) for nitrogen oxides (NOx)

L = fuel loading consumed (mass of forest fuel/unit land area burned)
A = land area burned
Ei = total emissions of pollutant "i" (mass pollutant)

Combining equations 1 and 2, we have:

Ei = Pi * L * A

Pi is given above for total hydrocarbons and for nitrogen oxides. The fuel loading is given in AP-42 for different regions of the United States and ranges from 9 to 60 tons per acre. Conservatively, we will estimate a low-end emission rate using 10 tons per acre which is associated with North Central U.S. conifer forests. Note that our results could increase by a factor of 6 were the high end of emissions expected.

Between June 21 and June 26, 1,650,003 hectares (4,077,246 acres) burned across Canada according to satellite measurement techniques employed by the Canadian Wildland Fire Information System (CWFIS)[iii]. Fires were most active within Quebec at this time and of the 1,650,000 hectares burned across Canada, 1,570,081 hectares (3,879,755 acres), or the equivalent area of the US State of Connecticut (1,435,700 hectares) burned across Quebec Figure 28). Daily area burned across Quebec showed an intense period of burning during the June 21-26 period, peaking at over 450,000 hectares in one day on June 22, 2023. Burn area is estimated by satellite. Cumulative burned area for all of Canada is given as blue bars while daily area burned in Quebec is given in hallowed orange bars. There is a burn area increase equivalent to the size of Connecticut between June 21 and June 26, 2023, leading to a large increase in emissions in that time period.

Assuming a lower threshold of emission per area burned the total hydrocarbon emissions from the period can be estimated to be:
Ehc = 24 lbs of HC / ton of forest fuel consumed * 10 tons fuel / acre * 3,879,755 acres
Ehc =931,141,200 pounds of HC
Ehc = 465,571 tons of HC emitted during the period from June 21 to June 26, 2023

Similarly for NO_x:
Enox = 4 lbs of NO_x / ton of forest fuel consumed * 10 tons fuel / acre * 3,879,755 acres
Enox = 155,190,200 pounds of NO_x
Enox = 77,595 tons of NO_x emitted during the period from June 21 to June 26, 2023

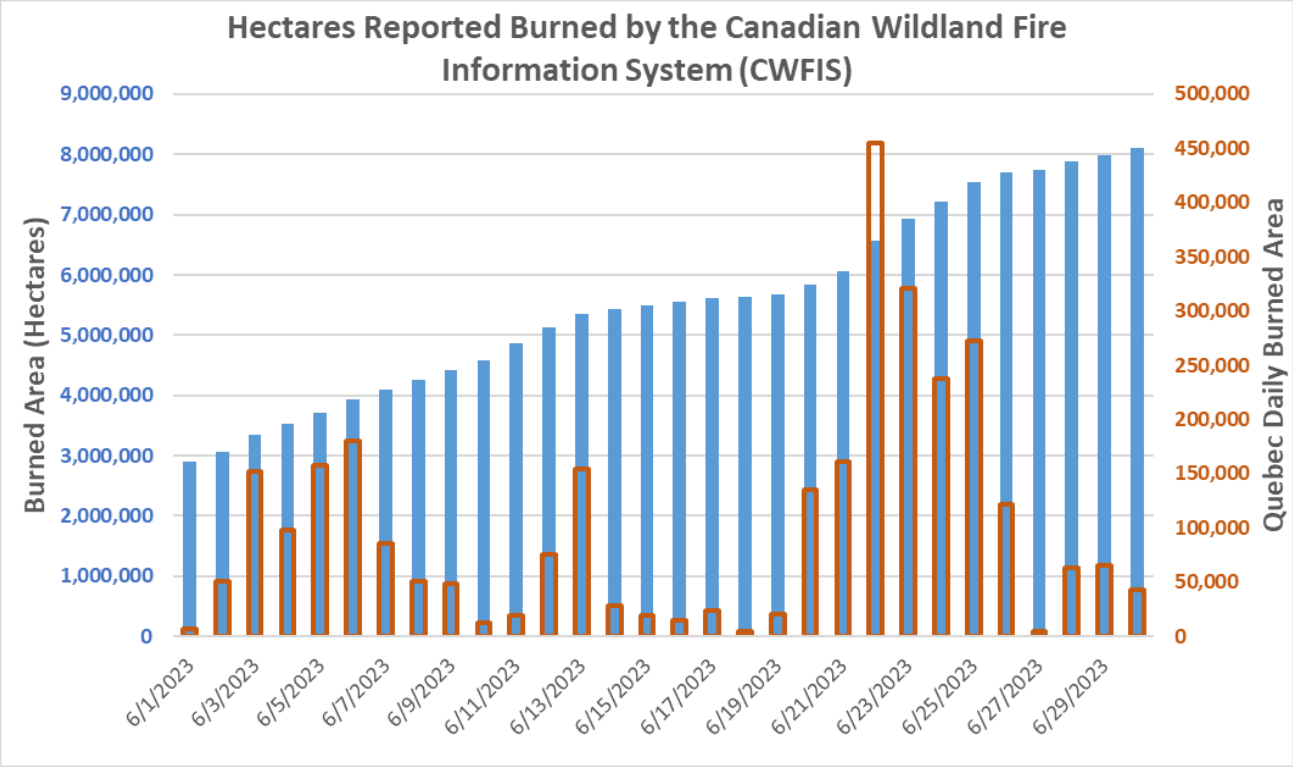

Figure 28: Hectares burned reported by Canadian Wildland Fire Information System (CWFIS).

Q is the total daily emission rate in tons per day of reactive hydrocarbons and nitrogen oxides. EPA recommends in the exceptional events guidance, that only 60% of the hydrocarbons should be considered reactive. Therefore, the reactive hydrocarbon emissions become rHC = 0.6 * Ehc or 0.6 * 465,571 = 279,343 tons of reactive HC emitted during the period of interest. No adjustments are suggested for the NO_x emissions. Total rHC and NO_x emissions over the period would therefore be 279,343 + 77,595, or 356,938 tons over the six days. On average, this results in a daily emission rate, or Q, of 59,490 tons per day.

3.3.2 Estimate of d

Based on the large distance, there will not be individual analyses completed for each monitor in the District but an estimate of the distance from Centroid of the fires (~ 49.37°N, 76.61°W) to the most distant monitor exceeding in the District will be calculated. In this event, the most distant monitor to exceed was the McMillan Reservoir site. Together, these points will supply a conservative, yet representative distance the smoke traveled to the District ozone network. Two distances are also offered - Euclidean and following the curved path through the Great Lakes. The direct path between

the two points yields a distance of approximately 1200 km; the curved path through the Great Lakes (a trajectory similar to figures above) covers a distance of 2,400 km. A representative value may be an average of these two, and as such, 1,800 km was therefore used for d, the distance smoke from Quebec fires traveled to the District.

3.3.3 Q/d Estimate

Using the values determined above, Q/d becomes 59,490 tpd divided by 1800 km or 33 tpd/km (Table 4). This value is well below the EPA recommended level of 100 tpd/km, indicating clear causality. If, instead, we aggressively assumed emissions from the out-of-control fire just on June 22, with 455,081 hectares (1,124,529 acres) burned, the District's Q/d value climbs to 57. Still below 100, but now within the range of Q/d values within demonstrations cited within the EE guidance.

Table 4: Q/d analysis for various scenarios

ACRES	Ehc (tons)	Enox	Q	No. days burning	d	Q/d	DESCRIPTION
3,879,755	465,571	77,595	356,938	6	1800	33.0	Standard Q/d
1,124,529	134,944	22,491	103,457	1	1800	57.5	June 22 emissions only
3,879,755	105,000	7,000	112,000	1	1800	62.2	Comparing to Appendix A2 fires
3,879,755	2,793,424	465,571	2,141,625	6	1800	198.3	Fuel loading at a maximum of 60 tons/arce instead of 10

Taking a slightly different approach, DOEE considered the basis for the EPA guidance and looked at emissions from one of the four fires EPA relied on in developing their guidance. Appendix A2 of the EPA Exceptional Event Guidance Document indicates that EPA based their conclusions on 12 km grid CMAQ modeling of four 2011 multiday fires: Wallow, Waterhole, Big Hill and Flint Hills. Emissions from the fires were based on a program called SMARTFIRE. Using information available on the Wallow Fire, DOEE approximated the emissions that might be calculated for the Quebec fires.

The Wallow Fire was located in eastern Arizona and western New Mexico from May 29, 2011, through July 8, 2011, and burned 841 square miles (538,240 acres) by June 26th. The maximum daily emissions from that fire were reported as approximately 15,000 tons of rVOC and 1,000 tons of NO_x. [Simulating Fire Event Impacts on Regional ozone and $PM_{2.5}$ and Looking Forward Toward Evaluation, Kirk Baker, EPA October 5, 2015 and Using SOAS and related field study data for scientific and regulatory modeling, Kirk Baker, EPA, undated; both are slide presentations] If this fire were scaled up by a factor of seven to approximate the total acreage burned in the Quebec fires, then the daily emissions were as high as 105,000 tons for rVOC and 7,000 tons for NO_x. These emissions produce a Q of 112,000 tpd, and Q/d becomes 62 for the District. From the EE guidance document: "The O3 values within the approved demonstrations generally were associated with Q/D values above 50 tpd/km (Figure A2-1)". A value of 62 while below 100, which is well within the range of accepted concurrences. Taking a less conservative approach and recalling that a worst-case fuel loading would increase our Q results by a factor of six, Q/d would, in this case, result in ~198 tpd/km, well above EPA's threshold of 100 tpd/km. Several of the potential scenarios show direct causal relationships given the EPA Q/d criteria. Such findings satisfy both Key Factors 1 and 2 in the EPA Exceptional Events Guidance and further suggest the smoke plume's impact on the District was exceptional in nature.

EPA guidance indicates that if a Q/d analysis compares favorably to analytical data from other fires, then the fire can be presumed to have had a causal effect on ozone concentrations at the point of concern. Since 2015, at least three major Canadian wildfire episodes have impacted the District: June 9-12, 2015 (as thoroughly described in Dreessen et al., 2015), May 25-26, 2016, and July 20-22, 2016. Thus, by EPA's Q/d definition, DOEE now has a small subset to compare other wildfire impacts on ozone within the contemporary emissions environment. A Q/d analysis for May and July 2016 was done in those exceptional event analyses. For June of 2015, Q/d was calculated using values in Dreessen et al., 2016, which listed 77,000 acres burned in a two (2) day period and smoke transported 3100 km from central Saskatchewan. Dreessen et al., 2016, goes on to show the impact of the smoke plume as it descended on the eastern Midwest and Mid-Atlantic on June 9-11, 2015, and showed clear wildfire signatures and influences on ozone.

Based on that research, Q/d for that ozone episode would have been 1.1 (Table 5 5). The May event demonstrated here had a Q/d four times as large (4.1). The July 2016 event had a Q/d of 1.8. Some research has noted the uncertainties in the influence of wildfire emissions in terms of strength and composition on ozone production (e.g., Hu et al., 2008). Thus, it is quite plausible that the value of 100 for Q/d is not relevant for long-range transport cases. It appears a more appropriate Q/d number for Canadian wildfire smoke transport cases to the District is closer to one (1), 100 times lower than the EPA suggested value. In the June 29-30, 2023 event, the Q/d value was 33, well below 100, despite immense smoke impacts indicated by fine particulate values in excess of 100 $\mu g/m^3$. The obvious smoke impacts logically lend to a much higher Q/d value than the recommended value of unity. At 33, the Q/d calculated as a baseline value for June 29-30 compared consistently and favorably with other fire events in the District, and DOEE believes this shows a clear causal relationship between the ozone and smoke.

ACRES	Ehc (tons)	Enox (tons)	Q (tons)	No. days burning	d (km)	Q/d	DESCRIPTION
368,187	44,182.00	7,364.00	33,873.20	2.5	3280	4.1	Fort McMurray - May 2016
271,134	32,536	5,423	24,945	4.0	3530	1.8	Northwest Territories - July 2016
77,000	5,544.00	1,540.00	7,084.00	2.0	3100	1.1	Lac La Ronge - June 2015

Table 5: Q/d Analysis for three Canadian Wildfire events impacting the District.

Noting the wide variability in emissions estimates from different approaches, and as the Q/d method does not generally easily apply to long-range transport scenarios in the District to clearly fit the expectation of a clear causal impact, other evidence is presented demonstrating that the smoke plume from Quebec fires caused elevated ozone levels in the District.

3.4 99th Percentiles

As part of demonstrating a clear causal relationship between ozone concentrations and the fire event, monitored concentrations were put in the context of historical observations. Observations at monitors falling at or above the 99th percentile in the past five years established statistical evidence that the

event was likely influenced by an exceptional event and are a "Key Factor" used to determine whether a Tier 2 application is appropriate. Following the Exceptional Events Guidance, the 99th percentile was calculated for all District monitors for all days of the ozone season (April – September) from 2019-2023. Additional 99th percentiles were calculated using subsets of days as summarized and presented previously in section 3.1 and in Figures 20-21. For convenience, a summary table with comparisons of all the 99th percentiles is given in Table 6 6.

	99th Percentile ppb					June 29, 2023			
Name	**AQSID**	**All Data**	**June Only**	**2022**	**2022-2023**	**All Data**	**June Only**	**2022**	**2022-2023**
McMillan	110010043	73	79	72.5	75.4	Yes	Yes	Yes	Yes
River Terrace	110010041	62.9	65	60	60	Yes	Yes	Yes	Yes

Table 6: 99th percentile values and comparisons to observations on June 29, 2023.

The two District monitors for which DOEE is seeking exclusion due to exceptional event influence have their 99th percentiles presented based on data from April 1 – September 30, 2019-2023, and other subsets as defined in section 3.1. The final four columns highlight which monitors exceed their 99th percentile level ("Yes") for a given data set and day.

3.4.1 Particles

$PM_{2.5}$ can be both a primary pollutant and a resultant secondary pollutant of wildfire emissions downstream, as photochemistry within the plume converts certain species to aerosols. The entire DOEE network showed a correlated increase in $PM_{2.5}$ 24-hour averages from June 29-30, which aligned with the onset of the smoke plume in the District (Figure 29). Additional episodes of smoke is visible on June 1-2 and 6-9. No other period of the month exhibited such a large, coherent increase across the entire District network. Though the late June period did not possess the highest particle observations of the month, it did exhibit the highest distribution and highest-low observation for the entire month, showing that even with slightly lower concentrations, the state was essentially uniformly impacted by smoke, as compared to earlier June when smoke was stronger in some areas than others. The fine particle observations, therefore, provided additional evidence that along with ozone and ozone precursors, fine particles were transported within the smoke-affected airmass and were a distinct indicator of wildfire emissions, particularly since speciated particles associated with wildfire emissions showed similar increases.

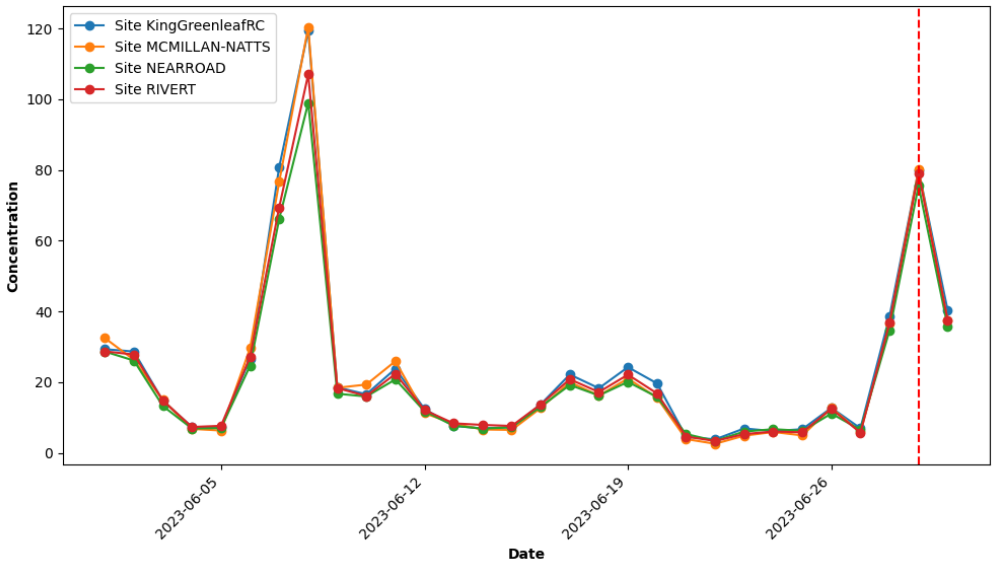

Figure 29: Daily averaged fine particle ($PM_{2.5}$) concentrations for all sites available in the District for the month of June 2023. June 29th is highlighted by the red vertical line.

3.4.2 3.5.3 Carbon Monoxide (CO)

CO, previously identified as a wildfire smoke indicator, can play a role in ozone production and followed similar trends to other pollutants over the lifetime of the event (Figure 30). McMillan Reservoir and the Near Road sites both had the highest CO concentration of the entire month of June on June 29, despite a second smoke event earlier in the month. This increase in CO was coincident with increased wildfire-related fine particle concentrations and provided irrefutable evidence for the direct impact of the smoke at the surface. The plume arrived over the District in agreement with the increased CO concentrations at the District surface monitors (Figure 30). Together, these observations indicated that wildfire-related ozone precursors were present to contribute to ozone production upstream across the Great Lakes and Ohio River Valley and then moved into the District by June 28.

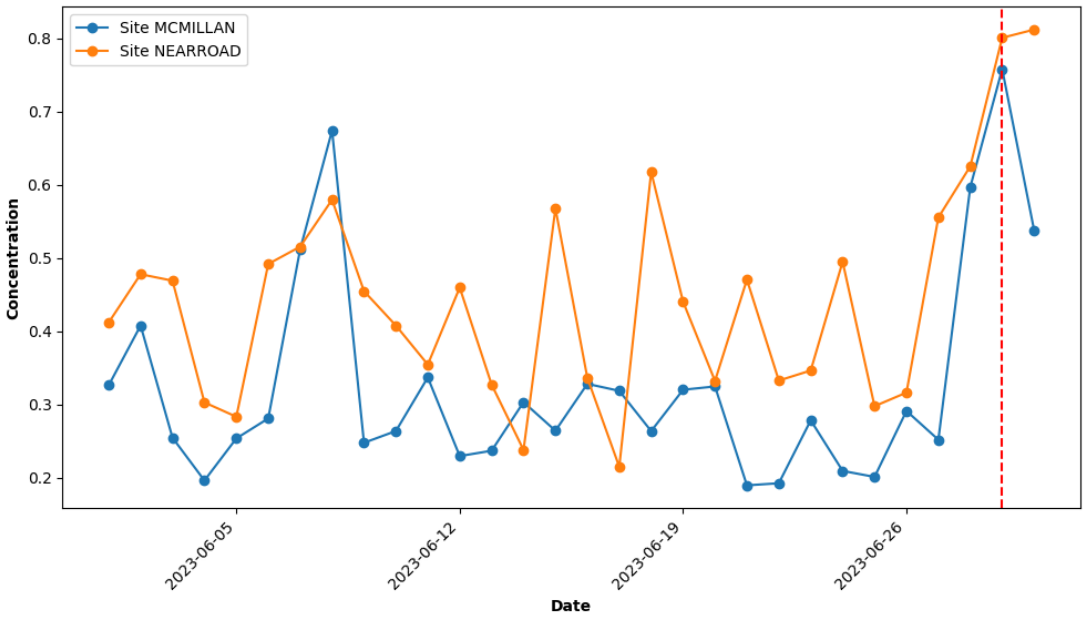

Figure 30: Daily Carbon Monoxide (CO) at available sites in the District on June 29th is highlighted by the red vertical lines.

3.4.3 Nitrogen Oxides

Singh et al. (2012) showed that ozone production rates from wildfires in California were dependent upon available NO_x (NO_x = sum of nitrogen oxide (NO) and nitrogen dioxide (NO_2)) and that NO_x from the fires themselves was relatively low. However, NO_x emissions from fires can vary greatly, and research has noted the uncertainties in the influence of wildfire emissions from one to another (e.g., Hu et al., 2008). In the current study, monitors observing the highest ozone concentrations were near urbanized areas (e.g. Essex, Maryland), suggesting the local NO_x contributions from these areas were contributing to ozone concentrations, see Figure 31. Here, hourly ozone concentrations from McMillan and River Terrace were compared to Piney Run (Maryland) and State College (Pennsylvania), both of which are located in rural areas. However, in smoke, ozone production may occur more rapidly than otherwise may occur due to additional precursors present. As such, NO_x in the District simply augmented ozone production within the smoky and already ozone-laden airmass since ozone concentrations within the smoke plume were already regionally increased, both in rural and urban areas. Ozone would not have reached the MD8AO concentrations observed during the event without the presence of the smoke. The augmentation of ozone was particularly likely and apparent given the spatial coherence of ozone and smoke on June 26-28 over the entire corridor of HMS analyzed smoke, with enhanced ozone from the Great Lakes to the East Coast (Figure 18).

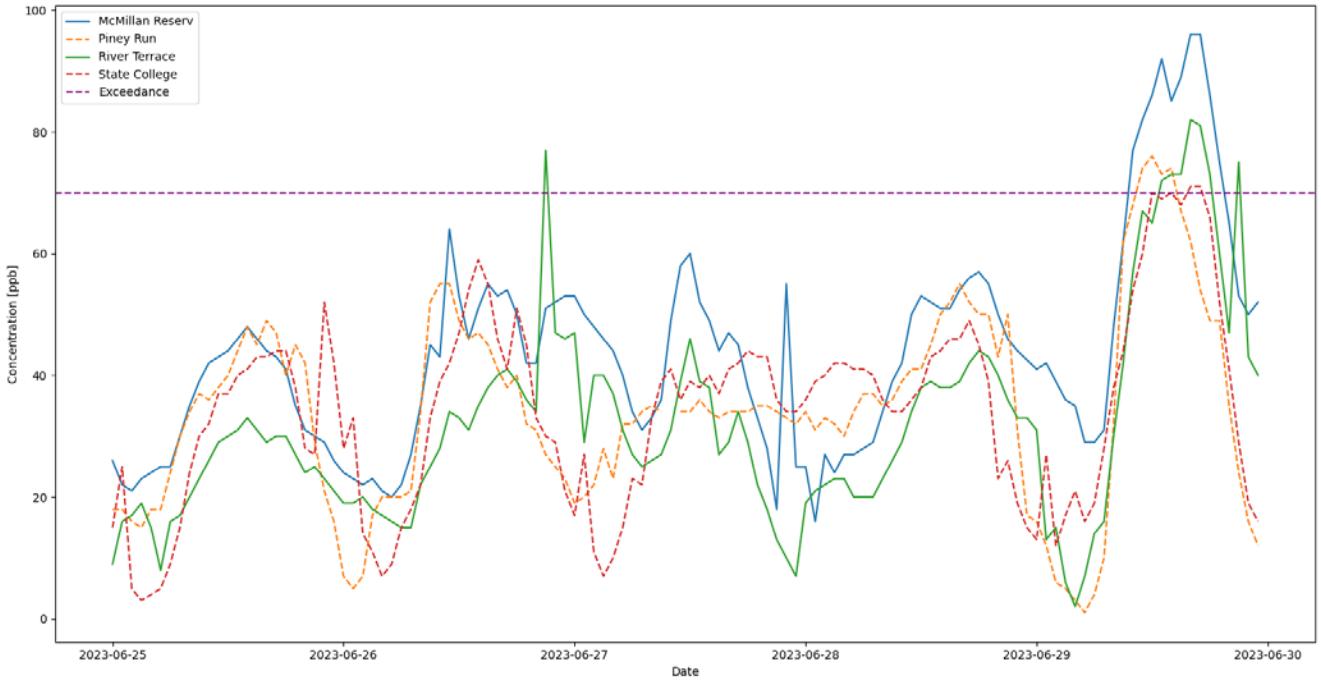

Figure 31: Comparison of hourly ozone concentrations from both urban District monitors vs rural monitors Piney Run (Maryland) and State College (Pennsylvania) from June 25th -June 29th.

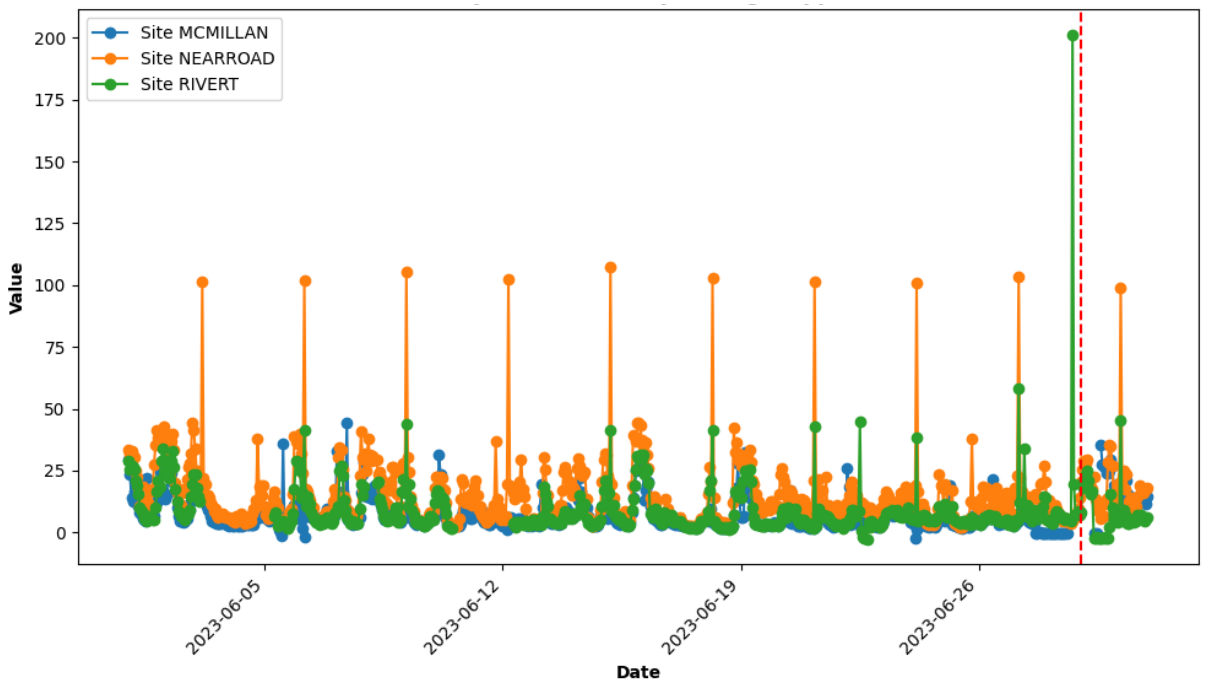

Figure 32: As in Figure 28, except for hourly nitrogen dioxide (NO_2) from available District monitors in June 2023.

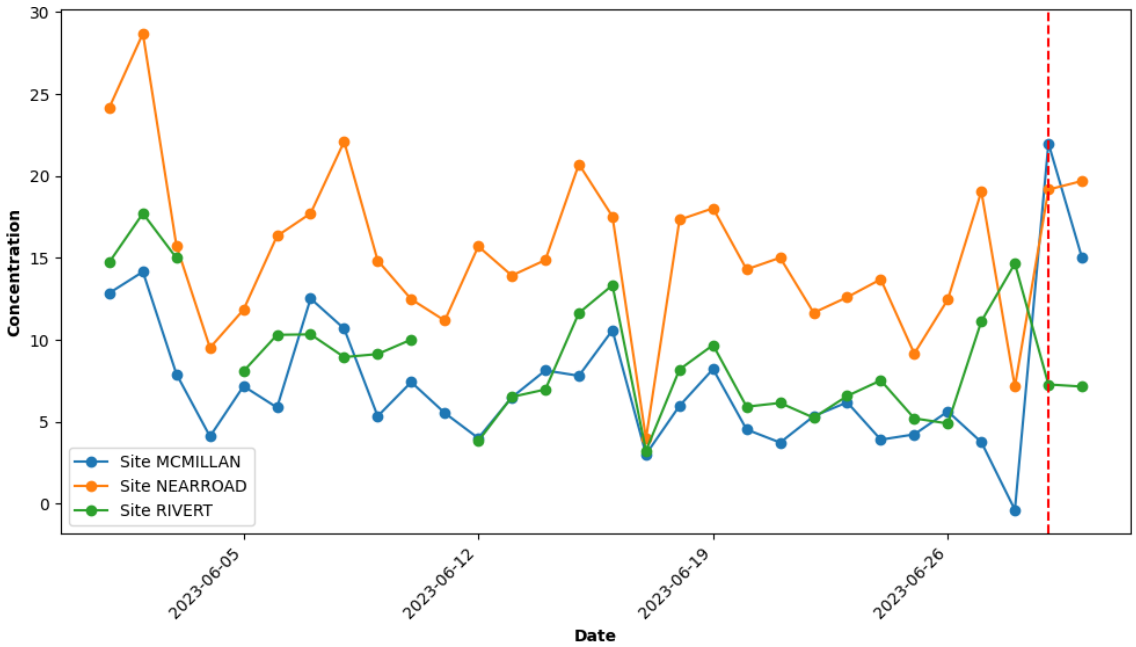

Figure 33: As in Figure 28, except for daily average nitrogen dioxide (NO_2) from available District monitors in June 2023.

3.4.4 NO_x Historical Context: Local June NO_x, Aged Nitrogen, and Total Reactive Nitrogen

If wildfire NO_x was stored within the smoke plume due to the abundance of VOCs, as discussed in Dreessen et al. (2016), strong evidence of aged NO_x would be present. Further study of the composition of the Nitrogen in the airmass showed that the total active nitrogen (NO_y) was both one of the largest NO_y observations in June in the past six years (Figure 34). Furthermore, NO_T, a measure of the reactivity and NO_x storage within an airmass, was also the highest in the last six years (Figure 35). All this is despite the lowest monthly June EGU NOx emissions upstream to date (Figure 5). Daily average NO_y concentrations for all June 2023 days at the District monitors showed that late June of 2023 had some of, if not the highest NO_y and NO_T observations exclusive of the other strong smoke periods in June of 2023, consistent with the time period of the smoke influenced airmass in Maryland on June 29, 2023. There was no doubt the airmass was characterized by abundant NO_x, not seen even when upstream EGUs were emitting larger amounts of NO_x prior to the 2017-2023 era.

Subjective analysis of nitrogen species allows some qualitative source attribution. Generally, it is difficult to distinguish NO_x sources from each other (i.e., point, mobile, wildfire). Fresh NO_x emissions tend to be dominated by Nitrogen Oxide (NO) rather than Nitrogen Dioxide (NO_2) or other non-NOx speciation (NO_T). NO has a shorter lifetime due to its high reactivity. Thus, an airmass dominated by NO_T tends to indicate aged emissions amid a reactive airmass. The composition of the NO_x was overwhelmingly composed of older and 'storage' nitrogen species on June 29. The high levels of NO_2 were indicative of an aged airmass, NO_x transport, and, therefore, non-local emissions. DOEE, therefore, contends the increased NOx observed during the ozone event was a result of efficient NOx storage within the smoke plume sourced from the fire itself and diminutive regional NOx contributions,

both of which caused NO_Y and NO_T to be beyond contemporary concentrations in the District, further leading to ozone at statistically extreme concentrations.

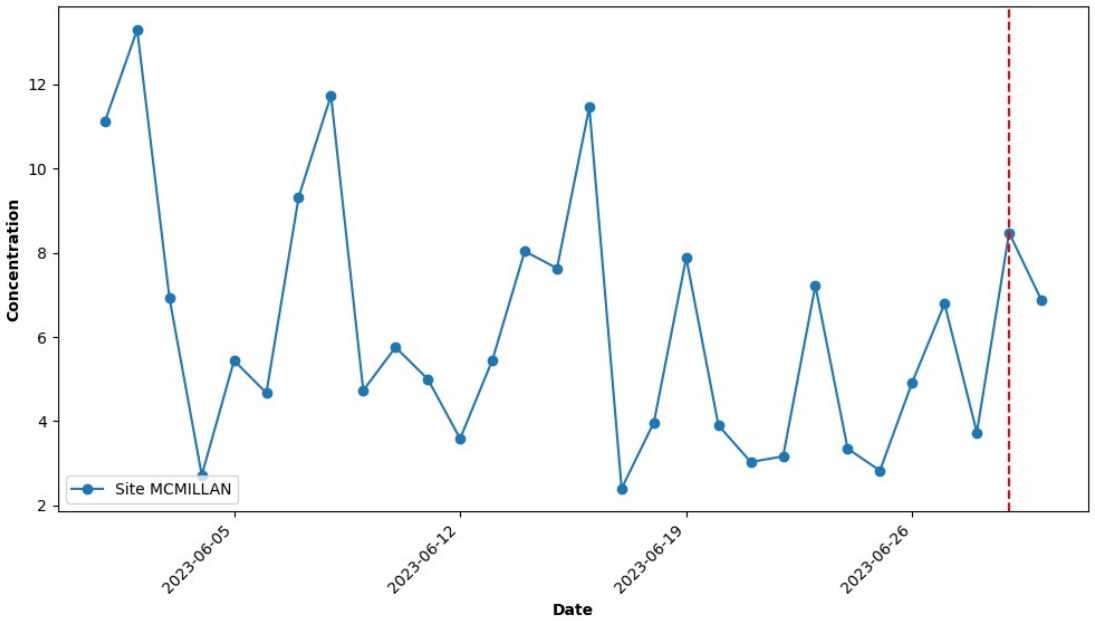

Figure 34: Daily oxides of Nitrogen concentrations at the District's McMillan site for the month of June.

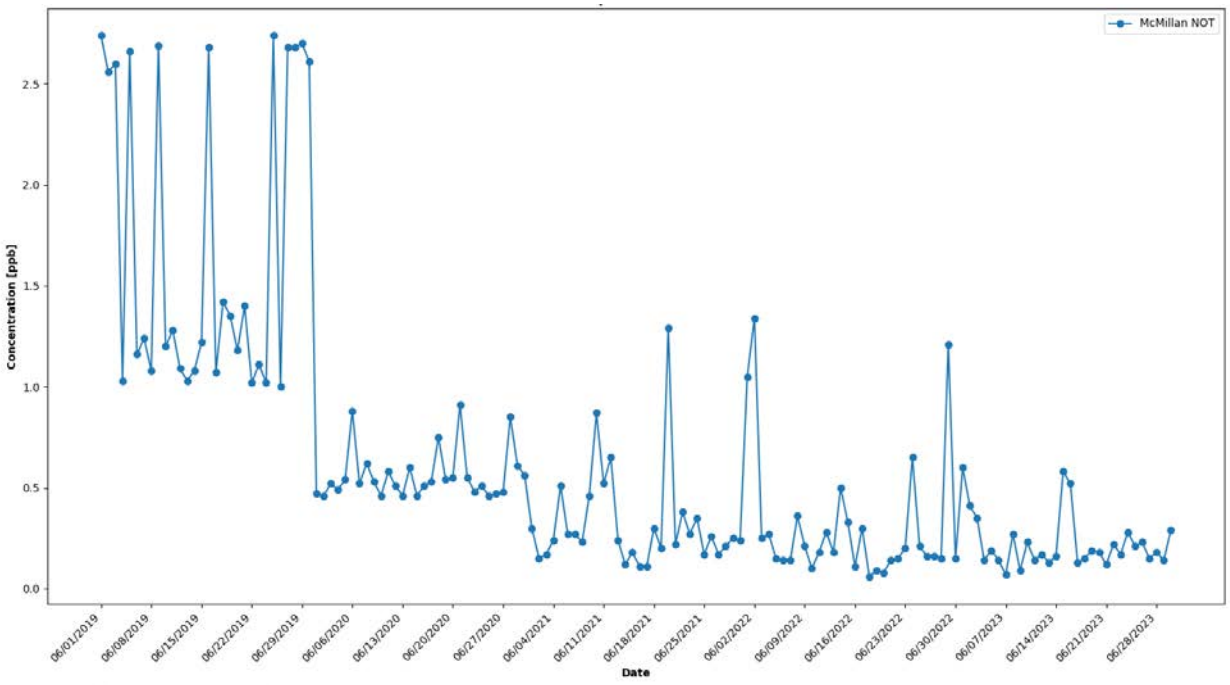

Figure 35: NOT concentrations from McMillan monitor for days in June from 2019 to 2023.

4.0 The Occurrence was a Natural Event

According to the Clean Air Act (CAA) and the Exceptional Events Rule (40 CFR § 50.14), an exceptional event must be "an event caused by human activity that is unlikely to recur at a particular location or a natural event." The Quebec fires were a "natural event." The Exceptional Events Rule defines a wildfire as "…any fire started by an unplanned ignition caused by lightning; volcanoes; other acts of nature; unauthorized activity; or accidental, human-caused actions, or a prescribed fire that has developed into a wildfire. A wildfire that predominantly occurs on wildland is a natural event." Based on the documentation provided in section 2 of this submittal, which discusses the origin and evolution of the wildfire events, the Quebec fires qualify as a "natural event" because they were unplanned fires on wildland ignited by lightning. A report put out by the Canada Natural Resources Department says that 120 fires were ignited by lightning in just one day. EPA generally considers the emissions of ozone precursors from wildfires on wildlands to meet the regulatory definition of a natural event as defined in the NAAQS. Accordingly, DOEE has shown that the event is a natural event and may be considered for treatment as an exceptional event.

5.0 The Occurrence was Not Reasonably Controllable or Preventable

Based on the documentation provided in section 2, the fires relevant in this demonstration were due to lightning that caused wildfire events on wildland. These fires were considered natural wildfire events by the EPA, were outside of the United States, and were therefore neither reasonably controllable nor preventable by the District of Columbia. No policy that the District enacted could have prevented the fire, or the smoke which it caused, to enter the United States, or DOEE was not aware of any evidence clearly demonstrating that prevention or control efforts beyond those actually made would have been reasonable. Therefore, emissions from these wildfires were not reasonably controllable or preventable and met the criterion for treatment as an exceptional event.

6.0 Public Comment

This is a draft for public comment. Analysis of the comments will be included in the final document.

7.0 Conclusions

On June 29, 2023, smoke associated with wildfires across Quebec, Canada was transported across the Great Lakes and Upper Ohio River Valley and delivered ozone and precursors to the District. This smoke plume produced ozone exceedances all along its track two days prior, with near ozone exceedances observed near the fires themselves in sections of remote Quebec, Canada. Upon arriving in The District, the smoke impacted all monitoring sites across the District's air monitoring network. The monitored MD8AO concentrations reached 89 ppb and 73 ppb on June 29 and resulted in at least one of the fourth-highest concentrations of 2023 at both sites and met or beat the 99th percentile at both sites on at least one or both days. The comparisons and analyses provided in sections 2 and 3 of this demonstration support DOEE's position that the June 29 wildfire event affected air quality in such a way that there exists a clear causal relationship between the specific event and the monitored concentrations on June 29, 2023, and thus satisfies the clear causal relationship criterion.

The analyses provided in this demonstration supports DOEE's position that the Quebec wildfires, particularly from June 21 - 25, affected air quality in the District by June 29 in such a way that there exists a clear causal relationship between the event (June 21-25, 2023, burn period in Quebec) and the monitored ozone exceedances in the District on June 29, 2023, and thus satisfies the clear causal relationship criterion for recognition as an exceptional event. Based on these facts, DOEE requests that EPA concur that the 2 MD8AO concentrations on June 29, 2023 (Table 8), exceeding the 70 ppb NAAQS at the following two monitors: McMillan Reservoir (110010043) and River Terrace Education Campus (110010041) were impacted by an exceptional event.

DOEE formally requests that the data from these two monitors on these days be concurred with as exceptional events and excluded from use for regulatory determinations.

8.0 References

Adam, M., M.Pahlow, V.A. Kovalev, J. M. Ondov, M.B. Parlange, and N. Nair. (2004) Aerosol optical characterization by nephelometer and lidar: The Baltimore Supersite experiment during the Canadian forest fire smoke intrusion. *J. Geophys. Res. Atmos.* (1984–2012) 109: D16. doi:10.1029/2003JD004047

Andreae, M.O., and P. Merlet. (2001) Emission of trace gases and aerosols from biomass burning. *Global biogeochem. Cycles 15*(4): 955–66. doi:10.1029/2000GB001382

Bytnerowicz, A., D. Cayan, P. Riggan, S. Schilling, P. Dawson, M. Tyree, L. Wolden, R. Tissell, and H. Preisler. (2010) Analysis of the effects of combustion emissions and Santa Ana winds on ambient ozone during the October 2007 southern California wildfires. *Atmos. Environ. 44*(5): 678–87. doi:10.1016/j.atmosenv.2009.11.014

Chai, T., H.-C. Kim, P. Lee, D. Tong, L. Pan, Y. Tang, J. Huang, J. McQueen, M. Tsidulko, and I. Stajner. (2013) Evaluation of the United States National Air Quality Forecast Capability experimental real-time predictions in 2010 using Air Quality system ozone and NO2 measurements. *Geosci. Model Dev. 6*(5): 1831–50. doi:10.5194/gmd-6-1831-2013

Colarco, P.R., M.R. Schoeberl, B.G. Doddridge, L.T. Marufu, O. Torres, and E.J. Welton. (2004) Transport of smoke from Canadian forest fires to the surface near Washington, DC: Injection height, entrainment, and optical properties. *J. Geophys. Res. Atmos.* (1984–2012) 109:D6. doi:10.1029/2003JD004248

DeBell, L.J., R.W. Talbot, J. E. Dibb, J. W. Munger, E.V. Fischer, and S.E. Frolking. (2004) A major regional air pollution event in the northeastern United States caused by extensive forest fires in Quebec, Canada. *J. Geophys. Res. Atmos.* (1984–2012) 109:D19. doi:10.1029/2004JD004840

Dreessen, J., Sullivan, J., & Delgado, R. (2016) Observations and impacts of transported Canadian wildfire smoke on ozone and aerosol air quality in the Maryland region on June 9–12, 2015. *Journal of the Air & Waste Management Association, 66*(9), 842-862.

EPA (1997) Peer Review of CASTNet, *Federal Register*, Vol. 62, No. 40 (1997): 9189. http://www.gpo.gov/fdsys/pkg/FR-1997-02-28/pdf/97-4967.pdf

EPA (2006) Air Quality Criteria For Ozone and Related Photochemical Oxidants (Final Report, 2006). U.S. Environmental Protection Agency, Washington, DC, EPA/600/R-05/004aF-cF, 2006.

Fiore, A.M., R.B. Pierce, R.R. Dickerson, M. Lin, and R. Bradley. (2014) Detecting and attributing episodic high background ozone events. *Environ. Manage. 64*: 22.

Flannigan, M.D., and van Wagner, C.E. (1991) Climate change and wildfire in Canada. *Canadian Journal of Forest Research. 21*(1)(Jan,1991) https://doi.org/10.1139/x91-010

Gégo, E.P., S. Porter, A. Gilliland, and S.T. Rao. (2007) Observation-based assessment of the impact of nitrogen oxides emissions reductions on ozone air quality over the eastern United States. *J. Appl. Meteorol. Climatol. 46*(7): 994–1008. doi:10.1175/JAM2523.1

District of Columbia Exceptional Event Demonstration and Analysis of the June 2023 Quebec Canada Wildfires and Their Impact on DC's Air Quality on June 29, 2023

Hu, Y., M.T. Odman, M.E. Chang, W. Jackson, S. Lee, E.S. Edgerton, K. Baumann, and A.G. Russell. (2008) Simulation of air quality impacts from prescribed fires on an urban area. *Environ. Sci. Technol. 42*(10): 3676–82. doi:10.1021/es071703k

Marlons, J.R., Bartlein, P.J., Walsh, M.K., Whitlock, C. (2009) Wildfire responses to abrupt climate change in North America. *Proceedings of the Nat'l Academy of Sciences 106* (8) 2519-2524, https://doi.org/10.1073/pnas.0808212106

Maryland Department of the Environment, Air and Radiation Management Administration. (2012) Creating a climate for clean air. *e'mde* 5 (4). http://mde.maryland.gov/programs/researchcenter/reportsandpublications/emde/pages/researchcenter/publications/general/emde/vol5no4/article%201.aspx#.VlM-5r_gKPV.

Maryland Department of the Environment. (2022) *Ambient air monitoring plan for calendar year 2023.* https://mde.maryland.gov/programs/air/AirQualityMonitoring/Documents/MDNetworkPlanCY2023.pdf

Maryland Department of the Environment. (2015) Linking weather and air quality using radar. Air and Radiation Management Administration, Monitoring Program. Last modified December 1, 2015. http://www.mde.state.md.us/programs/Air/AirQualityMonitoring/Pages/Radar.aspx

McKeen, S.A., G. Wotawa, D.D. Parrish, J.S. Holloway, M.P. Buhr, G. Hübler, F.C. Fehsenfeld, and J.F. Meagher. (2002) Ozone production from Canadian wildfires during June and July of 1995. *J. Geophys. Res. Atmos.* (1984–2012) 107 (D14): ACH–7. doi:10.1029/2001JD000697

McNamara, D. P., George Stephens, Mark Ruminski, and Tim Kasheta. (2004) The Hazard Mapping System (HMS)—NOAA's Multi-Sensor Fire and Smoke Detection Program Using Environmental Satellites. In *Proceedings of the 13th Conference on Satellite Meteorology and Oceanography*.

Morris, G.A., S. Hersey, A.M. Thompson, S. Pawson, J.E. Nielsen, P.R. Colarco, and W.W. McMillan. (2006) Alaskan and Canadian forest fires exacerbate ozone pollution over Houston, Texas, on 19 and 20 July 2004. *J. Geophys. Res. Atmos.* (1984–2012) 111(D24). doi:10.1029/2006JD007090

Pechony, O., Shindell, D.T. (2010) Driving forces of global wildfires over the past millennium and the forthcoming century. *Proceedings of the Nat'l Academy of Sciences 107*, 19167-19170, doi:10.1073/pnas.1003669107.

Putero, D., Landi, T. C., Cristofanelli, P., Marinoni, A., Laj, P., Duchi, R., ... & Bonasoni, P. (2014). Influence of open vegetation fires on black carbon and ozone variability in the southern Himalayas (NCO-P, 5079 m asl). *Environmental Pollution*, *184*, 597-60

Roberts, Sandra, et al. (2022) Multidecadal Trends in Ozone Chemistry in the Baltimore-Washington Region. *Atmopheric Environment, 285.*

District of Columbia Exceptional Event Demonstration and Analysis of the June 2023 Quebec Canada Wildfires and Their Impact on DC's Air Quality on June 29, 2023

Rolph, G.D., (2017) Real-time Environmental Applications and Display sYstem (READY) Website (http://ready.arl.noaa.gov). NOAA Air Resources Laboratory, Silver Spring, MD.

Ryan, William F. (2004) The low level jet in Maryland: profiler observations and preliminary climatology. *Report for Maryland Department of the Environment, Air and Radiation Administration*. Maryland State Implementation Plan, Appendix-G (2004).

Sapkota, A., Symons, J.M., Kleissl, J., Wang, L., Parlange,M.B., Ondov, J., Breysse, P.N., Diette, G.B., Eggleston, P.A., Buckley, T.J. (2004) Impact of the 2002 Canadian Forest Fires on Particulate Matter Air Quality in Baltimore City. *Environ. Sci. Technol., 39* (1), 24–32 https://doi.org/10.1021/es035311z

Singh, H.B., C. Cai, A. Kaduwela, A. Weinheimer, and A.Wisthaler. (2012) Interactions of fire emissions and urban pollution over California: Ozone formation and air quality simulations. *Atmos. Environ. 56*: 45–51. doi:10.1016/j.atmosenv.2012.03.046

Spichtinger, N., M. Wenig, P. James, T. Wagner, U. Platt, and A. Stohl. (2001) Satellite detection of a continental-scale plume of nitrogen oxides from boreal forest fires. *Geophys. Res. Lett. 28*(24): 4579–82. doi:10.1029/2001GL013484

Spracklen, D.V., Mickley, L.J., Logan, J.A., Hudman, R.C., Yevich, R., Flannigan, M.D., Westerling, A.L. (2009) Impacts of climate change from 2000 to 2050 on wildfire activity and carbonaceous aerosol concentrations in the western United States. *Journal of Geophysical Research, Atmospheres. 114*:D20 https://doi.org/10.1029/2008JD010966

Stein, A.F., Draxler, R.R, Rolph, G.D., Stunder, B.J.B., Cohen, M.D., and Ngan, F., (2015). NOAA's HYSPLIT atmospheric transport and dispersion modeling system, *Bull. Amer. Meteor. Soc., 96*, 2059-2077, http://dx.doi.org/10.1175/BAMS-D-14-00110.1

Westerling, A.L., Hidalgo, H.G., Swetnam, T.W. (2006) Warming and Earlier Spring Increase Western U.S. Forest Wildfire Activity. *Science 313*(5789): 940-943, DOI: 10.1126/science.1128834

[i] https://earthobservatory.nasa.gov/images/151507/canadian-smoke-reaches-europe

[ii] **https://www.cnn.com/2023/08/22/americas/canada-wildfires-climate-change-quebec/index.html [Source: Frederic Chouinard/SOPFEU/Anadolu Agency/Getty Images]**

[iii] https://cwfis.cfs.nrcan.gc.ca/datamart [Retrieved August 29, 2023]